



**Ministry of Environment  
and Food of Denmark**  
Environmental  
Protection Agency

# **Transport and transformation of biocides in construction materials**

## **Factors controlling release and emissions**

Pesticide Research No.  
177

November 2018

Publisher: The Danish Environmental Protection Agency

Editors: Ulla E. Bollmann, Kai Bester, Jes Vollertsen,  
Michał M. Urbańczyk, Elise A. Rudelle

Graphics: Ulla E. Bollmann

ISBN: 978-87-7038-007-2

The Danish Environmental Protection Agency publishes reports and papers about research and development projects within the environmental sector, financed by the Agency. The content of this publication do not necessarily represent the official views of the Danish Environmental Protection Agency. By publishing this report, the Danish Environmental Protection Agency expresses that the content represents an important contribution to the related discourse on Danish environmental policy.

Sources must be acknowledged.

# Contents

<b>Preface</b>	<b>5</b>
<b>Sammenfatning</b>	<b>6</b>
<b>Summary</b>	<b>8</b>
<b>1. Introduction and objectives</b>	<b>10</b>
1.1 Biocides: utility and emissions	10
1.2 Leaching process	12
1.3 Degradation and fate	13
<b>2. Materials and methods</b>	<b>14</b>
2.1 Materials	14
2.1.1 Biocides	14
2.1.2 Minerals & Acrylate	15
2.1.3 Render & Paints	16
2.2 Transport processes in the material	16
2.2.1 Influence of wet & dry cycles	16
2.2.2 Mobility controlled by different fractions	18
2.2.2.1 Partitioning between polymeric binder and water	18
2.2.2.2 Partitioning between minerals and water	19
2.2.2.3 Distribution constants for a model render	20
2.2.3 Diffusion controlled mobility	21
2.2.4 Depth resolved profiling	22
2.3 Photodegradation of biocides	24
2.3.1 Identification of photodegradation products	24
2.3.2 Biocide transformation on facade surfaces	25
2.3.3 Influence of pigments on photodegradation	26
2.3.4 Monitoring of photodegradation products	27
2.4 Extraction and analysis	27
2.4.1 Sample extraction for biocides and transformation products	27
2.4.2 Analysis of biocides	28
2.4.3 Analysis of transformation products	28
<b>3. Results &amp; Discussions</b>	<b>30</b>
3.1 Transport processes in the material	30
3.1.1 Influence of wet & dry cycles	30
3.1.2 Mobility controlled by different fractions	35
3.1.2.1 Polymeric binder	35
3.1.2.2 Minerals	38
3.1.2.3 Distribution constants for a model render	40
3.1.3 Diffusion controlled mobility	42
3.1.4 Depth resolved profiling	45
3.2 Photodegradation of biocides	52
3.2.1 Identification of photodegradation products	52
3.2.2 Biocide transformation on facade surfaces	56

3.2.3	Influence of pigments on photodegradation	63
3.2.4	Monitoring of photodegradation products	69
<b>4.</b>	<b>General conclusions</b>	<b>71</b>
4.1	Transport	71
4.2	Transformation	71
<b>5.</b>	<b>Perspectives</b>	<b>73</b>
<b>6.</b>	<b>References</b>	<b>74</b>
	<b>Appendix</b>	<b>79</b>



# Preface

The project about the transport and transformation mechanisms of biocides in construction materials has been conducted between 1<sup>st</sup> August 2014 and 31<sup>st</sup> December 2017 and was founded by the Danish Environmental Protection Agency - Pesticide Research Programme. The project was performed in collaboration between Aarhus University, Department of Environmental Science and Aalborg University, Department of Civil Engineering. Additionally, external partners (BAM, BFG, RMI, DTU, AGH) have been involved in parts of the project. The progress of the project has been followed and discussed by the working group EXPOSURE consisting of: Henrik F. Brødsgaard, Anne Munch Christensen and Anne Louise Gimsing from Danish EPA and the external members: Niels Lindemark, Anne Mette Madsen, Anne Fabricius, Jes Vollertsen, Carsten Suhr Jacobsen, Ulla E. Bollmann, Kristian Koefoed Brandt, Annette E. Rosenbom, Kai Bester, Hanne Ingmer, Birgitte Cordua, Michael Nielsen, Charlotte Rahbek, Jesper Lund-Larsen.

The report is split into two main topic transport processes in the materials and transformation, more accurate phototransformation processes. Parts of this project report have been published in international scientific journals. Additionally, the project results have been presented at several international conferences (Bilag 13).

K. Styszko, U.E. Bollmann, K. Bester. Leaching of biocides from polymer renders under wet/dry cycles - Rates and mechanisms. *Chemosphere* 2015, 138, 609-615.  
**=> Chapter 2.2.1 & 3.1.1**

U.E. Bollmann, Y. Ou, P. Mayer, S. Trapp, K. Bester. Polyacrylate-water partitioning of biocidal compounds: Enhancing the understanding of biocide partitioning between render and water. *Chemosphere* 2015, 119, 1021-1026.  
**=> Chapter 2.2.2.1 & 3.1.2.1**

M.M. Urbanczyk, U.E. Bollmann, K. Bester. Partition of biocides between water and inorganic phases of renders with organic binder. *Sci. Total Environ.* 2016, 573, 639-644.  
**=> Chapter 2.2.2.2 & 3.1.2.2**

M.M. Urbanczyk, K. Bester, U.E. Bollmann. Multi-layered approach to determine diffusion coefficients through polymer films: Estimating the biocide release from paints. *Building and Environment*, in press (DOI: 10.1016/j.buildenv.2018.11.011).  
**=> Chapter 2.2.3 & 3.1.3**

U.E. Bollmann, G. Minelgaite, M. Schlüsener, J. Vollertsen, T. Ternes, K. Bester. Photodegradation of octylisothiazolinone and semi-field emissions from facade coatings. *Sci. Rep.* 2017, 7, 41501.  
**=> Chapter 2.3.1, 2.3.2, 3.2.1 & 3.2.2**

U.E. Bollmann, G. Minelgaite, M. Schlüsener, J. Vollertsen, T. Ternes, K. Bester. Leaching of Terbutryn and Its Photodegradation Products from Artificial Walls under Natural Weather Conditions. *Environ. Sci. Technol.* 2016, 50, 4289-4295.  
**=> Chapter 2.3.1, 2.3.2, 3.2.1 & 3.2.2**

M.M. Urbanczyk, K. Bester, N. Borho, U. Schoknecht, U.E. Bollmann. Influence of pigments on phototransformation of biocides in paints. *J. Haz. Mat.* 2019, 364, 125–133.  
**=> Chapter 2.3.3 & 3.2.3**

# Sammenfatning

Det er almindelig praksis at der tilsættes biocider (dvs. algicider, fungicider, bactericider) til polymerbaseret puds og maling for at konservere dem mens de er på lager, samt beskytte dem efter at de er påført bygningerne. Tidligere studier har vist, at biociderne bliver vasket ud af materialerne når det regner på de behandlede overflader, hvorefter de ender i miljøet. Selvom kontakt med vand er essentiel for at udvaskning kan finde sted, er der også andre faktorer der påvirker udslippet af biocider, såsom transportmekanismer der styrer at biociderne når materialets overflade, samt nedbrydningsprocesser der gør, at noget af de aktive stoffer omsættes. Dette projekt har bidraget med viden om disse to faktorer.

## Transportmekanismer

Udvaskningsprocessen kan beskrives som en proces med flere trin: (1) fjernelse fra overfladen, som er (2) i ligevægt med de dybere lag af materialet, som (3) sørger for at overfladefilmen bliver konstant suppleret med biocider. I forhold til maling forgår transporten via diffusion igennem polymeren, mens der er forskellige muligheder når det drejer sig om komposit puds: diffusion igennem polymeren, mineralerne eller de vandfyldte porer, eller advektiv transport igennem de vandfyldte porer (fx transport drevet gennem fordampning af vandet i porerne). I dette projekt blev der udført forsøg med forskellige våde og tørre cykler, som gav indblik i transportprocessen fra de dybere lag til overfladen, såvel partitioneringsforsøg med enkelte stoffer (akrylat, mineraler), for at undersøge betydningen af de forskellige materialer på overgangen af biocidet fra materialet til vandfasen.

Resultaterne viste, at biocider i puds hovedsaglig transporteres gennem vandfyldte porer, mens tør diffusion ikke er relevant. Udvaskning af biocider var meget højere når pudset var udsat for intermitterende våd-tør faser end når det var kontinuerlig vådt. Det betyder, at tiden mellem de våde faser har en stor betydning for selve udvaskningen og det er her at overfladefilmen suppleres med biocider. I forsøgene hvor pudset var permanent fugtigt, var udvaskningen endnu højere end når pudset tørrede ud. Det tyder på at diffusionen gennem vandfyldte porer er vigtigere end advektiv transport med det fordampende vand.

Partitioneringsforsøgene viste, at polymerandelen i puds er den vigtigste faktor til fordeling af biociderne i vand-puds-systemet og selve fordelingskonstanten ( $\log D_{\text{render}}$ ) kunne forudsiges ud fra akrylat-vand fordelingskonstanten ( $\log K_{\text{AcW}}$ ). Nogle mineraler (fx talk, som bliver brugt søm fyldmateriale) adsorberer dog biocider til en vis grad, og kunne finde anvendelse i et nyt materiale design.

## Nedbrydningsprocesser

Nedbrydningsveje af biociderne terbutryn og *N*-octylisothiazolinone, blev undersøgt ved at nedbrydningsprodukter blev identificeret og efterfølgende analyseret i udvaskningsvand og miljøprøver. Massebalancen for terbutryn gik op, når der blev taget højde for fotonedbrydningsprodukterne. Der findes flere mulige årsager til, at der manglede en stor del i massen af *N*-octylisothiazolinone: flere ukendte nedbrydningsprodukter, mineralisering eller tab til atmosfæren. Alt i alt udgør fotonedbrydningsprodukter en stor del af den endelige massebalance af biocider i puds. Der er vigtig at tilføje, at en stor andel af produkterne – selvom de bliver formet på overfladen – forbliver i materialet og ikke bliver vasket ud med det samme. I regnvandsbassiner findes nedbrydningsprodukter i høje koncentrationer (op til 50 ng L<sup>-1</sup>). Det er derfor væsentligt at inkludere nedbrydningsprodukter i miljø-risikovurderinger.

Selve fotonedbrydningen foregår sandsynligvis via indirekte fotolyse. Derfor har materialeegenskaber, især pigmenter, antagelig en stor indflydelse på selve nedbrydningsprocessen, da de fx kunne agere som fotokatalysator. Forsøgene viste, at pigmenter forhindrer fotonedbrydning. Nedbrydningshastigheden er sammenlignelig ved de tre undersøgte pigmenter. Men da forskellige pigmenter viser forskellige nedbrydningsmønstre, er lys-pigment-biocid interaktionen evident og bør tages i betragtning ved fremtidig produktudvikling.

# Summary

It is state-of-the-art in material production, to equip polymeric resin-based paints and renders with biocides (i.e. algacides, fungicides, bactericides) to prevent the materials and the final coating films from biological deterioration. It is well-known that these biocides leach from the materials when they get in contact with rainwater and end up in the environment. However, although the water contact is crucial for the leaching, other factors need to be taken into consideration: the transport of the biocides to the coating surface as well as transformation reactions. This project contributed to a considerable knowledge gain in both fields.

## Transport processes

The leaching of biocides from render is a multi-step process: (1) removal from the surface layer, which is itself (2) in equilibrium with the deeper layers of the render, from which (3) the surface layer is constantly refilled. Considering paints, these transports must be diffusive through the polymer, while in the porous multiphase composite renders the transport can occur through any of the phases (polymer, minerals, or water filled pores. While transport through the polymer and the mineral phases would be diffusive, the transport through the water filled pores could be diffusive and advective especially (driven by the evaporative transport of the water). By conducting experiments with different wetting and drying cycles the processes leading to a refill of the surface layer were studied, while single component (acrylate-resin, minerals) partitioning experiments were used to determine the influence of the different fraction on the phase transfer.

The results showed that the transport of biocides in renders predominantly occurs through the water-filled pores, while the transport through the dry render was considerably less. As intermittent wetting generated considerably higher leaching rates than continuous wetting, it can be concluded that the equilibration time in between the leaching cycles has a major impact on the leaching as this would be the time to refill the surface layer. However, if the render was kept wet during the equilibration time the leaching was higher than in those cases when the render was left to dry. This indicates that the pore-water diffusion is more important than evaporative (advective) transport for the refill of the surface layer.

The single compound partitioning showed that the polymeric binder is in fact the most important part in the render-water partitioning. However, some minerals (e.g. talc, which is used as filler and lubricant during production) show low partitioning as well. The distribution constants to polyacrylate-based render ( $\log D_{\text{render}}$ ) can be predicted linearly from the polyacrylate-water partition constants ( $\log K_{AcW}$ ) as a first assessment.

## Transformation processes

The phototransformation pathways of two example compounds, terbutryn and *N*-octylisothiazolinone, were studied: transformation products were identified and analyzed in render leachates and environmental samples. As seen in the example of terbutryn, the mass balance can be closed if phototransformation products are included. However, as the mass balance of *N*-octylisothiazolinone cannot be closed, other factors must be considered: still unknown products, mineralization and loss to the atmosphere. Hence, it can be concluded that photochemical transformation products constitute a considerable mass fraction of the total balance of the biocides in render materials. As an important fact, it has to be mentioned that transformation products – though formed on the facade surface – are remaining in the depth of the material and are not leached immediately. In stormwater pond in- and effluent samples, transformation products were detected (up to 50 ng L<sup>-1</sup>) – often in as high as or even higher concentrations than the respective parent compound – showing the importance of transformation products being included in environmental risk assessments.

As the phototransformation is assumed to occur mainly via indirect photolysis, the material properties, especially pigments, were expected to have an influence on the phototransformation process, by, e.g., acting as photo-catalysts. In general, it could be shown that pigments shade/protect biocides from light irradiation. The influence of pigments on the degradation rates was rather low. However, as different pigments showed different degradation pattern, an interaction light-pigment-biocide was evident and should be considered in future material design.

# 1. Introduction and objectives

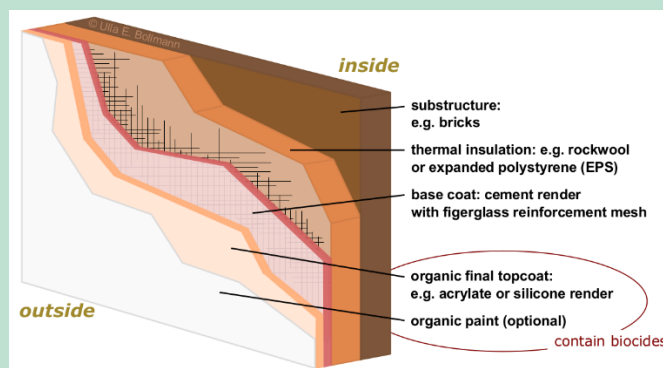
Modern polymeric resin based paints and renders are commonly equipped with biocides in order to prolong their shelf life and to protect the final coatings film. Nevertheless, several studies have shown, that these biocides leach out of the materials when they get in contact with rainwater and end up in storm- and wastewater systems and finally in the environment. Hence, the water contact is required. However, also other factors need to be taken into consideration: the transport of the biocides to the coating surface as well as transformation reactions.

## 1.1 Biocides: utility and emissions

Biocides are regulated in the European Union (EU) and defined in the European biocidal product regulation (BPR) [1] as substances designed *“to destroy, deter, render harmless, prevent action of, or otherwise exert a controlling effect on any harmful organism by chemical or biological means.”*

Due to rain, but more important, dew, building facades get wet and offer a good environment for microorganisms to grow. Especially polymeric based renders and paints are known to be very susceptible to algal and fungal growth, due to their specific physico-chemical properties [2].

Hence, in recent years more and more facade materials are equipped with biocides in order to prevent algal and fungal growth on the building facades. The increasing mounting of thermal insulation systems (Figure 1.1-1), which requires the usage of polymer based renders and paints, accounts for an increase in biocide containing materials.



**Figure 1.1-1** Principal construction of a biocide-containing external thermal insulation composite system (ETICS) - the top-paint-layer is optional; either the organic render or the paint or both layers may contain biocides.

Both renders and exterior paints can be equipped with film preserving compounds. It is known that triazines and phenylureas are used as algicides and carbamates as fungicides, while isothiazolinones are used as bactericides (in-can preservation) and fungicides (film preservation) for such purposes [3]. Besides the use as film preservatives, some of the biocides are only added to the products to increase shelf life of the formulated products until they are used (in-can preservatives) [4]. The concentration per single biocide is about  $0.1 - 2 \text{ g kg}^{-1}$  render, which corresponds to  $0.3 - 4 \text{ g m}^{-2}$  render-coated wall area [5]. In-can and film preservatives consist of mixtures of about one to eight different biocides, leading to a total content of biocides in render and exterior paints from 0.5 % to 1 % [5]. Besides the previous named biocides, triazoles are used for the preservation of wood, as they are very effective fungicides [6].

Few studies have focused specifically on the occurrence of biocides from building material in the aqueous environment. Hence, most of the available data is on used and previously pesticides such as terbutryn, diuron, tebuconazole, propiconazole or mecoprop [7-13]. Since dichloro-*N*-octylisothiazolinone and cybutryn are common antifouling boosters for ships, some studies on their occurrence in marine waters have been performed [14-19]. An overview of some concentration levels in the different water types for some biocides is given in Table 1.1-1. It is obvious that PNEC values are occasionally exceeded in stormwater and concentrations above the recommended annual average environmental quality standards can be detected in some types of water.

**Table 1.1-1** Selected biocide concentrations in direct facade runoff, stormwater, wastewater and surface waters [ng L<sup>-1</sup>] as well as soils next to houses [ng g<sup>-1</sup>] in comparison to annual-average environmental quality standards (AA-EQS) [ng L<sup>-1</sup>] and predicted no-effect concentration for surface waters (PNEC<sub>aquatic</sub>) [ng L<sup>-1</sup>].

Water type	Site	<i>N</i> -Octylisothiazolinone	Dichloro- <i>N</i> -octylisothiazolinone	Carbendazim	Terbutryn	Cybutryn	Diuron	Isoproturon	Mecoprop	Ref.
<b>AA-EQS</b>		-	-	-	64	2.5	300	200	-	[20]
<b>PNEC<sub>aquatic</sub></b>		7.1	34	34	34	2	20	-	-	[21, 22]
<b>Facade runoff</b>	CH	na	na	na	1-5*10 <sup>6</sup>	na	1-40*10 <sup>6</sup>	na	na	[23]
	DK	5.4/3.4*10 <sup>6</sup>	0.2/0.3*10 <sup>6</sup>	0.5/0.4*10 <sup>6</sup>	2.6/1.4*10 <sup>6</sup>	na	4.7/5.3*10 <sup>6</sup>	8.0/5.9*10 <sup>6</sup>	na	[24]
<b>Stormwater</b>	CH	na	na	50-1100	20-1800	na	<LOD	na	100-10000	[5]
	F	na*	na*	7-195	<1.2	na	25-795	3-53	na	[25]
	DK	<LOD-39	na	14-306	12-1840	<LOD-5	<LOD-101	<LOD-148	<LOD-25	[26]
<b>Wastewater</b>	ES	na	na	na	5-183	na	28-2526	1-90	na	[27]
	CH	na	na	60-80	16-24	4-6	30-50	10-50	420-600	[28]
	CN	2	6	110	na	na	na	na	na	[29]
	DK	<LOD	>LOD	14-78	5-55	<LOD-8	3-39	<LOD-43	<LOD-34	[30]
<b>Surface water</b>	D	<1	<1	18-94	5-169	1-11	9-32	7-113	10-126	[31]
	CH	<LOD	na	10-206	<20-50	<LOD	50-310	50-5500	50-1750	[32]
	ES	na	na	na	4-15	na	10-68	3-9	na	[27]
	DK	<LOD-38	<LOD-63	<LOD-10	<LOD-1	<LOD-3	<LOD-39	<LOD-7	<LOD-201	[24]
<b>Soil</b>	DK	<LOD-3.3	<LOD	<LOD-0.7	<LOD-7.6	-	<LOD-0.2	<LOD	-	[33]

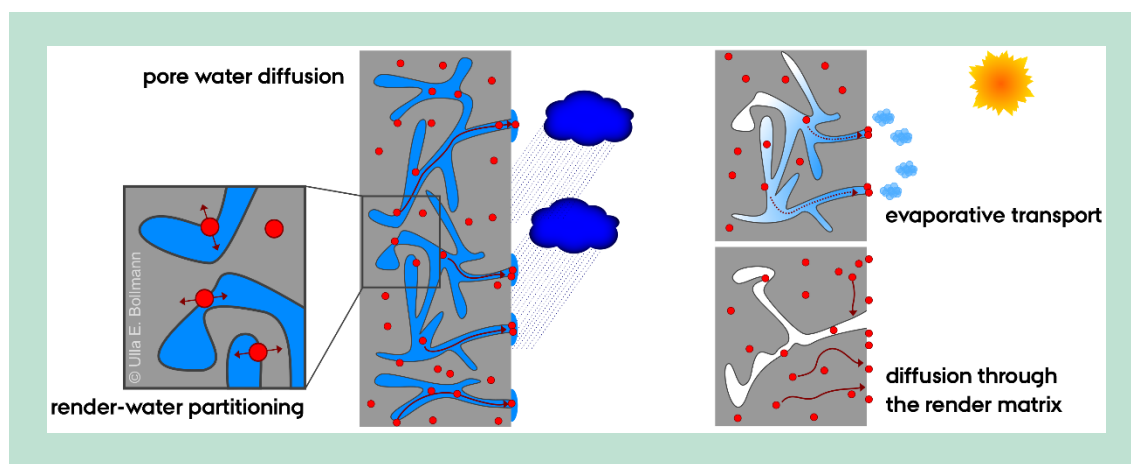
na: not analyzed, <: below limit of quantification, \* not stated which isothiazolinone analyzed

Often, facade runoff water is directly percolated into the ground or discharged to the environment via separated sewer systems, although biocide concentrations of several mg L<sup>-1</sup> have been detected in direct facade runoff water [23]. Biocides can be detected in soils surrounding houses with treated facades [33]. Due to dilution with unpolluted rainwater, concentrations in stormwater and small urban creeks, which mainly contain stormwater, usually drop down to a few hundred ng L<sup>-1</sup> [5, 32, 34]. Emission dynamic analysis during rain events in an entire stormwater catchment reveals that first-flush is not relevant for stormwater [26]. Concentrations in wastewater are usually in the lower ng L<sup>-1</sup> range. In- and effluent comparisons reveal that the removal of biocides is relatively low in the present wastewater treatment techniques [29, 31]. Comparisons between dry and wet weather demonstrates that not only wash-off from building materials during rainy periods but also household activities contribute to biocide occurrence in wastewater [30].

For a comprehensive study on the occurrence of biocides in Danish waters and emission dynamics in storm- and wastewaters the reader is referred to our previous report “*Water-driven leaching of biocides from paints and renders: Methods for the improvement of emission scenarios concerning biocides in buildings*” [24].

## 1.2 Leaching process

Both, laboratory test systems using constantly soaked material, dipping experiments or weather chambers [5, 35, 36], and semi field studies under natural weather conditions [23, 37] have proven that biocides leach from synthetic resin render in relatively high amounts. Several parameters having an influence on the leaching of biocides are discussed, including both material and compound properties. The water solubility and affinity of the organic substance to the matrix, the organic carbon content of the matrix [38], and the presence and leachability of other components (such as thickeners) in the matrix are mentioned [35, 36]. In addition, the surface structure or porosity of the matrix [35], temperature and light effects are pointed out [5]. First tests showed that the delivery of biocides is too fast to rely only on diffusion [39–41] and that active water transport such as that well-known in soils might be involved [42].



**Figure 1.2-1** Processes involved in the transport of biocides from the render to the coating surface.

In general, the leaching process of biocides from render is assumed to be a multistep process: (1) removal from the surface layer which is itself (2) in equilibrium with the deeper layers of the render, from which (3) a continuous refill of the surface layer occurs. Several processes might be crucial for the refilling of the surface layer (Figure 1.2-1): diffusion through the water filled pores as well as the render matrix [5, 35, 36, 41], transport with the evaporating water [35], and render-water partitioning [5]. Also the enrichment on the coating surface during drying cycles is discussed [5]. The transport through pore water as well as the partitioning requires water, hence, would occur during the respective rain event. The evaporative transport would occur after the rain finished leading to an accumulation of active ingredients on the coating surface during the dry period. Diffusion through the render matrix would take place both during and between rain events and would be needed in order to enable contact of biocides with water. To gain deeper understanding of the transport processes involved in the leaching process, the following research objectives were proposed:

**Objective 1** Test whether wet and dry cycles lead to different leaching.

**Hypothesis 1** The evaporating pore water will transport biocides actively to the surface of the material, thus wet/dry cycles will enhance biocide leaching.



**Objective 2** Test to which extent diffusion through the render (binder vs. filler) is decisive for the leaching.

**Hypothesis 2a** The diffusion of biocides through the render is occurring through the binder and the binder alone controls the diffusion of the biocides through the render.

**Hypothesis 2b** The polymeric binder and the binder alone controls the partitioning of the biocides between water and render.

### 1.3 Degradation and fate

Studies on the leaching of biocides under natural weather conditions over a longer period (1-5 years) show heavy leaching during the first months of exposure to natural weather [23, 24, 37], independent of the test setup used or the specific material tested. Concentrations in the first runoff samples ranging from about 1 to 100 mg L<sup>-1</sup> are detected. Afterwards, the emissions decrease drastically. During the first 30 L m<sup>-2</sup> runoff (corresponding to about 6-7 month) the cumulative emissions are roughly linear [23]. Afterwards the emissions nearly stagnate, although only maximum 13% of the initially applied content could be recovered in the runoff after 48 months [37].

Back extractions of the remaining fraction in the matrix do not cover the whole mass balance but leave gaps of up to 80% [23, 37]. Hence, other release or removal processes need to be taken into consideration [37]:

- Sublimation into the surrounding environment, which might be happening when the facade is heated up by sunshine.
- Migration into deeper layers in the coating or the substructure, which might affect the analysis if only the top coat is extracted.
- Formation of degradation and transformation products due to UV radiation, which might either be washed off as well or remain in the coating.
- Irreversible sorption to coating components; hence, biocides would neither be available for microorganisms nor accessible to analytical extraction.

Due to the lack of information on degradation products, Burkhardt et al. observed only the one known biodegradation product for terbutryn and cybutryn, M1 (N-tert-butyl-6-(methylsulfanyl)-1,3,5-triazine-2,4-diamine), as well as DCPMU (N-(3,4-dichlorophenyl)-N-methylurea), a degradation product of diuron, in the runoff water. While M1 was emitted with increasing amounts over time, DCPMU only accounted for up to 0.4% of the total mass balance for diuron [23]. In general, it seems that degradation is a crucial factor for the losses; hence, leading us to the following objective:

**Objective 3** Study for which compounds the solid-state photochemical degradation on the render materials is relevant and whether pigments are affecting the photodegradation.

**Hypothesis 3a** Photochemical transformation products constitute a considerable mass-fraction of the total balance of the biocides in render materials.

**Hypothesis 3b** The different pigments influence the photodegradation rates considerably as some might act as photo-catalysts, while others might just shade (protect) the biocides from light.

## 2. Materials and methods

### 2.1 Materials

#### 2.1.1 Biocides

This project covers a broad range of biocidal compounds used in renders and paints (Table 2.1-1); beyond these, algaecides, fungicides, and bactericides, used both as in-can and as film preservatives. Nevertheless, not all studies were performed for all biocides. The exact selection is noted in the respective method description.

**Table 2.1-1** Biocides covered within this project: Name, acronym, CAS-number, physical-chemical properties (Molecular weight ( $M_w$ ), molecular volume ( $M_v$ )<sup>1</sup>, octanol-water partition coefficient ( $\log K_{ow}$ )<sup>2</sup>, water solubility (WS)<sup>2</sup>, Henry's constant ( $k_H$ )<sup>2</sup>, vapor pressure ( $p_{vap}$ )<sup>2</sup>, and predicted-no-effect-concentration (PNEC)<sup>3</sup>, activity and product types registered under the biocidal product regulation coded product types (under review or \*approved)<sup>4</sup>. Additionally, usages in cosmetic products<sup>5</sup> and as pesticides<sup>6</sup> are listed.

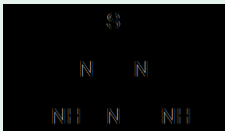
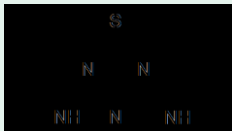
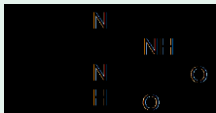

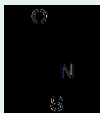



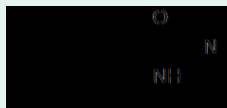
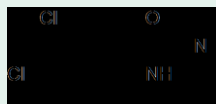
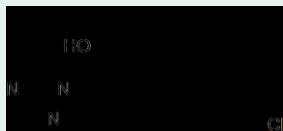
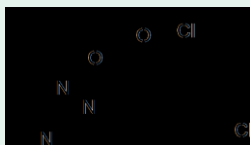

Group	Compound (Abbreviation) CAS-No.	Formula	Physical-chemical properties	Activity, Product types (BPR) Pesticide in DK
<b>Triazines</b>				
	<b>Terbutryn (TB) 886-50-0</b>		$M_w$ : 241.36 g mol <sup>-1</sup> $M_v$ : 230.62 Å <sup>3</sup> $\log K_{ow}$ : 3.77 WS: 42 mg L <sup>-1</sup> $k_H$ : 9.1*10 <sup>-9</sup> atm m <sup>3</sup> mole <sup>-1</sup> $p_{vap}$ : 2.4*10 <sup>-5</sup> mmHg PNEC <sub>aquatic</sub> : 34 ng L <sup>-1</sup>	Algaecide Biocide: PT 7, 9, 10 Pesticide: -
	<b>Cybutryn, Irgarol 1051 (IRG) 28159-98-0</b>		$M_w$ : 253.37 g mol <sup>-1</sup> $M_v$ : 236.84 Å <sup>3</sup> $\log K_{ow}$ : 4.07 WS: 20 mg L <sup>-1</sup> $k_H$ : 5.3*10 <sup>-9</sup> atm m <sup>3</sup> mole <sup>-1</sup> $p_{vap}$ : 3.7*10 <sup>-6</sup> mmHg PNEC <sub>aquatic</sub> : 2 ng L <sup>-1</sup>	Algaecide Biocide: not approved (PT 21 <sup>until 2016</sup> ) Pesticide: -
<b>Carbamates</b>				
	<b>Carbendazim (CD) 10605-21-7</b>		$M_w$ : 191.19 g mol <sup>-1</sup> $M_v$ : 165.80 Å <sup>3</sup> $\log K_{ow}$ : 1.55 WS: 3112 mg L <sup>-1</sup> $k_H$ : 1.5*10 <sup>-12</sup> atm m <sup>3</sup> mole <sup>-1</sup> $p_{vap}$ : 5.4*10 <sup>-9</sup> mmHg PNEC <sub>aquatic</sub> : 34 ng L <sup>-1</sup>	Fungicide Biocide: PT 7, 9, 10 Pesticide: c
	<b>Iodocarb (IPBC) 55406-53-6</b>		$M_w$ : 281.09 g mol <sup>-1</sup> $M_v$ : 182.91 Å <sup>3</sup> $\log K_{ow}$ : 2.45 WS: 436 mg L <sup>-1</sup> $k_H$ : 6.9*10 <sup>-9</sup> atm m <sup>3</sup> mole <sup>-1</sup> $p_{vap}$ : 4.6*10 <sup>-4</sup> mmHg PNEC <sub>aquatic</sub> : 500 ng L <sup>-1</sup>	Fungicide Biocide: PT 6*, 7, 8*, 9, 10, 13* Cosmetics Pesticide: a
<b>Isothiazolinones</b>				
	<b>Methylisothiazolinone (MI) 2682-20-4</b>		$M_w$ : 115.16 g mol <sup>-1</sup> $M_v$ : 95.67 Å <sup>3</sup> $\log K_{ow}$ : < 0 WS: 9.6*10 <sup>5</sup> mg L <sup>-1</sup> $k_H$ : 5.0*10 <sup>-8</sup> atm m <sup>3</sup> mole <sup>-1</sup> $p_{vap}$ : 0.031 mmHg PNEC <sub>aquatic</sub> : 3900 ng L <sup>-1</sup>	Bactericide/ Fungicide Biocide: PT 6, 11*, 12*, 13* Cosmetics Pesticide: -
	<b>Benzisothiazolinone (BIT) 2634-33-5</b>		$M_w$ : 151.19 g mol <sup>-1</sup> $M_v$ : 122.72 Å <sup>3</sup> $\log K_{ow}$ : 0.64 WS: 22204 mg L <sup>-1</sup> $k_H$ : 6.9*10 <sup>-9</sup> atm m <sup>3</sup> mole <sup>-1</sup> $p_{vap}$ : 2.6*10 <sup>-5</sup> mmHg	Bactericide/ Fungicide Biocide: PT 2, 6, 9, 10, 11, 12, 13 Pesticide: -

Table 2.1-1 continue.

Group	Compound (Abbreviation) CAS-No.	Formula	Physical-chemical properties		Activity, Product types (BPR) Pesticide in DK
	<b><i>N</i>-Octylisothiazolinone (OIT)</b> 26530-20-1		$M_W$ : 213.34 g mol <sup>-1</sup> $M_V$ : 219.47 Å <sup>3</sup> Log $K_{OW}$ : 2.61 WS: 309 mg L <sup>-1</sup>	$k_H$ : 3.6*10 <sup>-7</sup> atm m <sup>3</sup> mole <sup>-1</sup> $p_{vap}$ : 2.0*10 <sup>-4</sup> mmHg PNEC <sub>aquatic</sub> : 7.1 ng L <sup>-1</sup>	Bactericide/ Fungicide Biocide: PT 6, 7, 8*, 9, 10, 13 Pesticide: -
	<b>Dichloro-<i>N</i>-octylisothiazolinone (DCOIT)</b> 64359-81-5		$M_W$ : 282.22 g mol <sup>-1</sup> $M_V$ : 239.91 Å <sup>3</sup> Log $K_{OW}$ : 3.59 WS: 27 mg L <sup>-1</sup>	$k_H$ : 1.9*10 <sup>-7</sup> atm m <sup>3</sup> mole <sup>-1</sup> $p_{vap}$ : 2.3*10 <sup>-6</sup> mmHg PNEC <sub>aquatic</sub> : 34 ng L <sup>-1</sup>	Bactericide/ Fungicide Biocide: PT 7, 8*, 9, 10, 11, 21* Pesticide: -
Phenylureas					
	<b>Isoproturon (IP)</b> 34123-59-6		$M_W$ : 206.28 g mol <sup>-1</sup> $M_V$ : 211.28 Å <sup>3</sup> Log $K_{OW}$ : 2.84 WS: 92 mg L <sup>-1</sup>	$k_H$ : 1.9*10 <sup>-9</sup> atm m <sup>3</sup> mole <sup>-1</sup> $p_{vap}$ : 7.9*10 <sup>-6</sup> mmHg	Algaecide Biocide: PT 7, 10 Pesticide: -
	<b>Diuron (DR)</b> 330-54-1		$M_W$ : 233.09 g mol <sup>-1</sup> $M_V$ : 188.41 Å <sup>3</sup> Log $K_{OW}$ : 2.67 WS: 102 mg L <sup>-1</sup>	$k_H$ : 5.3*10 <sup>-10</sup> atm m <sup>3</sup> mole <sup>-1</sup> $p_{vap}$ : 4.7*10 <sup>-6</sup> mmHg PNEC <sub>aquatic</sub> : 20 ng L <sup>-1</sup>	Algaecide Biocide: PT 7, 10 Pesticide: c
Triazoles					
	<b>Tebuconazole (TBU)</b> 107534-96-3		$M_W$ : 307.82 g mol <sup>-1</sup> $M_V$ : 287.16 Å <sup>3</sup> Log $K_{OW}$ : 3.89 WS: 97 mg L <sup>-1</sup>	$k_H$ : 5.1*10 <sup>-10</sup> atm m <sup>3</sup> mole <sup>-1</sup> $p_{vap}$ : 4.6*10 <sup>-6</sup> mmHg PNEC <sub>aquatic</sub> : 1000 ng L <sup>-1</sup>	Fungicide Biocide: PT 7*, 8*, 10* Pesticide: a/b/c
	<b>Propiconazole (PPZ)</b> 60207-90-1		$M_W$ : 342.22 g mol <sup>-1</sup> $M_V$ : 283.81 Å <sup>3</sup> Log $K_{OW}$ : 4.13 WS: 11 mg L <sup>-1</sup>	$k_H$ : 14*10 <sup>-9</sup> atm m <sup>3</sup> mole <sup>-1</sup> $p_{vap}$ : 3.6*10 <sup>-6</sup> mmHg PNEC <sub>aquatic</sub> : 1600 ng L <sup>-1</sup>	Fungicide Biocide: PT 7*, 8*, 9* Pesticide: a
Phenoxy acids					
	<b>Mecoprop (MCP)</b> 93-65-2		$M_W$ : 214.65 g mol <sup>-1</sup> $M_V$ : 183.51 Å <sup>3</sup> Log $K_{OW}$ : 2.94 WS: 471 mg L <sup>-1</sup>	$k_H$ : 1.8*10 <sup>-8</sup> atm m <sup>3</sup> mole <sup>-1</sup> $p_{vap}$ : 4.6*10 <sup>-4</sup> mmHg	Algaecide Roof protection (not registered under BPR, since higher plants) Pesticide: b

1. Calculated with Molinspiration Cheminformatics<sup>®</sup>: <http://www.molinspiration.com/cgi-bin/properties>

2. Calculated with EPI Suite<sup>™</sup> v4.10 of the US EPA: <http://www.epa.gov/oppt/exposure/pubs/episuitd.htm>.

3. IRG, IPBC, MI, OIT, DCOIT, TBU, PPZ: respective assessment reports under BPR [22]; TB, CD, DR: Burkhardt et al., 2009 [21].

4. Compounds under review or \*approved [22]; Biocide product types [1]: 2 Disinfectants and algaecides not intended for direct application to humans or animals, 6 Preservatives for products during storage (In-can preservatives), 7 Film preservatives, 8 Wood preservatives, 9 Fiber, leather, rubber, and polymerised materials preservatives, 10 Construction material preservatives, 11 Preservatives for liquid-cooling and processing systems, 12 Slimicides, 13 Working or cutting fluid preservatives, 21 Antifouling products.

5. Cosmetic product directive [43]

6. Compounds marked (a) are used as pesticide in Danish agriculture (in 2016) [44], (b) are used as plant protection products in Danish private gardening (in 2016) [45], (c) found as pesticides on fruits and vegetables sold, but not produced in Denmark (in 2016) [46].

## 2.1.2 Minerals & Acrylate

### Polyacrylate dispersion

Plextol D498 obtained from Synthomer Deutschland (Marl, Germany) was used. This polymer is used in industry to produce organically modified renders and paints. Plextol D498 is characterised as thermoplastic methylmethacrylate and n-butyl-acrylate copolymer dispersion (50% w/w, density: 1.05 g mL<sup>-1</sup>) [47].

## Minerals

Minerals included in this project were barite, calcium carbonate, marble, kaolinite, and talc. Calcium carbonate was used as powder ( $\leq 30\ \mu\text{m}$  particle size, Sigma Aldrich) as well as marble chunks (VWR). Talc powder was acquired from Struers; kaolinite and barite from Sigma-Aldrich.

### 2.1.3 Render & Paints

#### Facade renders – commercial products

Within this project two commercially available facade renders with acrylate (KHK, Quick-Mix, Osnabrück, Germany) and silicone resin binder (HECK SHP KC1, BASF Wall Systems, Marktreidwitz, Germany) were applied. The content of organic binder was determined by measuring the losses during combustion at  $550^\circ\text{C}$ . This temperature releases carbon from organic matter but no carbon from calcium carbonate. The initial organic content was 10% in the dry acrylate render, while it was 15% in the silicone render. The dried acrylate render had a surface area of  $1.12\ \text{m}^2\ \text{g}^{-1}$  (determined as BET experiment following Brunauer–Emmett–Teller [48], a density of  $1.79\ \text{g}\ \text{mL}^{-1}$  and a calcium carbonate content of 66%. The dried silicone render had a BET surface of  $0.63\ \text{m}^2\ \text{g}^{-1}$ , a density of  $1.53\ \text{g}\ \text{mL}^{-1}$  and a calcium carbonate content of 25%. Electron microscopy reveal a composite structure of 10-100  $\mu\text{m}$  mineralic particles into which polymer particles are embedded. Polymer particle size seems to range 10-100  $\mu\text{m}$  for silicone, while they are around 1 mm for acrylate.

Both renders contained some of the studied biocides as purchased. Both renders contained amounts of BIT (approximately  $15\ \mu\text{g}\ \text{g}^{-1}$ ) and MI (approximately  $30\ \mu\text{g}\ \text{g}^{-1}$ ) while the acrylate render contained also OIT (approximately  $165\ \mu\text{g}\ \text{g}^{-1}$ ) and terbutryn (approximately  $263\ \mu\text{g}\ \text{g}^{-1}$ ) and the silicone render contained zinc pyriithione (not studied).

#### Paints – artificial, industry-like formulations

Four paints were prepared and provided by the Dr.-Robert-Murjahn-Institut (RMI, Ober-Ramstadt, Germany). The paints are industry-like formulations – however, with open ingredient list (Bilag 1.1). The only difference between the different paints were the pigments added to the formulation. The white pigment formulation was based on titanium dioxide stabilized with aluminum oxide, aluminum hydroxide and amorphous silica (Kronos 2160, KRONOS Worldwide, Inc., Dallas, Texas, United States). Red and black formulations were based on iron oxides: hematite ( $\alpha\text{-Fe}_2\text{O}_3$ , Bayferrox 130 M) and magnetite ( $\text{Fe}_3\text{O}_4$ , Bayferrox 318 M) (both LANXESS Deutschland GmbH, Cologne, Germany). In the pigment free formulation, the lack of pigment was compensated by adding more calcium carbonate in order to achieve the same total mass and the same mineral mass fraction.

Formulations with and without biocides were prepared. To the formulations with biocides different active substances (film preservatives), i.e. diuron (Algon P Paste), terbutryn (Algon PS Paste), carbendazim (Konservan ZSW) and octylisothiazolinone (Acticide OTW 8), (provided by Thor GmbH, Speyer, Germany), were added to give final concentrations of 500 mg/kg active ingredient in the paints. Equal concentrations of the active substances were applied to enable comparison based on physico-chemical properties of the substances. The paint formulations also contained in-can preservatives based on different isothiazolinones (i.e. MI, CMI, BIT).

## 2.2 Transport processes in the material

### 2.2.1 Influence of wet & dry cycles

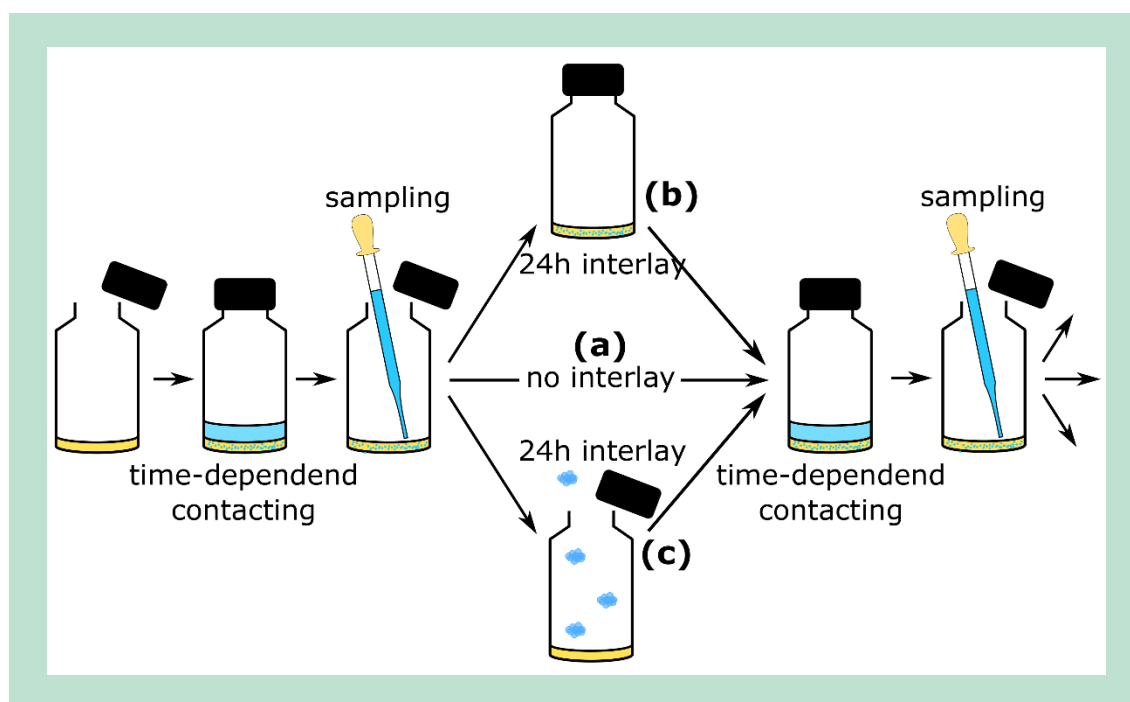
#### Preparation of render samples

Render samples with controlled amounts ( $10\ \mu\text{g}\ \text{g}^{-1}$ ) of all biocides included in this study (Table 2.1-1, except propiconazole and mecoprop) were prepared by spiking 10 g render with 1 mL biocide solution ( $100\ \mu\text{g}\ \text{mL}^{-1}$  of each biocide in a mix of methanol and acetonitrile). It is anticipated, that the resulting product is very similar to industry products after reaching the respective equilibria and evaporation of water and solvents, even though this is not following industry praxis in which formulated and not pure biocides would be used. The resulting con-

centrations were somewhat less than freshly formulated new product and represent renders at the middle of lifetime of real systems and not freshly applied ones. The resulting slurries were well mixed in a beaker. 2 g portions were placed into 30 mL glass vials each. These samples were air dried in the laboratory in 5 mm layers for two days. Thus, test render specimens with 5 cm<sup>2</sup> surface areas were obtained. The average weight of samples after airdrying was 1.75 g. In consequence, the concentrations of biocides in dried renders were 11.4 µg g<sup>-1</sup>.

### Leaching experiments

The render specimen were exposed to 1 mL water in the respective vials at room temperature (22°C). The duration of successive leaching steps were as follows: 3 s, 5 s, 10 s, 15 s, 30 s, 1 min, 10 min, 30 min and 60 min. To prevent concentration gradient formation in the water, the samples were shaken manually during the water contact (3 s – 1 min), while those performed for longer periods (i.e., 10 min, 30 min and 60 min) were conducted using of shaker. Afterwards, the water phase was collected and stored in the fridge until further analysis. Each render sample was weighted before and after each leaching steps which allowed assessing the amount of water taken up by the render. In the experiments three different kinds of cycles were considered (Figure 2.2-1).



**Figure 2.2-1** Setup for the (a) wet/wet, (b) wet/wet 24h, and (c) wet/dry experiments.

- (a) Wet/wet cycles (W/W). To mimic pure partitioning with suppressed evaporative or diffusive transports, leaching experiments were conducted as fast water contacting cycles in 2 min time intervals with the above mentioned contacting times of 3 s to 60 min. In these cycles, the renders always had water saturated pores, but no time for the diffusion through the pores.
- (b) Wet/wet 24h cycles (W/W 24h). To mimic diffusion through the water-filled pores (after partitioning in the pores), leaching experiments were performed with 24 h time intervals between the single leaching experiments with the above mentioned contacting times of 3 s to 60 min. In these experiments, the vials with render specimen stayed closed for 24 h after removing the supernatant water by means of a Pasteur pipette without allowing the pore water to evaporate. Hence, the materials were soaked with water, but had no water column above. (Diffusion through water filled pores possible; additionally, it might be possible that

biocides were desorbed from the polymers. However, partitioning has been demonstrated to be a relatively fast process, so in this respect, this experiment should be similar to experiment (a) as the same water volumes were used).

- (c) Wet/dry cycles (W/D). To mimic evaporative transport of water (and thus biocides) to the respective surfaces (after initial partitioning in the pores), leaching experiments were performed by drying the renders to dryness during 24 h time intervals between the water contacts. Thus, evaporative transports of biocides with the water to the surface of the material using the above mentioned contacting times of 3 s to 60 min was facilitated. Between the water contacts, the residual water on top of the surface was removed by means of a Pasteur pipette; the vials with render specimen stayed open for 24 h to allow pore water to evaporate from the render. The loss of water was controlled gravimetrically.

If the diffusion through the polymer would be the relevant mechanism, it was expected to determine the same transport during the wet/wet 24 h experiments as during the wet/dry experiments. After shaking the samples for the pre-defined contact time all of the supernatant water (but not the pore water, i.e. 1 mL) was removed. In some cases minor amounts of particles were detected in the solutions, thus the resulting extracts were centrifuged at 6000 rpm for 5 min for particle removal. Successively, exactly 700 µL of each supernatant was transferred to an autosampler vial and 50 µL internal standard solution was added for analysis. The experiments W/W were performed in duplicate, W/D and W/W 24 h in triplicate. The respective solutions were analyzed by duplicate injections each to the HPLC-MS/MS (see paragraph 0) and all values for the respective leaching experiment were averaged.

## 2.2.2 Mobility controlled by different fractions

Partition constants ( $K_d$ ) are typically calculated from the concentrations in the solid phase ( $c_s$ ) and the concentrations in the water phase ( $c_w$ ) at equilibrium using Eq. 4.2-1:

$$K_d = \frac{c_s}{c_w} \quad (\text{Eq. 4.2-1})$$

Nonetheless, render with organic binders are complex mixtures, which are described in standard EN 15824:2009. Typically, they consist of carbonates (30-60% weight percentage), organic binder (10-15%, such as acrylate or silicone), sand in different grain sizes and other additives. Schwarzenbach et al. [49] introduced the additivity concept in order to estimate sorption to soils, by assuming that (1) each sorption phase acts independently and comes to equilibrium with all other phases and (2) the total pollutant amount sorbed can be estimated as the sum of the pollutant amount in each phase. Transferring this concept to the render-water system, the render-water distribution constant ( $D_{render}$ , Eq. 4.2-2) can be described as the sum of the partitioning to the organic binder, minerals, sand particles and other render ingredients, where  $f$  describes the fraction of each of the different phases (i.e. binder, mineral, sand, water) and  $c$  the concentration of the biocide in each phase:

$$D_{render} = \frac{f_{organic\ binder} \cdot c_{organic\ binder} + f_{mineral} \cdot c_{mineral} + f_{sand} \cdot c_{sand} + \dots}{c_{water}} \quad (\text{Eq. 4.2-2})$$

In the following,  $D_{render}$  is used for the distribution of a biocide between the bulk render and water, while  $K_d$  describes the single phase partitioning.

### 2.2.2.1 Partitioning between polymeric binder and water

The experiments were performed for eleven compounds, of which ten are used as biocides in building materials (Table 2.1-1, all except MCP). The triazine atrazine was added for comparative reasons. Aqueous solutions were prepared from a stock solution (100 µg mL<sup>-1</sup> in acetonitrile) of the eleven compounds with Millipore-water at 10 ng mL<sup>-1</sup> (0.1% acetonitrile). Surrogate standards (1 µg mL<sup>-1</sup> in methanol) were used for mass spectrometric analysis: isoproturon-D6, terbutryn-D5, cybutryn-D9, tebuconazole-D6, and carbendazim-D4.

### Coating of glass fiber filters

The partitioning experiments in this study were performed using Plextol D498, a thermoplastic methylmethacrylate and n-butylacrylate copolymer dispersion obtained from Synthomer Deutschland (Marl, Germany). Since the total amount of polyacrylate per filter was aimed to be very low, Plextol D498 was diluted with Millipore-water to 20% w/w. Binder free glass fiber filters (Whatman GF/A, Ø = 25 mm, GE Healthcare, Little Chalfont, United Kingdom) were cleaned with methanol and Millipore-water before usage. After drying, the filters were coated with polyacrylate by adding a defined amount of diluted polymer dispersion onto the filter. Due to capillary forces the polymer dispersion was distributed over the entire filter surface and air dried at room temperature. Afterwards, the homogenous distribution was controlled by visual inspection and the added amount by weighing. Following this procedure, glass fiber filters were coated with 25, 50, and 80 mg polyacrylate.

### Kinetic study

In order to assure equilibrium sampling, a kinetic study was performed. Glass fiber filters coated with 80 mg polyacrylate were exposed to 20 mL aqueous biocide solution ( $10 \text{ ng mL}^{-1}$ ) while shaking at 200 rpm at room temperature. After different time points (1, 2, 6, 8, and 12 h) the partitioning was stopped and 90 µL of the aqueous phase were spiked with 10 µL surrogate standard and analyzed by HPLC-MS/MS (see paragraph 0). The experiments were performed in duplicate at room temperature.

### Polyacrylate coated glass fiber filter partitioning experiment

The polyacrylate–water partition constants were studied by analyzing the concentrations in water and polyacrylate phase at varying polyacrylate/water phase ratios. Glass fiber filters coated with 25 or 50 mg polyacrylate ( $m_{Ac}$ ) were exposed to 1, 2, 5, 10, 20, 50, or 100 mL aqueous biocide solution ( $10 \text{ ng mL}^{-1}$ ;  $V_W$ ). After shaking them 6 h at 200 rpm at room temperature the filters were removed from the biocide solution and back-extracted by 1 mL methanol. Both, 90 µL of the thus extracted aqueous biocide solution and 90 µL of the methanol extract were transferred to 150 µL HPLC-vials, spiked with 10 µL of surrogate standard, and analyzed by HPLC-MS/MS (see paragraph 0). All partitioning experiments were performed in triplicates at room temperature. The pH of the aqueous biocide solution was determined to be 5.5 (similar to rainwater) after the extraction. Mass balances ranging between 72% and 109% except for tebuconazole (58%) (for details see Bilag 4.1) were calculated in order to confirm total recovery of the added amount of biocides.

### Determination of partition constants from experimental data

Biocide concentrations in the water phase before ( $c_0$ ) and after equilibration ( $c_W(T_{eq})$ ) were determined for varying polyacrylate/water phase ratios ( $m_{Ac}/V_W$ ). The polyacrylate–water partition constant using polyacrylate coated glass fiber filters ( $\log K_{AcW}$ ) was obtained by non-linear regression of the relative concentration ( $c_{relative}$ ) as a function of the polyacrylate/water phase ratio ( $m_{Ac}/V_W$ ) according to Mayer et al. [50] (Eq. 4.2-3). By varying phase ratios, the influence of experimental artefacts can be minimized and precise partition constants can be obtained.

$$c_{relative} = \frac{c_W(T_{eq})}{c_0} = \frac{1}{1 + 10^{\log K_{AcW} \cdot (m_{Ac}/V_W)}} \quad (\text{Eq. 4.2-3})$$

Least square regressions were performed with GraphPad Prism v. 6.0. Due to low water phase concentrations after equilibration for the compounds with higher polyacrylate–water partition constants, regressions were based on 21 to 45 data points depending on the biocide.

#### 2.2.2.2 Partitioning between minerals and water

Compounds used in these experiments: carbendazim, diuron, iodocarb, isoproturon, cybutryn (irgarol 1051), octylisothiazolinone, terbutryn, and tebuconazole. Isoproturon-D6, terbutryn-D5, cybutryn-D9, tebuconazole-D6, and carbendazim-D4 were used as internal standards for quantitation with HPLC-MS/MS.

### Kinetic study

To ensure that partition experiments were performed under equilibrium conditions, a kinetic study was done. Ten glass vials with 200 mg of calcium carbonate were exposed to 7.5 mL biocides aqueous solution (0.1  $\mu\text{g mL}^{-1}$ , 1% MeOH) while shaking at 300 rpm. After different time points (1, 2, 6 and 8 h) the partition was stopped, two vials were taken and about 1.5 mL of the liquid phase with suspended  $\text{CaCO}_3$  was collected. The solid phase was separated by centrifugation in 2 mL autosampler vials. Successively, exactly 1 mL of the supernatant was transferred to a new 2 mL autosampler vial, spiked with 50  $\mu\text{L}$  internal standard solution for analysis and analyzed by HPLC-MS/MS (see paragraph 0). The experiments were performed at room temperature.

### Minerals-water partitioning of biocide

All minerals listed above were exposed to aqueous biocide solution in the ratio of 1:3 (i.e., 300 mg of material were exposed to 0.9 mL (equal to the 900 mg) aqueous biocide solutions). 10 different biocide concentrations varying between 0.1 and 1  $\mu\text{g mL}^{-1}$  were used. Minerals were exposed to aqueous biocide solution while shaking at 350 rpm for 12 hours in 2 mL glass autosampler vials. After the shaking period, the solid phase was separated by centrifugation. Successively, exactly 0.1 mL of the supernatant was transferred to a 2 mL glass autosampler vial with insert, spiked with 10  $\mu\text{L}$  internal standard solution and successively analyzed by HPLC-MS/MS. The pH of the aqueous phase after experiment was determined to be 5.5 (comparable to rainwater). By analyzing the biocide concentration in water and relating it to the total amount of the respective biocide in the system, the distribution between liquid and solid phase was determined. All partition experiments were performed in duplicate.

In order to ensure that the biocides losses due to e.g., adsorption on the glass or degradation during partitioning experiments are negligible, a back-extraction experiment was performed. Four 40 mL glass vials with 1 g of talc each were exposed to 3 mL of biocides aqueous solution (0.5  $\mu\text{g mL}^{-1}$ , 1% MeOH) while shaking at 300 rpm for 16 h. After shaking, exactly 0.5 mL of supernatant was collected in order to measure the biocide content in the water phase. The remaining material was dried, and then 10 mL of methanol was added to each vial in order to back-extract the biocides. The vials were shaken for 16 hours. After shaking, again precisely 0.5 mL of methanol supernatant was collected and the remaining talc was dried. The dried talc was contacted once again with 5 mL methanol for 16 h. After this time, 0.5 mL of the supernatant was collected. All collected samples were spiked with 50  $\mu\text{L}$  of internal standard solution and analyzed by HPLC-MS/MS (see paragraph 0).

#### 2.2.2.3 Distribution constants for a model render

In order to test the calculations for determining the distribution constants of the whole render system using parameters from single ingredients, an experiment with two artificial render formulations with known composition was performed. Both formulations consisted of the minerals and polyacrylate used in paragraph 2.2.2.1 and 2.2.2.2. The two renders were composed of the same ingredients in the same proportions: marble 32%,  $\text{CaCO}_3$  29%, acrylate 13%, water 20%. While one render contained 6% kaolinite, the other one contained 6% talc.

These artificial renders were prepared by mixing all the ingredients and successively drying them in a 3 mm layer. After that the materials were crushed, grinded and weighted. Finally, representative 1 g samples were exposed to 3 mL (i.e., 3000 mg) aqueous biocide solutions with four different concentrations varying between 0.25 and 1  $\mu\text{g mL}^{-1}$ . The exposures were conducted by shaking at 350 rpm for 17 hours in 20 mL glass vials. Successively, the solid phase was separated from the liquid one by centrifugation. Exactly 0.5 mL of the supernatant was transferred to a 2 mL glass autosampler vial, spiked with 50  $\mu\text{L}$  internal standard solution and successively analyzed by HPLC-MS/MS (see paragraph 0). By analyzing the biocide concentration in water and relating it to the total amount of the respective biocide in the system, the distribution between liquid and solid phase was determined. All partition experiments were performed in triplicates.



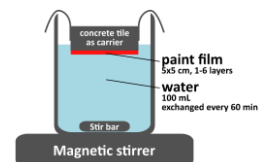
## 2.2.3 Diffusion controlled mobility

### Experimental procedure

Eight compounds with biocidal properties were used in the diffusion study: cybutryn (irgarol 1051), iodocarb, diuron, dichloro-*N*-octylisothiazolinone, *N*-octylisothiazolinone, tebuconazole, propiconazole, terbutryn. Seven internal standards were used: iodocarb-D6, diuron-D6, irgarol-D9, tebuconazole-D6, terbutryn-D6, *N*-octylisothiazolinone-D17, and propiconazole-D5. The experiment was performed using the black industry-like formulation from RMI (see paragraph 2.1.3). The paint was spiked with a biocide mixture (biocides dissolved in methanol) to give the final concentration of 0.07 mg/kg of each biocidal active ingredient in the paint.

Paint samples were prepared by applying paint with a roller paintbrush onto concrete tiles (Cement It Grey Mosaik, Class Tile, Maranello, Italy, 5 cm x 5 cm) serving as carriers. Samples of different thicknesses were prepared by applying different number of paint layers, starting with one layer and finishing with six. Additionally, samples of biocide-free paint were prepared to use as control. All samples were weighted: empty carriers, carriers with wet paint and after drying. Thickness of layers was measured after drying.

In order to measure the migration kinetics for selected biocides, the tiles painted on one side with biocide containing paint were suspended in 100 mL constantly stirred, deionised water. To provide perfect sink conditions for diffusing compounds, the water was replaced every hour for the total contact time of 30 h. Exactly 1 mL aliquots of the water were collected at each sampling point and spiked with 50 µL of internal standard solution. The obtained samples were analyzed without a prior concentration step by HPLC-MS/MS (see paragraph 0). All experiments were conducted in triplicates.



Experimental setup

### Calculation of diffusion coefficients

The release of biocides from a paint film matrix can be predicted by solving the equations for diffusion from a slab [51, 52]:

$$\frac{\partial C}{\partial t} = D \frac{\partial^2 C}{\partial x^2} \quad (\text{Eq. 4.2-4})$$

Where  $c$  is the concentration of a given biocide in the solid phase,  $D$  is the diffusion coefficient,  $t$  the time and  $x$  the distance that the compound needs to diffuse. The paint film is contacted with water only on one side, hence the sheet occupies the space  $0 < x < l$ , where  $l$  is the thickness of the paint. The solution of the diffusion equation in this case can be obtained by using the method of separation variables. The initial and boundary conditions are:

$$\begin{array}{llll} C=C_0 & 0 < x < l & t=0 & \text{paint film} \\ C=C_{ext} & x=l & t>0 & \text{surface} \end{array}$$

where  $C_{ext}$  is the biocide concentration in the receiving compartment.

The profiles of concentration  $C_{ext}$  at any time is described by the relation [52, 53]:

$$\frac{C-C_{ext}}{C_0-C_{ext}} = \frac{4}{\pi} \sum_{n=0}^{\infty} \frac{1}{2n+1} \sin\left(\frac{(2n+1)\pi x}{l}\right) \exp\left(-\frac{(2n+1)^2 \pi^2}{l^2} D t\right) \quad (\text{Eq. 4.2-5})$$

The amount of biocide transferred through the surfaces of the sheet is calculated by integrating the flux of substance ( $M_t$ ) through the surface with respect to time:

$$M_t = A l C_0 - \int_0^l C(x, t) A dx \quad (\text{Eq. 4.2-6})$$

where  $A$  is the area of paint film exposed to water, and the total amount of biocides initially within the matrix is  $M_0 = C_0 A l$ .

The total amount of biocide which has left the plane paint film of thickness  $l$  at time  $t$ ,  $M_t$ , could expressed after integration, as a fraction of the quantity initially present in the material  $M_0$  [53, 54]:

$$\frac{M_t}{M_0} = 1 - \frac{8}{\pi^2} \sum_{n=0}^{\infty} \frac{1}{(2n+1)^2} \exp\left(-\frac{D(2n+1)^2 \pi^2 t}{l^2}\right) \quad (\text{Eq. 4.2-7})$$

For the early stages of release the expression can be closely approximated by [52]:

$$\frac{M_t}{M_0} = 4 \left(\frac{Dt}{\pi l^2}\right)^{1/2} \quad \text{for } 0 \leq \frac{M_t}{M_0} \leq 0.6 \quad (\text{Eq. 4.2-8})$$

if Eq 4.2-8 is resolved to  $D$ :

$$D = \frac{s^2 l^2 \pi}{16} \quad (\text{Eq. 4.2-9})$$

where  $s$  is the slope of linear regression of  $\frac{M_t}{M_0}$  plotted against the square root of time. The approximation is valid at the beginning of the process when the transfer of matter is very high and the receiving volume is much higher in compare to the film volume [53].

#### 2.2.4 Depth resolved profiling

In this work package, the transport mechanisms that drives the delivery of biocides from the deeper layers of a render to its surface were studied. Contrary to paint, composite render is rather porous. Hence, inside a render, diffusion can proceed both through water in its pores or through its acrylate polymers. Diffusion was hence studied in dry render as well as wet render. Tiles of render were prepared from a façade acrylate render (KHK, Quick-Mix, Osnabrück, Germany) applied with a filling knife on 55 x 110 mm Plexiglas carriers. The render consists of a mix of acrylate binder, hydrated cement/lime, and sand of 2 mm grain size. The render was applied to a thickness of approx. 5 mm. Before application the wet render was spiked with biocides. A mixture of isoproturon, *N*-octylisothiazolinone, diuron, cybutryn, dichloro-*N*-octylisothiazolinone, and tebuconazole was prepared in acetonitrile and mixed with the render to concentrations of 100 µg g<sup>-1</sup> wet render. Terbutryn and *N*-octylisothiazolinone were already present in the render and measured in concentrations of 227 and 122 µg g<sup>-1</sup>, respectively. The render tiles were submitted to mobility tests as described in the following sections and then profiled by removing thin layers of render and collecting the material. For this purpose, a grinding machine was constructed that allowed depth-profiling the render tiles. It consisted of a grinder with a diamond grinding head and a sledge holding the render tiles (Figure 2.2-2). The rotation speed of the grinding head was slow and the render tiles continuously cooled with demineralized water to ensure that the render did not heat up and denaturize the biocides. The grinder was slowly and repeatedly moved over the render tile whereby some tenth of micrometers was removed per step. As the surface of a render tile was uneven, the first layer consisted of material grinded until the tile became flat. Then 320 µm was grinded off in many small steps. The whole slurry of fine render particles and all the water used to cool, transport and clean the particles of the machine was collected and stored in 100 ml glass bottle, ensuring that no biocide was lost. Then the next 320 µm were grinded, until a depth of 1-2 mm from the plastic carrier was reached. The remaining render could not be grinded due to issues with the structural strength of the remaining render on the Plexiglas tile. The grinding resulted in a total of typically 10 grinding material slurries per sample, representing a depth profiling with a resolution of approx. 1/3 mm.

#### Chemical analysis

The slurries of render powder in demineralized water were left for several days for sedimentation, upon which the supernatant was decanted and analyzed for biocides. The wet powder remaining in a bottle was freeze-dried and 1 g of the dried powder subjected to solvent extraction. Biocides extraction from render powder was performed by solvent extraction in acetonitrile using a Multiwave 3000 microwave oven (Anton Paar GmbH, Austria), following the recommendations of the EPA method 3546. An internal standard was added to the samples prior to extraction, and the recoveries ranged between 77% and 106%.

Biocide concentrations were determined in the water samples and the solvents of the render extraction. The analysis was performed by HPLC-MS using electrospray ionization in positive mode (ESI(+)) on a Dionex Ultimate 3000 HPLC-system coupled to a Thermo Scientific MSQ Plus single quadrupole Mass Spectrometer (Dionex, Sunnyvale, CA, USA). The separation was performed at 30°C using a Synergy polar-RP column (L = 150 mm, ID = 2 mm, particles = 4 µm, Phenomenex, Torrance, CA, USA). Both water and acetonitrile eluents were acidified at 0.1% v/v formic acid. The multi-step HPLC-gradient consisted of water (A) and acetonitrile (B): 0-1 min 30% B, 1-10 min 30-90% B, 10-14 min 90% B, 14-19 min, 30% B. All samples were diluted 10 times in acetonitrile and an internal standard was added before analysis.

Total solids (TS) and volatile solids (VS) were determined following Standard Methods (APHA, AWWA, WEF, 2017).



A render tile on a 55 x 110 mm Plexiglas carrier



**Figure 2.2-2** Grinding machine. Upper left picture: The diamond grinding head. Upper right picture: the sledge holding the render tile. Lower picture: The grinding machine on a lab table.

### Experimental procedures

For quantification of biocide mobility in dry render, tiles spiked with biocides were put in contact with tiles without biocide spiking. Each tile was first grinded to create a smooth surface. The two tiles – the one with and the one without spiked biocides – were then placed on top of each other with the smooth surfaces in close contact and pressed tightly together. The tiles were left for 4 months. The upper few mm of one set of tiles were grinded and analyzed for biocides as described above.

For quantification of biocide mobility in wet render, two setups were constructed, one which held render tiles continuously wet (Figure 2.2-4) and one which allowed tiles to undergo wet-dry cycles. The continuously wet setup held 12 tiles and was constantly fed with demineralized water, ensuring that the water always held negligible biocide concentrations and hence did not hinder free diffusion from the tiles. The setup was operated for half a year and a tile was removed from the reactor every 2 weeks and dried. Of these 7 were grinded and analyzed.



**Figure 2.2-3** Setup for creating continuously wet leaching conditions.

The wet-dry setup held 36 tiles where sets of 12 tiles were located at the same level in the setup. Every 3 days, demineralized water was fed to the reactor submerging the 12 tiles at the lowest position. The tiles stayed submerged for 12 hours after which the water was drained off. Every 6 days also the next set of 12 tiles were submerged, and every 9 days also the last set of tiles were submerged. The first set of tiles hence was wet for 12 hours every 72 hours, the second set was wet for 12 hours every 144 hours, while the last set was wet for 12 hours every 216 hours. The principle is illustrated in Figure 2.2-4. Each month a tile was removed, dried, and stored. Of the 12 tiles per level, the 6 were grinded and analyzed.

Day	0	1	2	3	4	5	6	7	8	9	10	11	12	13	14	15	16	17	18
L1																			
L2																			
L3																			

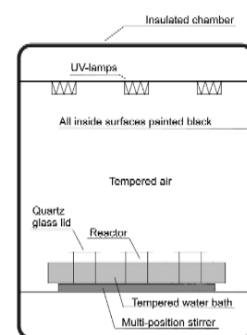
**Figure 2.2-4** Wet-dry cycles for intermittently wet render tiles.

## 2.3 Photodegradation of biocides

### 2.3.1 Identification of photodegradation products

100 mL of an aqueous terbutryn and *N*-octylisothiazolinone solution ( $10 \mu\text{g mL}^{-1}$ , tap water with 1% methanol) were irradiated with monochromatic UV-light (three 254 nm-lamps of 5 W) for 48 h. The setup was located in a temperature controlled chamber and the samples were cooled during irradiation as described previously by Minelgaite et al. [55]. Samples were taken at different time points (0 h, 5 h, 10 h, 20 h, 25 h, 30 h and 48 h). Afterwards the samples were stored at  $4^\circ\text{C}$  until analysis.

- **Non-target screening.** The identification of degradation products was performed on an HPLC (1200 Series, Agilent Technologies, Waldbronn, Germany) coupled to a QToF-MS (TripleTOF 5600, AB Sciex, Framingham, MA, USA) according to Schlüsener et al. [56]. The separation was performed on an Agilent Zorbax Eclipse Plus C18 Narrow Bore RR ( $2.1 \times 150 \text{ mm}$ ;  $3.5 \mu\text{m}$ ) using a water-acetonitrile (both with 0.1% formic acid) multistep gradient. The QToF-MS was operated in full scan mode ( $100\text{--}1200 \text{ m/z}$ ), with automatic product ion scans ( $30\text{--}1200 \text{ m/z}$ ) on all peaks exceeding 100 cps. Both positive and negative mode acquisitions were performed. Afterwards purchased / synthesized standards for



**Experimental setup**  
Adapted from Minelgaite et al. [57]



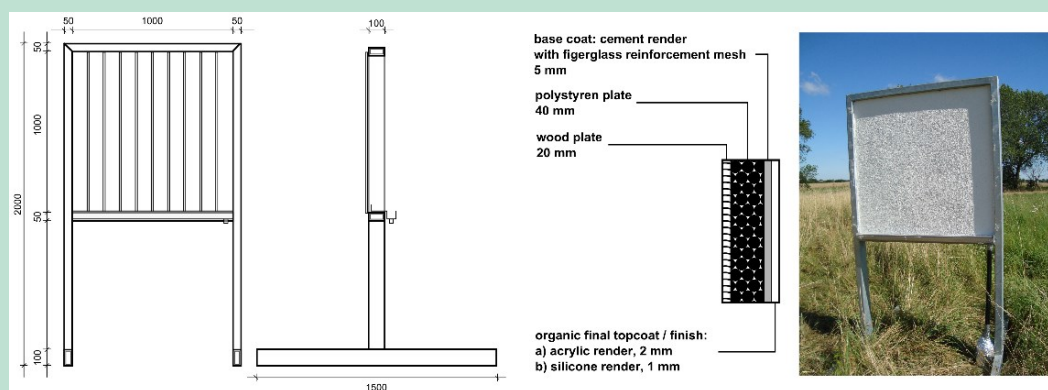
the suggested compounds were validated and quantified by triple quadrupole mass spectrometry (see paragraph 2.4.3) using retention time and product ion scans.

- **Suspect screening.** Additionally to the transformation products found in the non-target approach, suspects were hypothesized from the literature on DCOIT and MI/CMI: octylmalonic acid, octyloxamic acid, and 2-octylcarbamoyl-1-ethene sulfonic acid. Some panel samples were screened for those suspects. The suspected suspects were purchased / synthesized if possible and their presence in the samples was verified by comparison of retention time and mass spectrometric data for samples and true standard.

## 2.3.2 Biocide transformation on facade surfaces

### Construction of panels

Six panels were constructed according to usual industrial construction practice. A 1 m x 1 m polystyrene plate was attached on a wooden plate in a metal frame 1 m above the ground. A cement based, biocide free render with fiberglass reinforcement mesh was applied which was then coated with white acrylate (N = 3) and silicone (N = 3) finishing render, respectively. For the finishing render, two commercial products were used after modifications (acrylate resin render: KHK, Quick-Mix, Osnabrück, Germany; silicone resin render: HECK SHP KC1, BASF Wall Systems, Marktredwitz, Germany). The application thicknesses were 2 mm (acrylate) and 1 mm (silicone), respectively; hence, final amounts applied were 3 kg m<sup>-2</sup> (acrylate) and 2 kg m<sup>-2</sup> (silicone). Prior to the application of the finishing render, terbutryn and *N*-octylisothiazolinone were added as an industrial suspension and stirred well. Final concentrations in the renders were 1.7 and 4.6 g kg<sup>-1</sup> (acrylate) and 1.2 and 3.3 g kg<sup>-1</sup> (silicone render) for terbutryn and *N*-octylisothiazolinone, respectively. Due to the experimental setup the materials contained similar amounts of other isothiazolinones (MI, BIT, DCOIT) as well. The leaching of MI, BIT and DCOIT were subject of a previous report [24], while we focus in this report on the photodegradation of terbutryn and OIT.



**Figure 2.3-1** Experimental setup.

### Sampling and analysis

Panels were setup in Roskilde, Denmark (55.696°N, 12.103°E) and exposed to natural weather between August 2012 and March 2014, facing south-west. A metal rain gutter in the bottom of the panel was connected to a 2 L-glass bottle, which was exchanged after every rain event. The total run-off of about 80 L, equal to 70 rain events, was collected and analyzed. While the first 30 events were analyzed separately, events 31 to 70 were analyzed as composite samples of about 5 L run-off each.

For the analysis of terbutryn and *N*-octylisothiazolinone the first samples were diluted with methanol (event 1-14 1:100, event 15-54 1:10), while the samples from event 55-70 were analyzed directly. For transformation products, all samples were analyzed directly. To 1 mL of

(diluted) sample 50  $\mu\text{L}$  surrogate standard (terbutryn-D5 & *N*-octylisothiazolinone-D17, 1  $\mu\text{g mL}^{-1}$  in methanol) was added and analyzed by HPLC-MS/MS (see paragraph 0 & 2.4.3).

After 19 months of exposure, one acrylate and one silicone render panel were sampled and the remaining fraction of biocides analyzed. 10 samples (finishing together with reinforcement render,  $\sim 60\text{ cm}^2$  each) were taken, representing an even distribution across the panel, and individually crushed in a mortar. Subsamples (1 g) of each sample were extracted and analyzed according to paragraph 2.4.1.

#### Weather during the sampling period

A weather station 900 m linear distance away provided rain, humidity, temperature, radiation, pressure, wind speed and direction data at 2 m height, corresponding to the elevation of the panels above ground [19]. In total 1044 mm rain was recorded within the sampling period, of which 277 mm fell within the first 30 events. Average wind direction and speed during the first 30 rain events was SSW ( $202.5^\circ$ ) and  $6\text{ m s}^{-1}$  (full weather data Bilag 10.1).

Two heavy storm events occurred: St Jude storm/ storm Christian on October 28th, 2013 and storm Xaver on December 6th, 2013 with wind speeds  $> 100\text{ km h}^{-1}$ . During the first storm, three panels toppled over (one acrylate, two silicone panels). However, the sampling bottles stayed, so that samples could be analyzed, while all bottles were destroyed during the second storm.

### 2.3.3 Influence of pigments on photodegradation

#### UV transformation experiment

Samples for phototransformation studies were prepared by painting clean  $5\text{ cm} \times 5\text{ cm}$  glass plates. Two layers of paint equaling  $0.730\text{ g} \pm 0.06\text{ g}$  (in wet state), resulting in about  $0.54\text{ g}$  of dry weight were applied to each sample area of  $16\text{ cm}^2$ . The samples were stored in dark at  $20 \pm 2^\circ\text{C}$  for about 2 weeks prior to UV exposure. The photolysis experiment was conducted by exposing paint samples to UVA radiation in a commercial UVTest® Fluorescent / UV Instrument (Atlas Material Testing Technology, Illinois, USA) equipped with Atlas UVA-340 sun-lamps utilizing a continuous spectrum (see UV Bilag 11.1). The irradiation energy used was  $1.2\text{ W m}^{-2}$  at 340 nm resulting in about  $66\text{ W m}^{-2}$  for the whole spectrum of applied UVA radiation. The temperature within the set-up was  $40^\circ\text{C}$ .

Painted glass samples were exposed to UV radiation in triplicates, and withdrawn from the reactor at designated time intervals, ranging from 0 to 1056 h of total irradiation time. The selected radiation energy and time periods in these experiments were meant to be strong and long enough to show transformation reactions, but not necessarily to reflect the radiation energy that painted surfaces are exposed to under use conditions. 'Dark control' samples were exposed to the same conditions as other samples (temperature, humidity) under the exclusion of light by reversing the sample holders. After irradiation, paint samples were removed from the glass carriers and extracted with methanol ( $0.5\text{ g}$  of paint -  $5\text{ mL}$  of methanol) by sonicating for 1 h (SonorexSuper 10P, Bandelin, Berlin, Germany). The extraction was repeated 3 times for each sample, with supernatant collection in between. For the analysis of parent compounds, the samples were diluted 100 times with methanol. For quantitation of the transformation products, all samples were analyzed directly. To  $1\text{ mL}$  of (diluted) sample,  $50\text{ }\mu\text{L}$  of surrogate standard [carbendazim-D<sub>4</sub>, diuron-D<sub>6</sub>, octylisothiazolinone-D<sub>17</sub> and terbutryn-D<sub>5</sub>,  $1\text{ }\mu\text{g mL}^{-1}$  in methanol] was added. The parent compounds were analyzed according to paragraph 0 with a minor modification: the chromatographic method was shortened to 11 min, by removing other biocides from the method not used in this study. Transformation products were analyzed according paragraph 2.4.3.

Recovery rates were calculated by spiking a biocide free paint formulation with a known amount of biocides and performing the extraction process described above. Relative recovery rates ranged between 108 and 137% (Bilag 11.2).



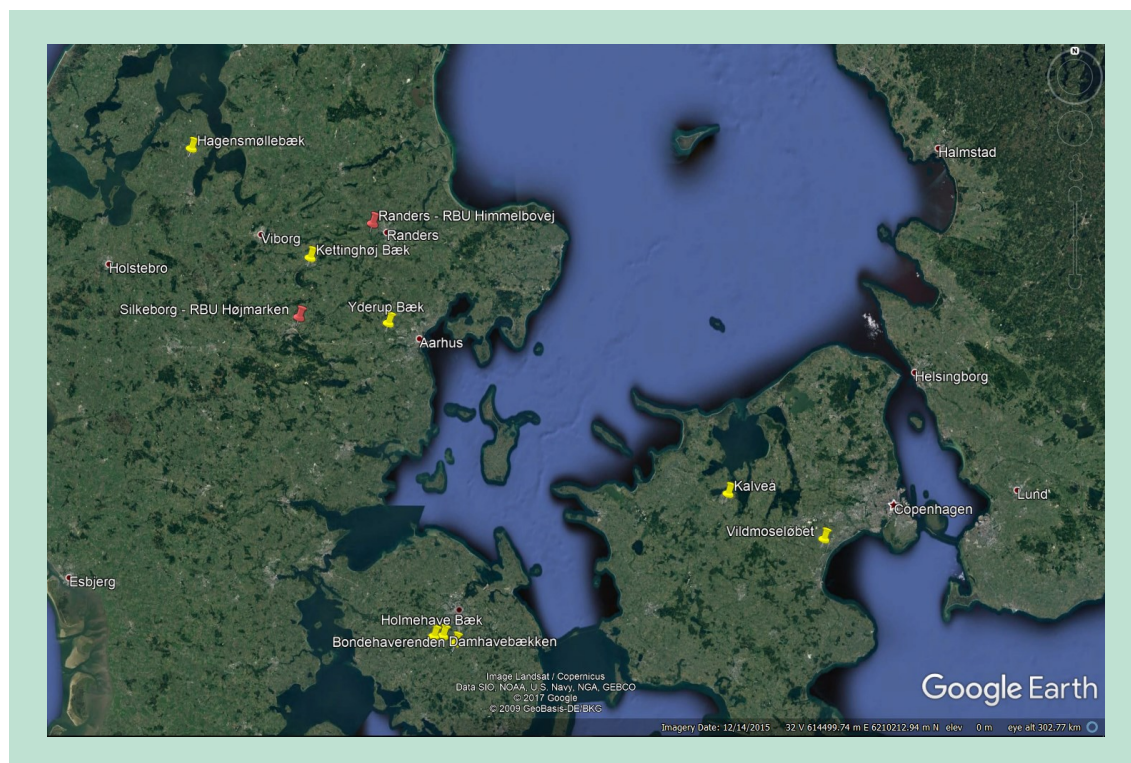
**Paint samples**  
Black (1), pigment-free (3),  
red (3), and white (1) paint

### Total solar reflection and FT-IR spectra

Total solar reflection of the paint films was measured in order to compare interactions of the differently pigmented paints with the applied UV radiation (for details see Bilag 11.3). Additionally, FT-IR spectra were recorded to determine eventual changes of the binder polymers due to the UV irradiation (details Bilag 11.4).

### 2.3.4 Monitoring of photodegradation products

In autumn 2017, 14 samples were collected in 2 L glass bottles and stored in darkness at 4°C until extraction. Sampling locations were distributed over Denmark (Figure 2.3-2). In total, eight surface waters as well as two rainwater basins (in- and outlet sampled) were sampled. While the surface waters were sampled with a single grab sample, the stormwater ponds were sampled over several days as flow proportional composite samples.



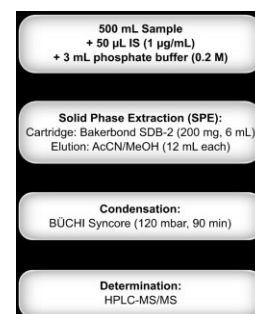
**Figure 2.3-2** Sampling locations for monitoring of transformation products in natural samples (yellow: surface waters, red: stormwater ponds).

## 2.4 Extraction and analysis

### 2.4.1 Sample extraction for biocides and transformation products

#### Solid phase extraction (SPE) from water samples

In a volumetric flask 500 mL sample was spiked with 50  $\mu\text{L}$  of internal standard ( $1\mu\text{g mL}^{-1}$  in methanol). In addition 3 mL of a 0.2M phosphate buffer was added to adjust to pH = 7. A Bakerbond SDB-2 (6 mL, 200 mg) SPE-cartridge was conditioned with 12 mL acetonitrile and successively, 12 mL water. After adding the sample ( $\sim 2\text{ mL min}^{-1}$ ) the cartridge was washed with 12 mL water and centrifuged to remove water residues (10 min, 3000 rpm). The cartridge was eluted with 12 mL acetonitrile and afterwards 12 mL methanol. The combined eluates were condensed to 1 mL by BÜCHI Syncore® (50°C, 280 rpm, 100 mbar,  $\sim 90\text{ min}$ ). The extracts were transferred to 1.5 mL vials using Pasteur pipettes and analyzed by HPLC-MS/MS (see paragraph 0 & 2.4.3). Relative extraction recoveries ranged between 86-113% for the individual compounds (see Bilag 2.1).



Extraction procedure

Octylamine was not recovered at all in the original extraction procedure. Hence, the extraction needed to be performed differently. In a volumetric flask 500 mL sample was spiked with 50 µL of internal standard ( $1\text{ }\mu\text{g mL}^{-1}$  in methanol). In addition 2.5 mL of a 0.2M phosphate buffer was added to adjust to pH = 7. A Strata-X-CW (Phenomenex, 200 mg, 6 mL) SPE-cartridge was conditioned with successively 15 mL methanol and 15 mL water (pH 7.6). After loading the sample, the cartridge was dried under vacuum. The cartridge was eluted with 15 mL of acidified methanol (5 vol% formic acid) and acidified acetonitrile (5 vol% formic acid) and ultimately by 15 mL of acidified methanol/acetonitrile (50:50, both 5 vol% formic acid). Combined eluates were condensed in a BÜCHI Syncore® to 1 mL (50°C, 280 rpm, 100 mbar, ~ 90 min). The extracts were transferred to 1.5 mL vials using Pasteur pipettes and analyzed by HPLC-MS/MS (see paragraph 0 & 2.4.3). Relative extraction recovery was 113%.

#### **Accelerated solvent extraction (ASE) from render material**

1 g of render, mixed with 1.5 g Hydromatrix, was extracted by accelerated solvent extraction (ASE 200, Dionex, Sunnyvale, CA, USA) in duplicate. Free space in the 11 mL cells was filled up with Ottawa-Sand. The cells were extracted at 110 °C and 1600 psi, using methanol (Li-Chrosolv gradient grade, Merck, Darmstadt, Germany) as a solvent. In total 3 extraction cycles were performed with the following settings: static time 5 min, preheating time 1 min, flush 60%, purge 60%. Afterwards, 500 µL extract was diluted with 1 mL methanol, spiked with 50 µL surrogate standard ( $1\text{ }\mu\text{g mL}^{-1}$  in methanol) and analyzed by HPLC-MS/MS (see paragraph 0 & 2.4.3). Extraction recoveries ranged between 69 and 120% for the individual compounds (see Bilag 2.1).

### **2.4.2 Analysis of biocides**

Biocides were analyzed by high performance liquid chromatography coupled to tandem mass spectrometry (HPLC-MS/MS) using electrospray ionization in positive mode (ESI(+)) on an Ultimate 3000 dual gradient low pressure mixing HPLC-system (*Dionex*, Sunnyvale, CA, USA) coupled to an API 4000 triple-quadrupole-MS (*AB Sciex*, Framingham, MA, USA) according to Bollmann et al. [26]. For HPLC gradients and column parameters see Table 2.4-1. Mass spectrometric parameters can be found in Bilag 1.

### **2.4.3 Analysis of transformation products**

Besides the analysis of the parent biocides, several transformation products of terbutryn and octylisothiazolinone were analyzed. Terbutryn transformation products were partly analyzed with a neutral gradient (water/methanol) and partly with an acidified gradient (water/acetonitrile with 0.2% formic acid), while the octylisothiazolinone transformation products were all analyzed with an acidified gradient, but with two different stationary phases. Additionally, 1-(3,4-dichlorophenyl)-3-methyl urea (DCPMU, diuron transformation product), 1-(4-Isopropylphenyl)-3-methylurea (IPPMU, isoproturon transformation product) and aminobenzimidazole (carbendazim transformation product) were analyzed. For HPLC gradients and column parameters see Table 2.4-1. Mass spectrometric parameters can be found in Bilag 2.



**Table 2.4-1** HPLC gradients and column parameters used for the analysis of the biocides and degradation products (TPs).

Compounds	Column	Gradient
<b>Biocides</b>	Synergy 4u Polar-RP	Water (A) and methanol (B): 250 $\mu\text{L min}^{-1}$
	80Å, 150 x 2 mm	0-3 min 0% B, 3-5 min 0→50% B, 5-15 min 50→80% B, 15-15.5 min 80→100% B, 15.5-19 min 100% B, 19-20 min 100→0% B, 20-25 min 0% B
	Phenomenex, Torrance, CA, USA	
	5°C	Post column acidification: 0.2% formic acid in water (30 $\mu\text{L min}^{-1}$ )
<b>TPs neutral</b>	Synergy 4u Polar-RP	Water (A) and methanol (B): 300 $\mu\text{L min}^{-1}$
Terbutometon	80Å, 150 x 2 mm	0-2.5 min 0% B, 2.5-3.5 min 0→50% B, 3.5-9.5 min 50→100% B, 9.5-11min 100% B, 11-11.5min 100→0% B, 11.5-15min 0% B
Terbutryn-sulfoxide	Phenomenex, Torrance, CA, USA	
Desethyl-terbutryn	5°C	Post column acidification: 0.2% formic acid in water (30 $\mu\text{L min}^{-1}$ )
Desthiomethyl-terbutryn		
Desethyl-desthiomethyl-terbutryn		
Desbutyl-desthiomethyl-terbutryn		
DCPMU		
IPPMU		
<b>TPs acidic</b>	Synergy 4u Polar-RP	Water/ 0.2% formic acid (A) and acetonitrile/ 0.2% formic acid (B): 300 $\mu\text{L min}^{-1}$
Octylamine	80Å, 150 x 2 mm	
N-Octylformamide	Phenomenex, Torrance, CA, USA	0-1 min 2% B, 1-2 min 2→40% B, 2-10 min 40→75% B, 10-10.5 min 75→100% B, 10.5-12 min 100% B, 12-12.5 min 100→2% B, 12.5-15 min 2% B
N-Octylacetamide	5°C	
N-Octylprop-2-enamine		
3-Octylthiazol-2(3H)-one		
Desbutyl-2-hydroxy-terbutryn		
Desethyl-2-hydroxy-terbutryn		
2-Hydroxy-terbutryn		
Aminobenzimidazole		
<b>TPs acidic 2</b>	Kinetex 2.6u PFP	Water/ 0.2% formic acid (A) and methanol/ 0.2% formic acid (B): 250 $\mu\text{L min}^{-1}$
N-Octyl malonamic acid	100Å, 50 x 2.1 mm	
N-Octyl oxamic acid	Phenomenex, Torrance, CA, USA	0-1 min 0% B, 1-4.5 min 0→100% B, 4.5-6.5 min 100% B, 6.5-6.8 min 100→0% B, 6.8-12.5 min 0% B
	25°C	

## 3. Results & Discussions

### 3.1 Transport processes in the material

#### 3.1.1 Influence of wet & dry cycles

##### Water uptake by the renders

During the experiments, the renders took up water. This effect was probably involved in changing the emission of biocides. During the wet/wet experiment (with no equilibration time in between the exposures) the amount of water taken up by the renders was limited by the relatively short time of the whole experiment (120 min). During these 120 min of contact time, each render sample took up about 0.26 g and 0.39 g of water, which constituted 14.7% and 23.1% of mass of the acrylate and silicone renders, respectively. The measured water uptake is documented in the Bilag 3.1.

The duration of the entire wet/dry experiment (with 24 h drying phases in between the exposures) was 193 h and the amount of water in the renders was limited by drying process between each leaching steps. The weight of each sample after a complete wet/dry cycle including drying was identical to its initial weight. Thus, complete evaporation of moisture was reached within 24 h drying. The measured water uptake increased with the exposure time of the render with water (see Bilag 3.1).

The duration of the entire wet/wet 24 h experiment (with 24 h equilibration time under 100% humidity) was also 193 h but the render samples were not dried between the leaching steps. The total mass of water taken up by the render during these 193 h was about 0.43 g and 0.86 g or 24.4% and 50.3% for acrylate and silicone renders, respectively. The measured water uptake is documented in Bilag 3.1.

While the water in the material in the wet/wet 24 h samples could be assumed to be in equilibrium after the 24 h period, this was clearly not the case for the wet/dry intervals and also some exchange must be assumed during the wet/wet experiments. Additionally it must be considered that the water was moving into deeper layers of the material if water was present over longer periods. Thus, during the wet/wet 24 h experiments more water enters the render than in the wet/wet experiment due to a considerably longer experimental time (193 h versus 120 min).

##### Biocide partitioning

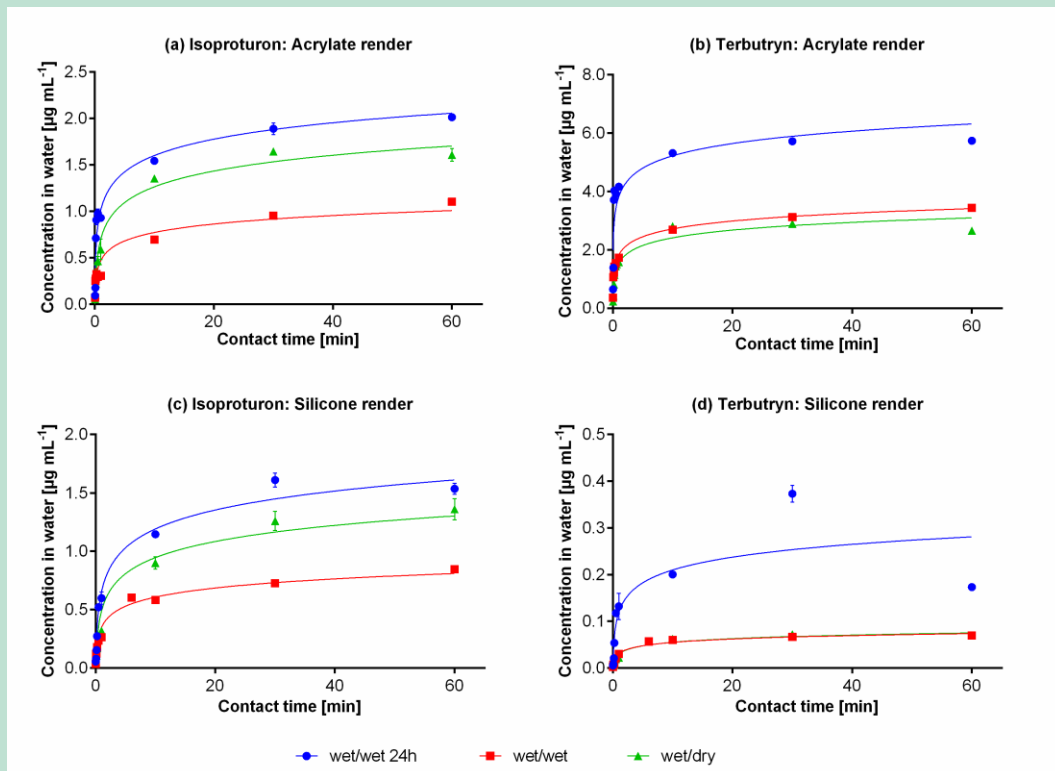
###### *Comparison aqueous concentrations vs water solubility and partitioning*

The biocide concentrations reached in the water were high (typically a few  $\text{mg L}^{-1}$ ), but considerably below the solubility in water. The concentrations of isoproturon reached in the water were up to  $1.61 \text{ mg L}^{-1}$  for the silicone render and to  $2.03 \text{ mg L}^{-1}$  for acrylic render. The highest concentration of terbutryn reached in the water was  $0.38 \text{ mg L}^{-1}$  for silicone render and  $5.9 \text{ mg L}^{-1}$  for acrylic render. Thus, it could clearly be shown that the concentrations in the water were not determined by the solubilities of the compounds in the water (compare Table 2.1-1). Concentrations in  $\text{mg L}^{-1}$ -range are comparable to those measured previously in different leaching studies by Wangler et al. [36] and Schoknecht et al. [35] using dipping, immersion experiments. The huge difference in final concentrations between the two different render systems highlight the strong influence of the render matrix on biocide leaching.

###### *Concentration dynamics*

In principle the concentrations dynamics proved similar for all experiments: Starting with very low concentrations at low contact times and reaching the highest concentrations after several minutes contact time – depending on compound and system (Figure 3.1-1). The maximum concentrations, established with typical contact times larger than 10 min, were in the same range as those determined in earlier pure partitioning experiments [38] (Table 3.1-1). Indeed,

from the experiments two phases can be observed: a phase of intensive transport (typically 3 s–10 min) and an equilibrium steady state (typically 10 min and more). Interestingly, the different leaching experiments led to different equilibrium concentrations. Thus, the cycle type (drying, soaked interval or direct water contact) is not only influencing the speed of leaching but also the equilibrium constants.



**Figure 3.1-1** Concentrations of isoproturon (a & c) and terbutryn (b & d) in the leachate under three different wetting regimes and for two different render systems in dependence of different wetting times at room temperature (22°C). In (d) the graphs for wet/wet and wet/dry are so close that they overlap in most places.

#### Comparison of different cycles

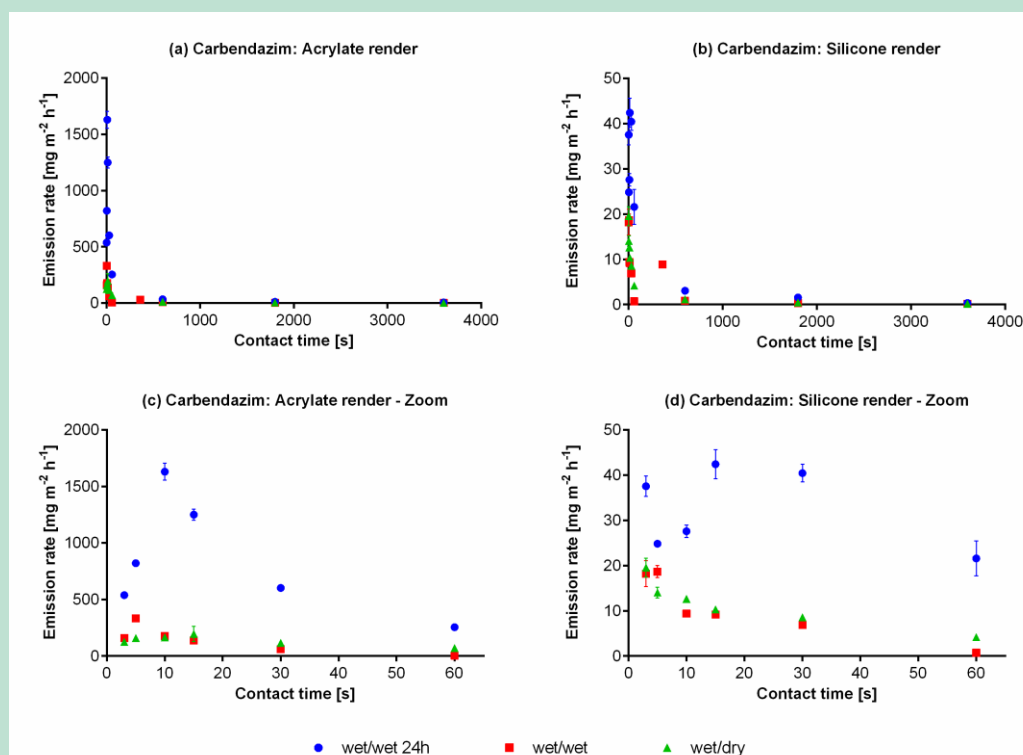
Surprisingly, in all leaching experiments (including different renders and a multitude of different compounds), the wet/wet cycles with 24 h equilibrium time (diffusion through water) gave the highest concentrations in the leachate during the intensive transport as well as the equilibrium phase. This clearly indicates that the water in the render (pore water) is an important mediator to the biocide transport in the materials. Usually the biocide concentrations in the leachate from the wet/wet 24 h experiments were factor 2-3 higher than those obtained by the other cycles, which is demonstrated for isoproturon and terbutryn for both renders in Figure 3.1-1. The wet/dry cycles (e.g. due to evaporative transports) resulted in considerably lower concentrations in the leachate than the wet/wet 24 h (diffusion through pore water). Hence, evaporative transport seems to be not relevant under these conditions. Consequently, it must be concluded, that diffusion through the pore water in the water-filled pores is contributing considerably to the biocide transport within the material. Whether wet/dry or a wet/wet without equilibration time turned out to give the higher concentrations in the leachate, was dependent on render system and compound.

**Table 3.1-1** Comparison of distribution constants ( $D_{render}$ ) in  $L\ kg^{-1}$  of biocides between renders obtained during different cycles and compared to pure thermodynamic data [38]. The data were calculated from triplicate samples obtained during the time of equilibrium, typically at 24–60 min contact time.

	Acrylate modified render				Silicone modified render			
	wet/dry	wet/wet	wet/wet 24h	$D_{render}$ [38]	wet/dry	wet/wet	wet/wet 24h	$D_{render}$ [38]
Carbendazim	7.9	11.3	1.0	33.8	107	146	31	310.
Isoproturon	5.5	8.5	4.1	8.1	7.4	10.7	6.2	9.8
Diuron	14.1	17.2	8.6	17.9	21.9	30.6	15.6	21.4
Cybutryn	64.7	62.3	18.0	26.0	192	190	19.0	121.4
Tebuconazole	61.7	81.9	35.0	65.8	480	558	67	700
Iodocarb	48.6	135	17.8	9634	78.0	81.3	42.4	70.8

### Equilibrium partitioning

Though the process is not truly thermodynamic equilibrium partitioning, distribution constants  $D_{render}$ , calculated from the equilibrium phase of the experiments (Eq. 4.2-2), were similar to those derive from powdered material [38]. Thus, indeed equilibrium had been reached at the longer contact times (Table 3.1-1). However, a clear difference was found between the different wetting experiments. During those experiments in which a huge water uptake was determined (wet/wet 24 h), the equilibrium partitioning led to higher concentrations in the water phase. Thus, the water soaked render sorbed less biocides than a dry one.



**Figure 3.1-2** Mass flow of carbendazim through acrylate and silicone render under different cycles. To allow deeper insight the x-axis in the lower plot is enlarged.

### Comparison of acrylate and silicone render in respect of wet/dry and wet/wet experiments

Significant differences in concentrations in the water were observed for most compounds when comparing the acrylate and the silicone render systems. When the silicone render was

used, the aqueous biocide concentrations were usually considerably lower which may be attributed to its higher organic matter content. In the acrylate system wet/dry was giving higher concentrations for methyl-, benz- and *N*-octylisothiazolinone, carbendazim, isoproturon, diuron, iodocarb and tebuconazole than wet/wet cycles. Wet/dry and wet/wet cycles without equilibration time were reaching similar values for terbutryn and cybutryn.

In the silicone render wet/dry experiments were giving higher concentrations for methyl- and dichloro-*N*-octylisothiazolinone, isoproturon and diuron, while wet/dry and wet/wet without equilibration time gave similar results for carbendazim, iodocarb, terbutryn, *N*-octylisothiazolinone and tebuconazole. On the other hand, cybutryn gave higher values for the wet/wet cycles than for the wet/dry.

**Table 3.1-2** Cumulative mass of biocides per unit area ( $\text{mg m}^{-2}$ ) emitted from silicone render (SR) and acrylic render (AR) under three different wetting regimes: wet/dry, wet/wet and wet/wet 24h. Values in parenthesis is weight percent of initial mass of biocides leached from the respective renders during the experiments.<sup>1</sup>

	unit	MI	BIT	CD	IP	DR	IPBC	TB	IRG	OIT	TBU	DCOIT	
Silicone render	wet/dry	[mg m <sup>-2</sup> ]	122.99	61.78	0.87	8.92	3.46	1.18	0.54	0.52	2.84	0.21	0.04
		[%]	nd	nd	(2.1)	(21.3)	(8.7)	(2.9)	(1.3)	(1.2)	(6.2)	(0.5)	(0.1)
	wet/wet	[mg m <sup>-2</sup> ]	106.2	65.92	0.75	12.12	2.92	1.15	0.57	0.59	2.45	0.21	0.02
		[%]	nd	nd	(1.8)	(28.9)	(7.5)	(2.8)	(1.4)	(1.3)	(5.4)	(0.5)	(0.1)
	wet/wet 24h	[mg m <sup>-2</sup> ]	294.88	141.92	2.67	11.93	5.01	2.08	2.17	4.06	13.61	1.13	0.24
		[%]	nd	nd	(6.2)	(27.6)	(12.3)	(5.0)	(5.0)	(8.7)	(28.9)	(2.5)	(0.6)
Acrylate render	wet/dry	[mg m <sup>-2</sup> ]	251.5	104.59	10.82	12.82	5.97	2.09	28.03	1.68	82.16	1.71	0.18
		[%]	nd	nd	(24.5)	(29.0)	(14.3)	(4.9)	nd	(3.5)	(12.9)	(3.7)	(0.5)
	wet/wet	[mg m <sup>-2</sup> ]	211.36	82.82	7.48	15.83	4.78	1.05	33.28	1.79	59.68	1.25	0.05
		[%]	nd	nd	(17.7)	(36.3)	(11.6)	(2.5)	nd	(3.8)	(9.8)	(2.7)	(0.1)
	wet/wet 24h	[mg m <sup>-2</sup> ]	465.02	188.68	34.39	15.75	7.98	3.21	61.62	6.11	217.26	3.64	0.13
			nd	nd	(77.0)	(35.2)	(18.9)	(7.5)	nd	(12.7)	(34.5)	(7.7)	(0.3)

(1) "nd" is used when the initial amount of the respective biocide is uncertain as an industrial product with not too clearly defined biocide content for some compounds was used.

MI: Methylisothiazolinone, BIT: Benzisothiazolinone, CD: Carbendazim, IP: Isoproturon, DR: Diuron, IPBC: Iodocarb, TB: Terbutryn, IRG: Cybutryn, OIT: *N*-Octylisothiazolinone, TBU: Tebuconazole, PPZ: Propiconazole

### Mass balance of biocides

During these experiments, a significant difference between those compounds with a relative high sorption toward the renders  $D_{\text{render}}$  (i.e., carbendazim, isoproturon, iodocarb, diuron, terbutryn, cybutryn, octylisothiazolinone, and tebuconazole) and those with low  $D_{\text{render}}$  (methyl- and benzisothiazolinone) on the other hand were experienced. While most studied biocides are used to protect the coating film and thus the whole service life outdoors, methyl- and benzisothiazolinone are used as in-can preservatives and not to stabilize the film as such. Consequently, a fast leaching is acceptable for these two biocides.

The calculation of the total leached fraction of biocides at the end of the wet/wet 24 h experiment showed that less than 20% of iodocarb, cybutryn and tebuconazole were leached from the acrylate render, while for carbendazim, isoproturon and diuron a significant fraction (>20%) was leached (Table 3.1-2). For the silicone-based render, generally less leaching was observed. Less than 20% were leached considering carbendazim, diuron, iodocarb, terbutryn, cybutryn, tebuconazole, and DCOIT. Significant amounts (>20%) were leached for octylisothiazolinone and isoproturon. However, it can clearly be recognized that also in this mass balance assessment the wet/wet 24 h leads to the highest emissions by far. This finding is indicating toward soaked materials, for example during longer rainy periods with dry periods with high relative humidity in between, should be emitting the most.

The total emissions during the 9 cycles were considerably higher for the acrylate render system in comparison to the silicone render system, which is in agreement with the earlier partitioning experiments.

### Transport fluxes

The transport fluxes [ $\text{mg m}^{-2} \text{h}^{-1}$ ] through the silicone render usually started with maximum values, which then decreased slowly but constantly. Contrary, the transport fluxes through acrylate renders increased through the first 10 s of exposure for the acrylate (as demonstrated for carbendazim in Figure 3.1-2) reaching a maximum at 10 s contact time after which the fluxes decreased continuously. This indicates toward a layering of the acrylate render – either in respect of the biocide concentration or in respect of material composition. All in all the curve for the silicone render is considerably flatter than those obtained for the acrylate render. Thus, a more constant delivery of biocides to the surface of the material can be expected from the silicone render than for the acrylate render.

### Mechanisms

With the presented data it is obvious that the transport is occurring predominantly through water filled pores. There are three possible transport scenarios when applying a constant gradient:

- (1) The flux through the material is high and the surface transition (crossing the phase border between solid and dissolved) is the limiting factor if the leaching. This would result in a leap in potential from render to bulk water, a continuous flow through the material and no biocide-gradients in the render (leading to constant mass flows across the boundary layer).
- (2) Crossing the phase barrier between render and bulk water is easy in comparison to the diffusion through the material. This would result in a decreasing flow with time in parallel with establishing biocide gradients within the render material.
- (3) The transport of the biocide through the bulk water is limiting the process: this would lead to decreased transport with time and gradients within the water.

Mechanism (3) can be excluded for the experimental setup, as the water was heavily mixed by shaking. In reality, the water film running down the render system is most probably highly turbulent as the surfaces are rough. The data seem to indicate that rather mechanism (2) is relevant as the biocide emission is dependent on the contact time. Decreased flows have also been observed in the literature [35, 36].

### Influence of wet & dry cycles – Key findings

- Transports of biocides through polymeric render as well as equilibria in the render/water system are dependent on the water content of the respective render.
- Generally speaking, the more hydrophilic compounds like MI are more rapidly transported through the systems than the more lipophilic ones
- Transport of biocides in renders predominantly occurs through the water-filled pores; the transport through the dry render considerably less; evaporative driven transports of biocides through render materials is negligible.
- Transport of biocides is highest when the render is in fresh contact with unpolluted water.

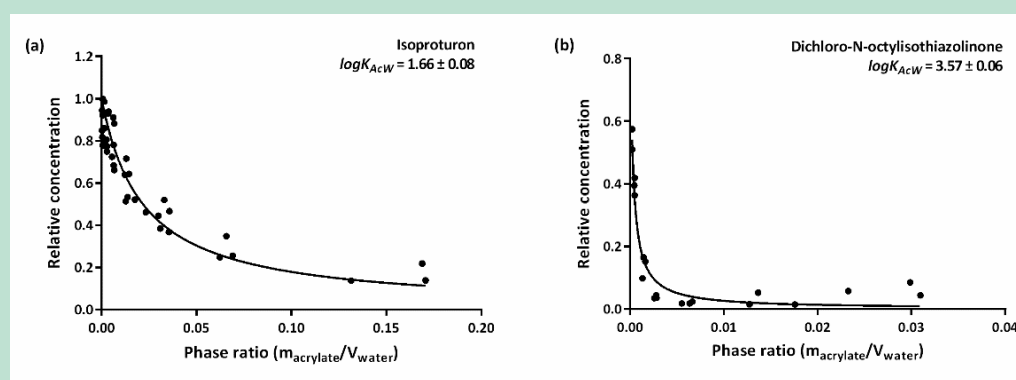
### 3.1.2 Mobility controlled by different fractions

#### 3.1.2.1 Polymeric binder

##### Confirmation of equilibrium partitioning

Equilibrium partitioning between water and polymer is dependent on (1) partitioning between water and polymer surface as well as (2) the transport of the biocide into the polymer volume. The polyacrylate coating on the glass fiber filter was thus kept very thin ( $< 1$  mm) and in the same order as for polyacrylate coated SPME fibers (85  $\mu\text{m}$ ) which in earlier studies were equilibrated within minutes to less than one hour [57-59]. Internal concentration gradients within the polymer coating can thus be neglected after some hours of exposure.

The concentration ratios ( $c_{\text{acrylate}}/c_{\text{water}}$ ) were increasing rapidly until 6 h of exposure for isoproturon, carbendazim, diuron, and atrazine, iodocarb, terbutryn, propiconazole, tebuconazole. No significant increase ( $< 5\%$  relative standard deviation) of the ratio was determined even after 12 h of exposure. Thus, equilibrium time was reached after 6 h for the studied biocides (see Bilag 4.2).



**Figure 3.1-3** Relative concentrations ( $c_{\text{W}}(T_{\text{eq}})/c_0$ ) after 6 h of contact time with the coated glass fiber filter plotted against the polyacrylate/water phase ratios for two representatives: (a) isoproturon, the compound with the lowest, and (b) dichloro-*N*-octylisothiazolinone, the compound with the highest polyacrylate-water partitioning constant ( $\log K_{\text{AcW}}$ ).

##### Partition constant between polyacrylate and water

By plotting relative concentrations against the polyacrylate/water phase ratio, hyperbolic graphs were obtained. As an example, Figure 3.1-3 shows the plots for the two biocides with the highest (dichloro-*N*-octylisothiazolinone:  $\log K_{\text{AcW}} = 3.57 \pm 0.06$ ) and the lowest (isoproturon:  $\log K_{\text{AcW}} = 1.66 \pm 0.08$ ) polyacrylate-water partition constants, which ranged from 46 to 3715  $\text{L kg}^{-1}$  (Bilag 4.3). The line in the plot is based on the non-linear regression of the relative concentration as a function of the polyacrylate/water phase ratio according to Eq. 4.2-3. The coefficients of determination ( $R^2$ ) varied between 0.80 (tebuconazole) and 0.98 (diuron). Polyacrylate-water partition constants and coefficients of determination ( $R^2$ ) for all compounds are summarized in Table 3.1-3. A good comparison with literature is only possible by using atrazine: Endo, Droge [60] studied the partitioning of a broad range of organic compounds between polyacrylate and water using solid phase micro extraction (SPME). Their experimental polyacrylate-water partition constant for atrazine was  $\log K_{\text{AcW}} = 2.40$ , which is in accordance with the results of the present study using polyacrylate coated glass fiber filters ( $\log K_{\text{AcW}} = 2.41 \pm 0.08$ ). The polyacrylate-water partition constants (SPME) for atrazine determined by Haftka et al. [61] and Verbruggen et al. [62] are lower than the one in the present study ( $\log K_{\text{AcW}} = 2.28 \pm 0.02$  and  $\log K_{\text{AcW}} = 1.95 \pm 0.02$ , respectively). Lambropoulou et al. [18] studied the polyacrylate-water partitioning of the two antifouling biocides cybutryn (Irgarol 1051) and dichloro-*N*-octylisothiazolinone (Sea Nine 211) using solid phase micro extraction. Their partition constants were slightly higher ( $\log K_{\text{AcW}} = 3.05$  and  $\log K_{\text{AcW}} = 3.83$ , respectively) than



those in the present study ( $\log K_{AcW} = 2.87 \pm 0.09$  and  $\log K_{AcW} = 3.57 \pm 0.06$ , respectively). Zambonin and Palmisano [63] reported an polyacrylate-water partition constant (SPME) for terbutryn of  $\log K_{AcW} = 5.32$ , which is much higher than the one in the present study ( $\log K_{AcW} = 2.89 \pm 0.10$ ). So far, no comparable polyacrylate-water partition constants are available in the literature for the other 7 compounds.

The octanol-water partition constant ( $\log K_{OW}$ ) is often used in order to predict partitioning between water and organic phases. Figure 3.1-4a shows that the determined polyacrylate-water partition constants of this study have a positive linear correlation to previously, experimentally determined octanol-water partition constants. This correlation is highly significant ( $r = 0.77$ , significant at  $P < 0.01$ ). However, in agreement to Vaes, Hamwijk [58] the polyacrylate-water partition constants are lower than the octanol-water partition constants for more lipophilic compounds ( $\log K_{AcW} = 0.454 \log K_{OW} + 1.20$ ).

**Table 3.1-3** Polyacrylate-water partition constants ( $\log K_{AcW}$ ) with 95%-confidence interval as well as coefficient of determination ( $R^2$ ) from the non-linear regression model for the studied compounds; N number of data points.

	$\log K_{AcW}$ (P = 95%)	$R^2$	N
Carbendazim	$2.23 \pm 0.07$	0.9093	42
Iodocarb	$2.66 \pm 0.09$	0.8951	37
Isoproturon	$1.66 \pm 0.08$	0.8569	41
Diuron	$2.19 \pm 0.04$	0.9774	45
Atrazine	$2.41 \pm 0.08$	0.8768	41
Terbutryn	$2.89 \pm 0.10$	0.8398	45
Cybutryn	$2.87 \pm 0.09$	0.8800	45
N-Octylisothiazolinone	$2.28 \pm 0.08$	0.8972	39
Dichloro-N-octylisothiazolinone	$3.57 \pm 0.06$	0.9582	21
Tebuconazole	$3.28 \pm 0.08$	0.7966	45
Propiconazole	$2.95 \pm 0.08$	0.8309	42

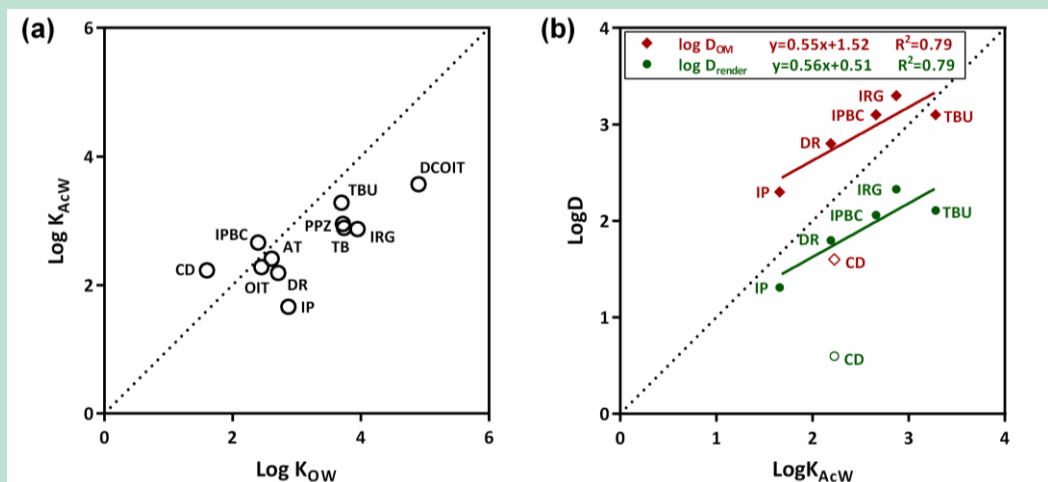
#### Comparison of polyacrylate-water partition constants with distribution constants between polyacrylate-based render and water

Stysko et al. [38] determined the distribution constants of selected biocides between polyacrylate-based render and water. The used render contained mainly polyacrylate (10%), carbonate (66%) and quartz sand. As described in that study, the render-water distribution constant is pH-dependent, hence, for comparison only distribution constants at pH 5.6 were used. Further, Stysko et al. [38] demonstrated that increasing the fraction of polyacrylate in a polyacrylate-based render reduced the desorption from the render for iodocarb, dichloro-N-octylisothiazolinone, tebuconazole, cybutryn, and carbendazim but not for isoproturon and diuron. Hence, the desorption of iodocarb, dichloro-N-octylisothiazolinone, tebuconazole, cybutryn, and carbendazim seemed to be dependent on the fraction of polyacrylate in the render, while the desorption of diuron and isoproturon was almost not affected by the polyacrylate fraction.

According to Eq. 4.2-2 the render-water distribution constant would be directly correlated to the polyacrylate-water partitioning. If the render partitioning would be solely dependent on partitioning between polyacrylate and water the normalized render-water distribution constant would equal the polyacrylate-water partition constant. The comparison of the polyacrylate-water partition coefficient (numerical values from this study, Table 3.1-3) and the desorption constant from polyacrylate-based render normalised to the organic matter content [38] showed a positive significant ( $P < 0.05$ ) linear correlation between the two constants only if carbendazim was excluded from the linear correlation ( $r = 0.79$ ) (Figure 3.1-4b). The Pearson correlation coefficient for all compounds, including carbendazim, is insignificant ( $r = 0.65$ ),



while Spearman's rank correlation, which tests the monotone relation and is robust against outlier and extreme values, gives a correlation coefficient of  $r_s = 0.79$ . Thus, by excluding the data points for carbendazim we can no longer reject the significance of a linear correlation between adsorption to render and to polyacrylate. Since carbendazim is having a  $pK_a$  of 4.5 about 10% carbendazim would occur cationic at pH 5.5. Minerals in the render would interact differently with the ionic form and would increase the sorption. However, the correlation with polyacrylate-water partition constants determined by solid phase micro extraction (Bilag 4.4) supports the hypothesis that the carbendazim data might be an outlier. The polyacrylate-water partition constant of carbendazim determined by solid phase micro extraction (SPME) is much lower than the one determined with the coated glass fiber filter (Bilag 4.4) and would fit better into the regression.



**Figure 3.1-4** (a) Correlation between the polyacrylate-water partition constant  $\log K_{AcW}$  (pH 5.5) and the octanol-water partition constant  $\log K_{OW}$  (pH 7) [3, 64]. (b) Correlation between the polyacrylate-water partition constant ( $\log K_{AcW}$ ) and the distribution constant to polyacrylate-based render ( $\log D_{render}$ ) as well as the one normalised to the organic matter content (organic matter content = 10%,  $\log D_{OM}$ ) determined by Styszko et al. [38] (trendline and correlation mathematically established without carbendazim). OIT: *N*-octylisothiazolinone, DCOIT: dichloro-*N*-octylisothiazolinone, IRG: cybutryn, TB: terbutryn, AT: Atrazine, TBU: tebuconazole, PPZ: propiconazole, DR: diuron, IP: isoproturon, IPBC: iodocarb, CD: carbendazim. Dotted 1:1-line for guidance purposes, not mathematically calculated).

### Comparison of partitioning to leaching

As described in paragraph 1.2, the leaching process of biocides from render is assumed to be a multistep process. The polyacrylate-water partitioning only reflects the transfer of biocides from the render material into the water phase, might it be inside the pores or first on the render surface. Other influencing factors, as availability of water in the render, are obviously not described. Based on the determined polyacrylate-water partitioning constants the partitioning of the biocides into the water phase would be in the following order: isoproturon > diuron > carbendazim > *N*-octylisothiazolinone > iodocarb > cybutryn > terbutryn > propiconazole > tebuconazole > dichloro-*N*-octylisothiazolinone. During leaching tests from facade render under natural weather conditions, Burkhardt et al. [23] analyzed seven biocides. Based on that study, the leaching ability could be sorted according to isoproturon > diuron > iodocarb > *N*-octylisothiazolinone > cybutryn > terbutryn > dichloro-*N*-octylisothiazolinone. Schoknecht et al. [65] achieved similar results using short term immersion tests according to EN 16105:2011: diuron ~ *N*-octylisothiazolinone > iodocarb > terbutryn ~ carbendazim > dichloro-*N*-octylisothiazolinone. The comparison of the results from the artificial walls as well as the la-

laboratory studies with the estimated ones based on acrylate-water partitioning constants indicates that polyacrylate indeed is the dominant phase for the partitioning of most biocides in the render-water system. Therefore, even though several processes might influence the desorption of biocides from polymer-based render into water, the concept of estimating the desorption behaviour based on the partition constants from the pure polymer (e.g. polyacrylate or polydimethylsiloxane) seems to be a useful tool, based on a rapid and easy method.

### 3.1.2.2 Minerals

#### Confirmation of equilibrium partitioning

The concentration ratios ( $c_{\text{CaCO}_3} / c_{\text{water}}$ ) were changing until 6 h of exposure for all of the compounds except methylisothiazolinone. No changes (<5% RSD) of the concentration ratios were determined between 6 and 8 h of exposure (Bilag 5.1). Hence, equilibrium time was determined to be reached after 8 h for the studied biocides. This study was performed in order to test how the concentrations of biocides in both phases are changing with time. Thus, minerals in the next experiments were contacted with the biocide aqueous solution for 12 h and thus certainly exceeding the 8 hours determined in this pre-experiment to be minimum for reaching equilibrium.

#### Equilibrium partitioning of biocides between minerals and water

The resulting values presented in Table 3.1-4 are calculated using Eq. 4.2-1 for each experiment, and averaging the data points representing different biocide concentrations used in the experiments. This way also the standard deviations were calculated. Additionally, results for talc are presented as graphs of  $c_s$  to  $c_w$  ratios, results in Figure 3.1-5.

The higher the  $K_d$  value the more biocides tend to sorb on the surface. The partition equilibria of biocides differ largely for different minerals. While almost all minerals sorb biocides to some extent, only talc seems to sorb biocides in significant amounts.

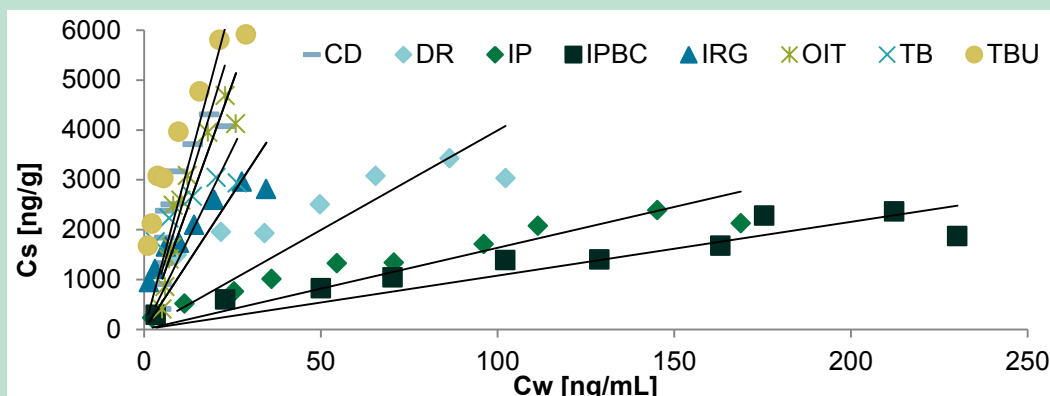
**Table 3.1-4** Partition constants ( $K_d$ ) of biocides between analyzed minerals and water phase, including the measurement uncertainties as standard deviations as indicated by ( $\pm$ ) in  $\text{mL g}^{-1}$ .

	Calcium carbonate	Talc	Kaolinite	Barite
Carbendazim (CD)	$0.3 \pm 0.2$	$263.0 \pm 45.2$	$3.0 \pm 0.1$	$0.4 \pm 0.2$
Isoproturon (IP)	$0.5 \pm 0.8$	$31.2 \pm 6.9$	$0.2 \pm 0.3$	$0.2 \pm 0.1$
Diuron (DR)	$0.2 \pm 0.4$	$68.1 \pm 15.9$	$0.3 \pm 0.1$	$0.1 \pm 0.2$
Irgarol (IRG)	$0.4 \pm 0.2$	$260.2 \pm 67.6$	$0.4 \pm 0.2$	$0.1 \pm 0.2$
Tebuconazole (TBU)	$0.3 \pm 0.2$	$683.7 \pm 124.9$	$0.6 \pm 0.02$	$0.1 \pm 0.1$
Iodocarb (IBPC)	$5.2 \pm 0.5$	$21.3 \pm 7.5$	$-0.1 \pm 0.003$	$-0.3 \pm 0.01$
Octylisothiazolinone (OIT)	$0.3 \pm 0.2$	$205.8 \pm 23.6$	$3.4 \pm 0.1$	$2.3 \pm 0.1$
Terbutryn (TB)	$0.5 \pm 0.2$	$280.2 \pm 66.4$	$0.5 \pm 0.4$	$-0.2 \pm 0.1$

#### Calcium carbonate (fine powder and marble stones/chunks)

Partition constants of all analyzed biocides on fine calcium carbonate range from 0.2 to  $5.2 \text{ mL g}^{-1}$  with the highest value for iodocarb  $K_d = 5.2 \text{ mL g}^{-1}$  (Table 3.1-4). Unfortunately, this biocide also undergoes hydrolysis [66] and hence, it might “disappear” from the system. All in all, the sorption to calcium carbonate is very low, and thus, the uncertainties are relatively high, without changing the central result: sorption is very low. Electrostatic interactions play a possible role in controlling the amount of biocides adsorbed on the calcium carbonate surface. According to [67], the calcium carbonate particles are uncharged or to some extent positively charged at pH 7.5, which favors the sorption of negatively charged compounds. However, at pH 9.5 calcium carbonate is negatively charged and repulsive towards compounds with negative charge. Under the experimental conditions (pH 5.5 equivalent to rainwater) the calcium carbonate as well as the biocides would be charged positively, thus the low interaction is easi-

ly understandable. As expected, no sign of adsorption was detected on marble samples. Marble is a stone completely or largely composed of calcium carbonate. Its high density, hardness and very low porosity might be an explanation for its lack of sorption properties [68].



**Figure 3.1-5** Sorption isotherms of biocidal compounds between talc and water.

#### Talc

Partition constants of biocides to talc ranged from 21.3 to 683.7 mL g<sup>-1</sup> (Table 3.1-4). Tebuconazole was the compound, which showed the highest partition towards talc (683.7 mL g<sup>-1</sup>). This finding can be explained with hydrophobic properties of this biocide. Other biocides with high K<sub>ow</sub> such as cybutryn and terbutryn also show high partition constants for talc, i.e., 260.2 mL g<sup>-1</sup> and 280.2 mL g<sup>-1</sup>, respectively. Talc has only small capacities to donate or accept electrons and, thus, limiting possibilities to form hydrogen bonds, which makes talc a relatively non-polar agent [69]. This fact might explain why talc in comparison sorbs relatively high amounts of the rather non-polar biocides, terbutryn, cybutryn, and tebuconazole. However, the talc content in renders might be limited, because of its other properties and the final purpose of the render. The addition of talc makes it easier to achieve a smooth surface of fillers and primers; it also provides good intercoat adhesion. Unfortunately, extensive use of talc in exterior conditions leads to the formation of fine powder on the surface of the paint film due to weathering; a process that is commonly described as chalking [70].

**Table 3.1-5** Mass balance on the talc partitioning including the measurement uncertainties as standard deviations as indicated by (±) in ng.

	IP	IPBC	DR	TB	IRG	OIT	TBU	CD
<b>Amount of biocides used in study [ng]</b>	789.0	2272.5	1953.8	1833.8	1048.5	836.3	2513.3	2757.8
Determined amount of biocide in water phase after partitioning [ng]	65.1 ± 1.9	363.6 ± 9.7	67.6 ± 2.9	13.6 ± 0.6	10.9 ± 0.7	1.7 ± 0.2	12.0 ± 0.8	2.3 ± 0.4
Theoretical amount of biocide adsorbed on talc [ng]	723.9 ± 1.9	1908.9 ± 9.7	1886.2 ± 2.9	1820.1 ± 0.6	1037.6 ± 0.7	834.6 ± 0.2	2501.2 ± 0.8	2755.5 ± 0.4
Amount of biocide extracted after 1st extraction [ng]	602.9 ± 12.7	1665.6 ± 44.6	1531.9 ± 49.6	1504.4 ± 43.6	916.6 ± 36.2	756.9 ± 23.2	2098.1 ± 39.1	939.8 ± 34.8
Amount of biocide extracted after 2nd extraction [ng]	114.7 ± 5.5	315.8 ± 15.8	291.1 ± 12.9	284.4 ± 12.7	179.3 ± 7.6	144.8 ± 12.6	378.3 ± 23.7	307.4 ± 7.3
Amount of biocide extracted in total [ng]	717.6 ± 11.4	1981.4 ± 39.0	1823.0 ± 45.7	1788.8 ± 44.8	1095.8 ± 39.4	901.7 ± 24.2	2476.4 ± 58.2	1247.2 ± 32.6
Amount of biocide determined in extracts plus in the aqueous phase [ng]	782.7 ± 12.3	2345.0 ± 37.0	1890.6 ± 45.3	1802.4 ± 45.3	1106.7 ± 39.7	903.4 ± 24.3	2488.4 ± 58.9	1249.4 ± 32.5
<b>Mass balance [%]</b>	99	103	97	98	106	108	99	45

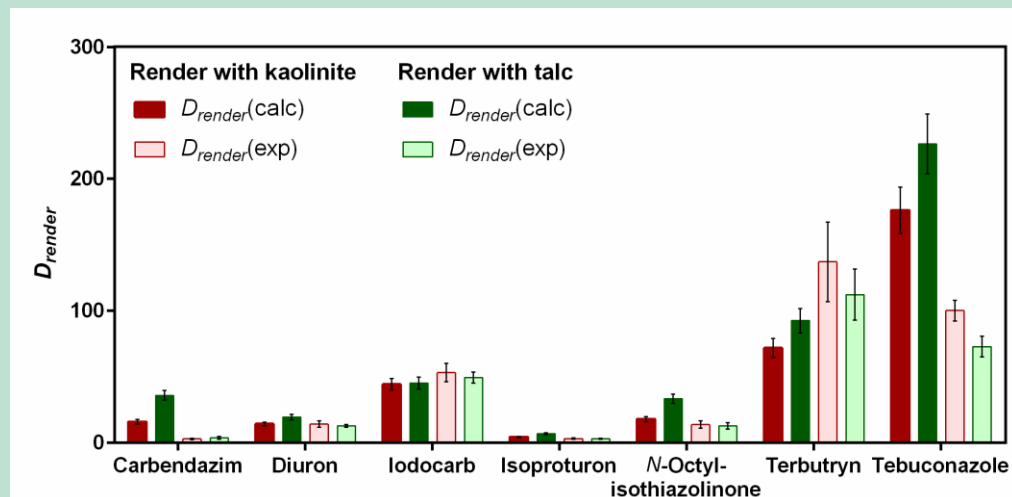
To test whether only partitioning or, additionally, other reactions are relevant, the talc was extracted after the incubation. Usually the sum of the single biocide found in the aqueous and those extracted from the solid phase added up to the initial amount, thus, indicating towards pure partitioning processes (Table 3.1-5). Only carbendazim was an exception, for this compound less than the initial amount was found in the two phases. However, the second extraction yielded nearly as much carbendazim than the first one indicating rather to an incomplete extraction than unknown processes.

#### Kaolinite

Partition constants ranged from  $-0.1$  to  $3.4 \text{ mL g}^{-1}$  (Table 3.1-4). Highest partition constants were determined for carbendazim ( $3.0 \text{ mL g}^{-1}$ ) and octylisothiazolinone ( $3.4 \text{ mL g}^{-1}$ ). Sorption of carbendazim to kaolinite is probably due to protonation of the biocide molecule, which is interacting with the negative surface charge of kaolinite [71]. Kaolinite shows a permanent negative charge, as a result of some of the centers in the tetrahedral layer of kaolinite being occupied by  $\text{Al}^{3+}$  ions instead of  $\text{Si}^{4+}$  ions. In consequence kaolinite acts as a cation exchanger with a given cation-exchange capacity [72]. Adsorption of biocides on the kaolinite surface should mainly occur due to electrostatic interaction forces between the compounds and the kaolinite surface.

#### Barite

Partition constants ranged from  $-0.3$  to  $2.3 \text{ mL g}^{-1}$ . Similar to kaolinite, the highest partition constants were obtained for carbendazim ( $0.4 \text{ mL g}^{-1}$ ) and octylisothiazolinone ( $2.3 \text{ mL g}^{-1}$ ) (Table 3.1-4). Barite belongs to a group of polar minerals [73]. Oxygen atoms in Barite ( $\text{BaSO}_4$ ) are linked both by covalent and ionic bonds. S and O atoms in  $(\text{SO}_4)^{2-}$  are linked together with  $\text{sp}^3$  hybrid covalent bonds. Further  $(\text{SO}_4)^{2-}$  are held together by Ba-O bonds with dominantly ionic character. In result, although most atoms are charged, barite has not a lot of surface charges [74].



**Figure 3.1-6** Comparison between calculated distribution constants ( $D_{\text{render}}(\text{calc})$ ) of biocides in render/water systems and experimental data ( $D_{\text{render}}(\text{exp})$ ).

#### 3.1.2.3 Distribution constants for a model render

The detailed compositions of commercial renders with organic binders and paints are usually unknown due to trade secrets. However, Schoknecht et al. [35] suggested a general render recipe – a modified recipe was used in this work, containing the most important technical in-

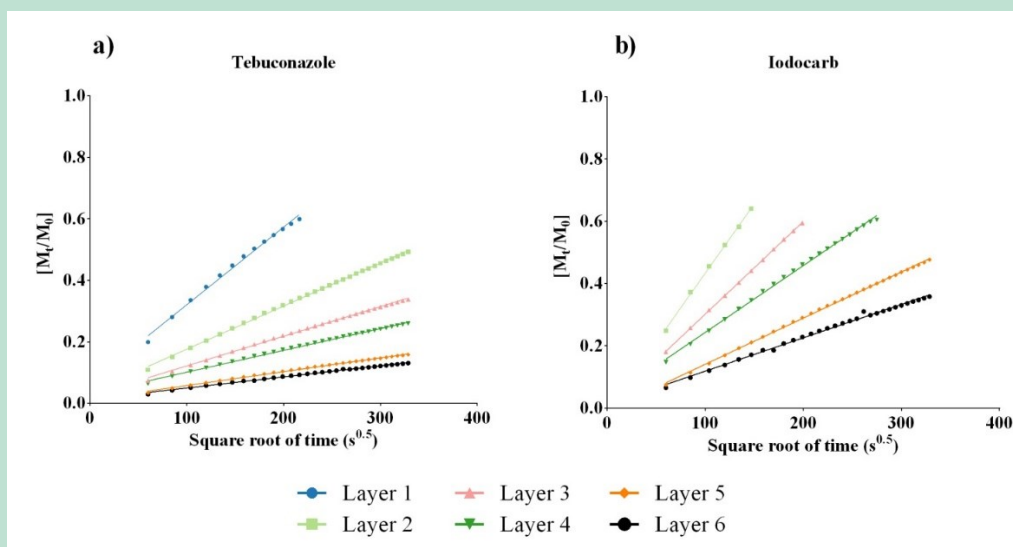
gredients commonly used in the industry. The composition was modified by substituting kaolinite with talc for this experiment to check whether predictions can be made and verified. Results of the partitioning experiment between water and render formulations were a) determined and b) compared with simple mathematical model (Eq. 4.2-2) from the single phase results (Table 3.1-3 & Table 3.1-4). The results are presented in Figure 3.1-6. In general, the experimental results for both of the renders formulation agreed with the calculated ones (Figure 3.1-6). For the talc render the closest match was for terbutryn with a partitioning constant of 112.3 (experimental) and 92.6 (calculated). Also the predictions for diuron for kaolinite render matched very well. The worst match between experimental and predicted was found for the talc render for carbendazim with 3.8 (experimental) and 36.0 (calculated). However, the experimentally determined partition constant for the talc containing render for carbendazim is similar to the one found by Styszko et al. [38] for a commercial render (i.e.,  $4.0 \pm 0.8$ ). It is worth to remind at this point that carbendazim was the only biocide without a positive correlation between partition constant for polyacrylate and desorption constant from acrylate-based render normalized to the organic matter content. As it is also not sorbing strongly to any mineral phase, it must be concluded that in respect of some interactions the polymer and the mineral phases do not act independently but give something like a third phase. However, the distribution constants for the renders with talc and kaolinite did generally not differ significantly from each other. The only biocide which shows differences was tebuconazole: for this compounds, the value obtained for kaolinite render in the experiments is higher. However, based on the calculations the opposite would have been expected. There is a possibility that other ingredients of the render influence the sorption of this hydrophobic compound. However, the experimental results for the designed renders (Figure 3.1-6) match those found for an industry render ( $130.2 \pm 1.2$ ; [38]) very well. This is indicating towards the different phases of the render interact with each other in some cases and thus do not give independent results in composite materials.

### Mobility controlled by different fractions – Key findings

- Partitioning of biocides in the render-water system is dependent on the polyacrylate-water partitioning and the polyacrylate fraction in the render. Mineral phases do contribute to the partitioning of biocides in renders, but to a much smaller extent than the polymer.
- Differences in sorption ability between minerals can be explained by the different properties, such as hydrophobicity or the surface charge.
- Distribution constants of biocides from render can be predicted to some extent by summarizing partition constants of single ingredients; The distribution constants to polyacrylate-based render ( $D_{render}$ ) can be predicted linearly from the polyacrylate-water partition constants ( $\log K_{AcW}$ ) as a first assessment.
- New render recipes with different mineral/acrylate contents might reduce leaching of biocidal compounds.

### 3.1.3 Diffusion controlled mobility

The migration of biocides from paint films with different number of paint layers applied was tested. Figure 3.1-7a and b show the kinetic plot for relative mass flows versus square root of time of tebuconazole and iodocarb into water, as an example for all analyzed compounds. These plots were used to calculate the diffusion coefficients considering Eq. 4.2-9. The plots show that there is a basic linear relationship between the mass flows of biocides and square root of time. Thus, it is following Fick's law of diffusion. The plots also show a y-intercept that is zero, which is the ideal situation. Graphs for remaining biocides are shown in Bilag 7.1, additionally plots showing mass flows versus time are added in Bilag 7.2. Nevertheless, when plotted functions exceed an  $M_t/M_0$  of 0.6 they start to bend, as the polymeric films get seriously depleted. Furthermore, in case of iodocarb, *N*-octyl-isothiazolinone, tebuconazole and diuron the biocide concentrations in the first layers were too low and migration too fast; consequently, some time points were excluded based on the restriction  $M_t/M_0 < 0.6$  (Bilag 7.2).



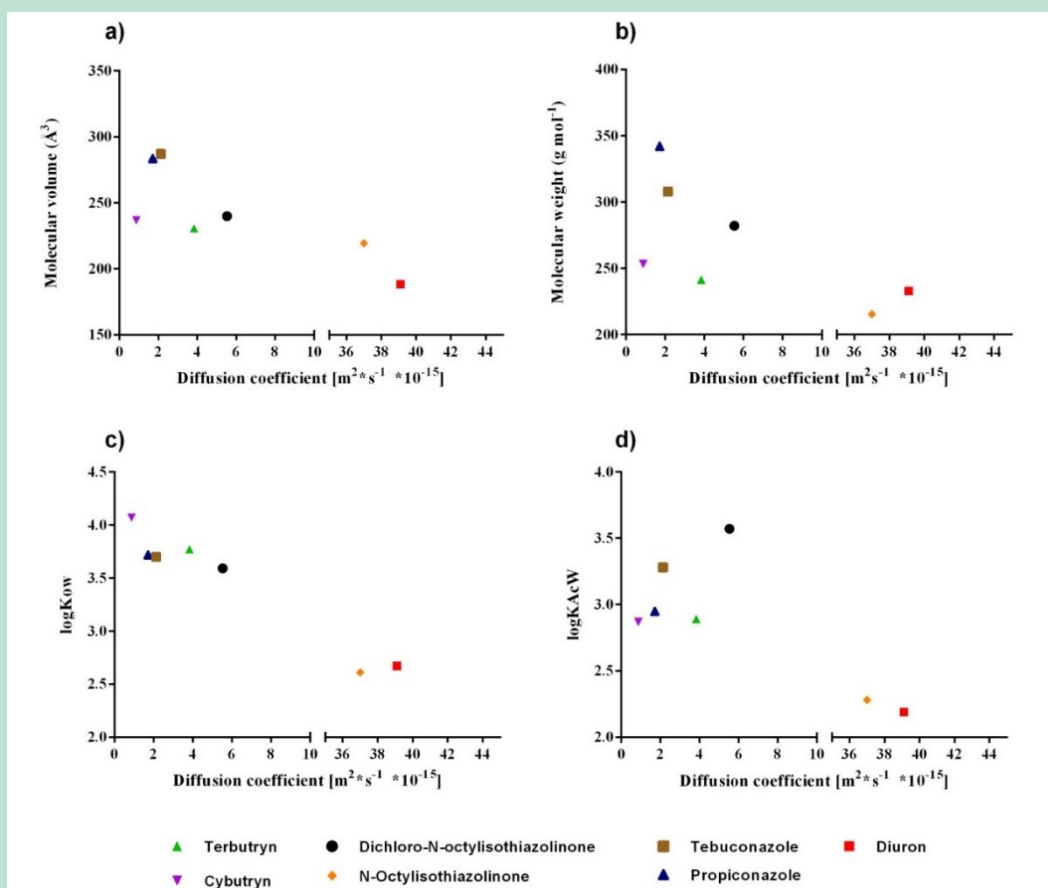
**Figure 3.1-7** Migration of a) tebuconazole and b) iodocarb from layered paint films into water represented as the fraction of biocide desorbed from paint film as a function of square root of time. Tebuconazole is one of the compounds with the slowest diffusion in this experiment, while iodocarb is the biocide with the highest diffusion coefficient in the dataset. The layer 1 data for iodocarb is not shown, as iodocarb was rapidly depleting from the paint.

There is a strict relation between the slope of the linear regression and the thickness of the paint (Eq. 4.2-9). The thickness of the paint layers was assessed by using an electronic calliper. This gave more contributions to the uncertainty than originally planned as the surfaces needed to have some roughness to maintain a good contact between tile and polymer film. The slope of the linear regression multiplied by paint layers thickness was used to calculate the diffusion coefficients in accordance to the Eq. 4.2-9 (Table 3.1-6). The final diffusion coefficient was calculated by averaging individual diffusion coefficients for separate layers. Slope values for tebuconazole presented in Figure 3.1-7a were one of the lowest among analyzed biocides, while iodocarb values (Figure 3.1-7b) were the highest. Hence, iodocarb showed the highest diffusion coefficient among all analyzed compounds ( $591 \cdot 10^{-15} \text{ m}^2 \text{ s}^{-1}$ ), while cybutryn showed the lowest one ( $0.876 \cdot 10^{-15} \text{ m}^2 \text{ s}^{-1}$ ). For comparison, the diffusion coefficient value found by Styszko and Kupiec [75] for cybutryn in acrylate renders was  $1.53 \cdot 10^{-9} \text{ m}^2 \text{ s}^{-1}$ . It is important to state that irgarol presented high acrylate-water partition constants (see paragraph 3.1.2.1) and Styszko and Kupiec reported problems with proper diffusion coefficient estimation for compounds with high partition constants. Another reason for such a difference between our

and their study is the different materials in question. This paper describes the diffusion in paints, not organic resin based renders, which are more complex materials.

**Table 3.1-6** Experimental diffusion coefficient values.

Biocide	$D_{\text{experimental}} [ \cdot 10^{-15} \text{ m}^2 \text{ s}^{-1} ]$
Iodocarb	591
Diuron	39.1
Terbutryn	3.83
Cybutryn	0.876
N-Octylisothiazolinone	37
Dichloro-N-octylisothiazolinone	5.53
Tebuconazole	2.13
Propiconazole	1.72



**Figure 3.1-8** Relationships between diffusion coefficient  $D$  and a) molecular volume b) molecular weight c) octanol-water partitioning coefficient  $\log K_{ow}$  d) acrylate-water partitioning coefficient  $\log K_{AcW}$  (Table 3.1-3). Iodocarb ( $591 \cdot 10^{-15} \text{ m}^2 \text{ s}^{-1}$ ) was excluded from the graphs to keep clarity.

In Figure 3.1-8 the diffusion coefficient  $D$  is related to (a) molecular volume, (b) molecular weight, (c) octanol-water partitioning coefficient  $\log K_{ow}$ , and (d) acrylate-water partition constant  $\log K_{AcW}$ , respectively. A good correlation between molecular volumes (Table 2.1-1) of the



migrating compounds to their diffusion coefficients can be found (Figure 3.1-8a). Generally speaking, the smaller the molecule, the faster the diffusion. The smallest molecule investigated in our study was iodocarb (182.91 Å<sup>3</sup>) and it was also the compound characterised with the highest diffusion coefficient. Diuron is slightly larger (188.41 Å<sup>3</sup>) with second highest diffusion coefficient in our dataset. The largest compound is tebuconazole (287.16 Å<sup>3</sup>) showing a very slow diffusion of  $2.13 \cdot 10^{-15} \text{ m}^2 \text{ s}^{-1}$ . Nonetheless, cybutryn seems to be an outlier, which probably is due other properties of this compound.

Comparing molecular weight of the respective biocide to the diffusion coefficients gave no clear correlation (Figure 3.1-8b), but lighter biocides seem to have higher diffusion coefficients. Between the lightest compound *N*-octylisothiazolinone ( $M_w$  215.36 g mol<sup>-1</sup>) and the heaviest compound propiconazole ( $M_w$  342.22 g mol<sup>-1</sup>), it was found a difference of an order of magnitude in the diffusion coefficient ( $37$  and  $1.72 \cdot 10^{-15} \text{ m}^2 \text{ s}^{-1}$ , respectively). For compounds with a similar molecular weight, other factors seemed to have influenced their diffusion coefficients. Obviously, size and weight are to some extent interdependent.

It can be seen in Figure 3.1-8c and d that the diffusion coefficient tends to decrease with increasing octanol-water and acrylate-water partition constants. However, some outliers are visible.

Only few studies have attempted to estimate diffusion of biocides in paints or other similar materials. Bergek et al. [76] measured the diffusion coefficient for *N*-octyliso-thiazolinone migrating from varnish coatings. In that study, a comparison between encapsulated biocides and biocides added in free state to the coating was made. Additionally, tests were performed on coatings dried for 7 and 28 days prior to the experiment. The diffusion coefficient for *N*-octylisothiazolinone added in the free state and dried for 7 days was  $30.7 \cdot 10^{-15} \text{ m}^2 \text{ s}^{-1}$ , which is very similar to the value obtained in our study  $37 \cdot 10^{-15} \text{ m}^2 \text{ s}^{-1}$ . The diffusion coefficient in case of the coating dried for 28 days was  $0.07 \cdot 10^{-15} \text{ m}^2 \text{ s}^{-1}$ . Experiments with encapsulated biocide resulted with values  $16.3 \cdot 10^{-15} \text{ m}^2 \text{ s}^{-1}$  and  $0.3 \cdot 10^{-15} \text{ m}^2 \text{ s}^{-1}$  for coatings dried 7 and 28 days, respectively.

### Diffusion controlled mobility – Key findings

- Diffusion coefficients of biocides in paints were around  $10^{-15} \text{ m}^2 \text{ s}^{-1}$ .
- Pure diffusion processes were able to drain the paints significantly from biocides within 30 h.
- The proposed experiment enables the assessment of the diffusion part of the leaching process.

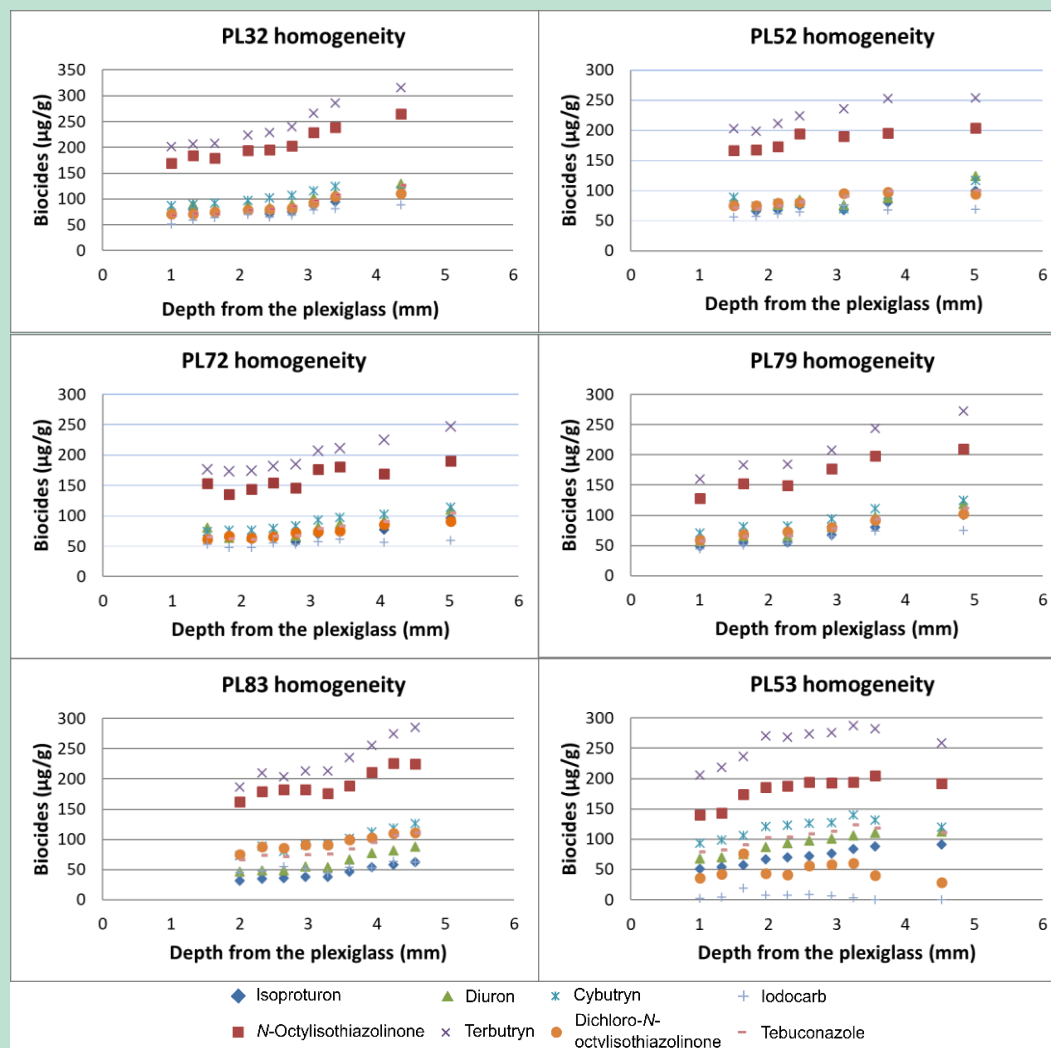


### 3.1.4 Depth resolved profiling

#### Characteristics of the render tiles

##### Homogeneity of render

The homogeneity of biocides inside the render prior to any treatment was assessed by identifying biocide profiles in 6 tiles that had not been subjected to any experimental procedures (Figure 3.1-9). The biocide concentrations were nearly always higher close to the render surface, indicating a systematic phenomenon causing the inhomogeneity.



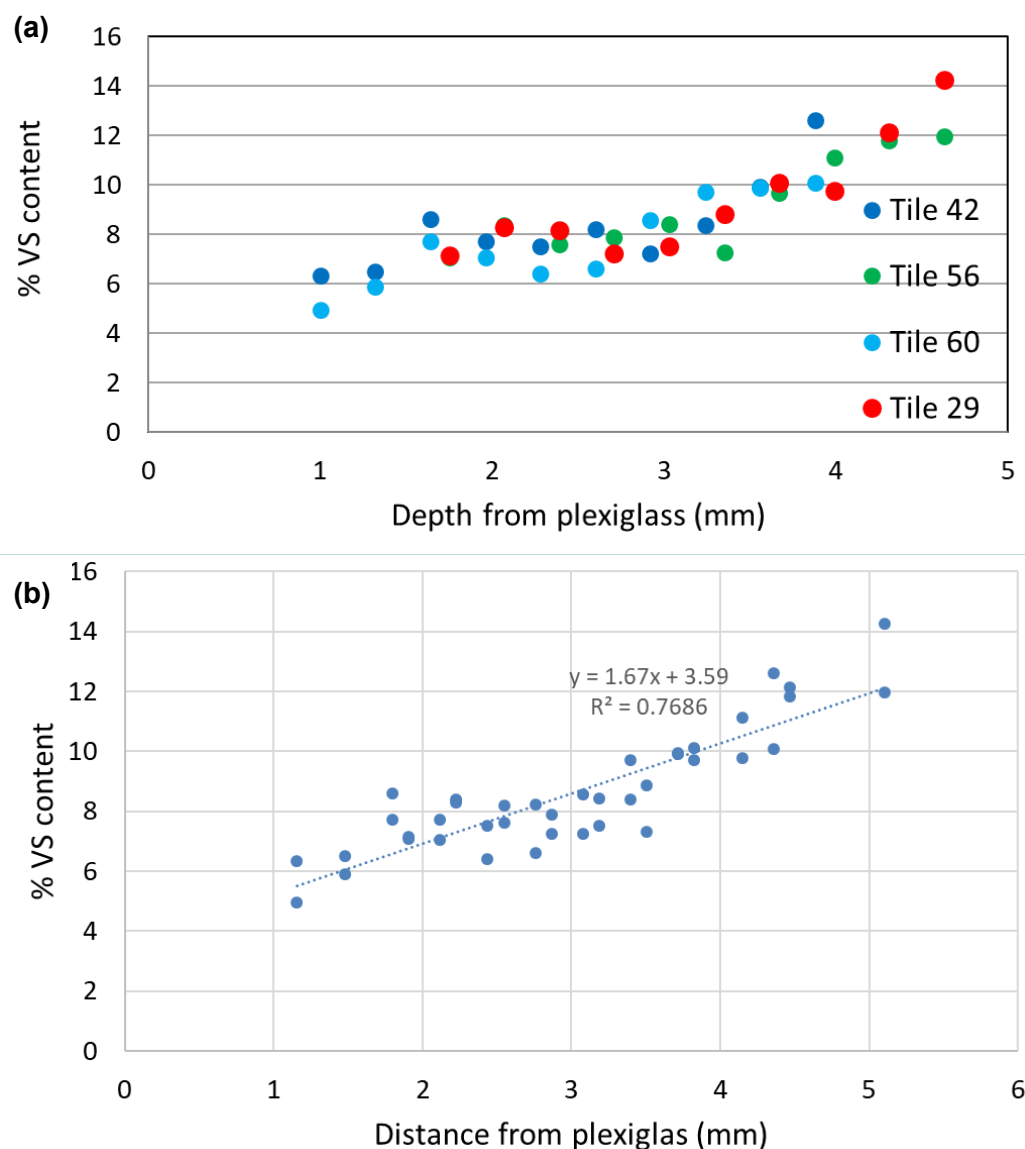
**Figure 3.1-9** Homogeneity of biocides in render tiles.

Slicing the render with the grinding machine, it was seen that the content of sand (2 mm grain size) was not homogeneously distributed through the depth of the render. There was a higher sand content closer to the Plexiglas surface. Biocides do not sorb significantly to sand (see paragraph 3.1.2.2) and the sand inhomogeneity in the render tiles will hence cause an inhomogeneity in biocide concentration.

This variation in sand content was probably an artefact of the application method; it is possible that the application with a filling knife forced the sand grains towards the Plexiglas tile. When the wet render was applied on the Plexiglas tiles, the tile was placed with the flat side up and the render applied. The render was then left to harden in the same position. It does though seem unlikely that gravity can have caused preferential settling of the sand grains during

drying, as such behavior was not observed in the moist render mixture while it was kept on stock for many months.

Whatever the cause of the inhomogeneity, the relative high concentration of sand close to the Plexiglas surface meant that the other materials constituting the render, the acrylate binder and the hydrated cement/lime, were at higher concentration at the top of the render. This was assessed by profiling the ratio of volatile solids (VS, the organic part of the render) to total solids (TS). The profiling of the organic content of the render material showed an increase from approx. 8% at depths of 1.5-3 mm to approx. 12% close to the render surface (Figure 3.1-10).



**Figure 3.1-10** Fraction of volatile organic solids (VS) profiled with the depth of the render.

For later use in analysis of the data, where it was needed to convert from TS to VS, the correlation between depth and VS-content was assessed. A simple linear correlation gave a coefficient of determination ( $R^2$ ) of 0.7686 (Figure 3.1-10b). Higher order correlations were also assessed but did not yield significantly better  $R^2$ -values. It was hence decided to use the linear correlation when converting from TS to VS where such was needed.

#### Porosity of intact render tiles

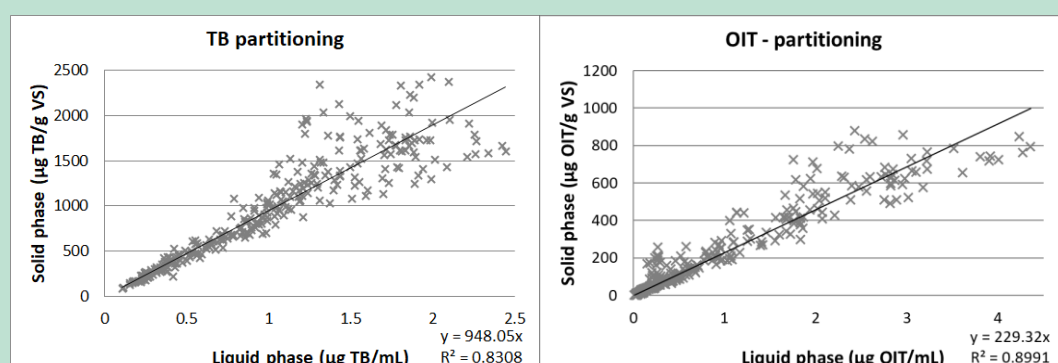
The porosity of the render, i.e. the fraction of the volume of voids over the total volume of the render, was found as the average of 3 tiles to be  $35.1\% \pm 1.3\%$ . The tiles were freeze dried and weighted, soaked in water for 2 days and weighted again. The porosity was found as the ratio of the mass of soaked up water to the total volume of the render (i.e. assuming a water density of  $1 \text{ g/cm}^3$ ).

#### pH of suspended render powder

The pH inside a render tile is governed by an equilibrium with the alkaline render compounds, mainly the cement/lime fraction, and the pore water. As a first approximation it was assumed that the pH of the render powder and demineralized water mix from the grinding of the tiles could represent the pore water pH. The render powder used for assessing the pH was from tiles that had been intermittent wet for 1 year. pH was determined on depth-profiled samples of 3 tiles, each containing 10 depth fractions. The depth profiling did not show a systematic change in pH with the depth into the render. The pore water pH was hence calculated as the mean of all 30 samples and found to be  $9.21 \pm 0.23$ .

#### Render-water distribution of biocides

The distribution of biocides between solid and liquid was estimated from the measured biocide concentrations in the supernatants and the wet powders. In total 31 tiles were included in this analysis, covering a total of 299 individual measurements of biocides in both liquid and solid phase (Figure 3.1-11 shows terbutryn and *N*-octylisothiazolinone as examples, all other figures in Bilag 3.1). There was quite some spread in the experimentally determined distribution data which might have been due to inhomogeneity in the sorbent and sorbate distribution within the render. The sorption showed no trend towards saturation at high liquid phase concentration and for all substances a linear sorption relation was hence assumed.



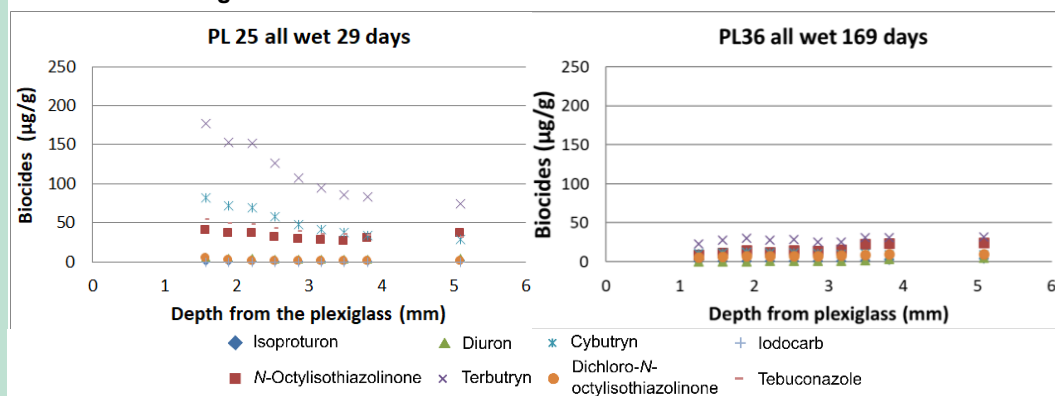
**Figure 3.1-11** Render-water distribution of biocides. The regression line was forced through zero.

#### Biocide profiles in render tiles subject to wetting

Examples of biocide profiles in render tiles after exposure to continuously wet condition (Figure 3.1-12), intermittent wetting (Figure 3.1-14) and dry diffusion (Figure 3.1-13) are shown in the following (the complete data set is shown in Bilag 8.2- Bilag 8.5). From the latter it is seen that diffusion in dry render occurred at a very low rate. The most significant diffusion was for IRG, where the biocide-spiked tile showed a decrease of roughly  $35 \mu\text{g/g}$  at the surface, which was reflected in a similar increase at the surface of the tile without spiked biocides. It seemed to have penetrated approx. 0.5 mm into the render during the 4 months of contact. For the other biocides that were spiked to the render, IP, TP, and DR showed a similar albeit less pronounced behavior. When comparing these low diffusion rates to diffusion under wet conditions it becomes obvious that the transport rates in a dry render were negligible com-

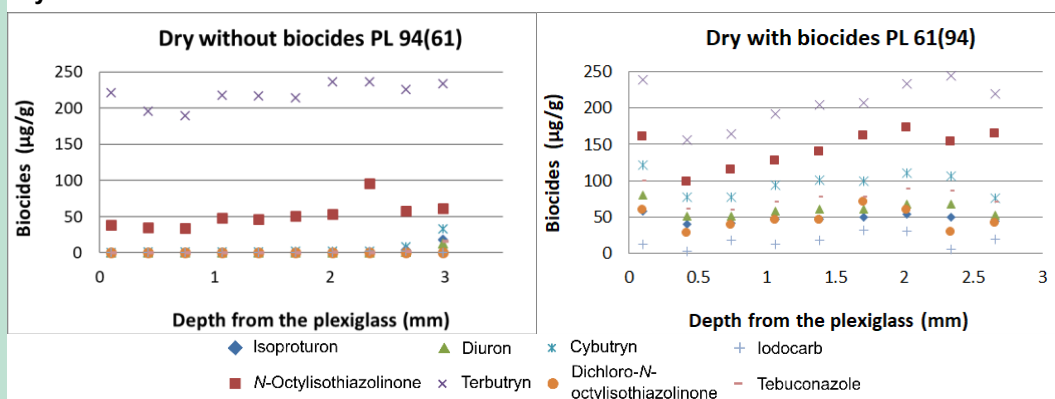
pared to those in a wet render. It can hence be concluded that transport via water in the pores of the render is the primary mechanism for the delivery of biocides to the render surface. In the tiles that were permanently wet or intermittently wetted, the biocide concentration closest to the surface decreased the fastest, followed by a general decrease of the biocides in the render. This general behavior is in good agreement with what can be expected when diffusion is the main transport process, as it here is the concentration gradient that drives the diffusion rate.

### Continuous wetting



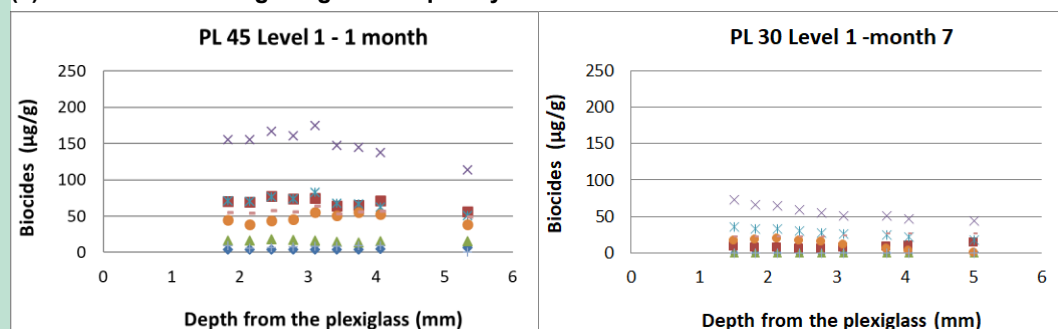
**Figure 3.1-12** Biocide profiles in render tiles subject to 29 (left) and 169 days (right) of continuous wetting.

### Dry diffusion

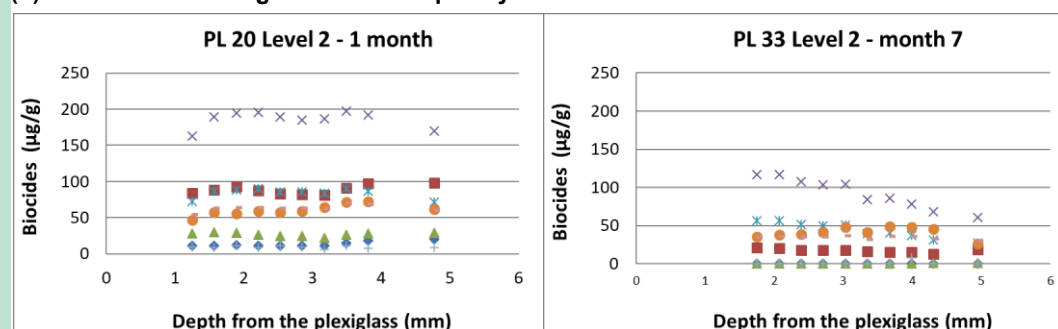


**Figure 3.1-13** Biocide profiles in render tiles subject to dry diffusion. Left tile “without biocides” was in direct contact with the right tile “with biocides” for 4 months.

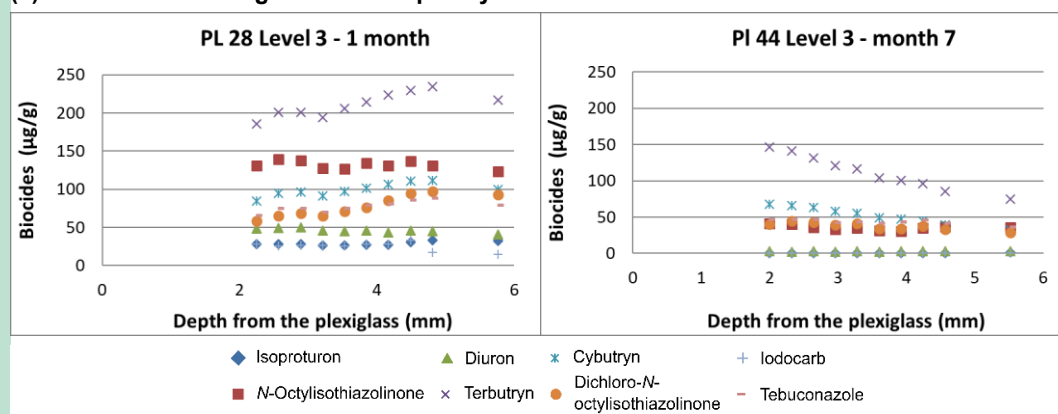
**(a) Intermittent wetting – highest frequency**



**(b) Intermittent wetting – medium frequency**

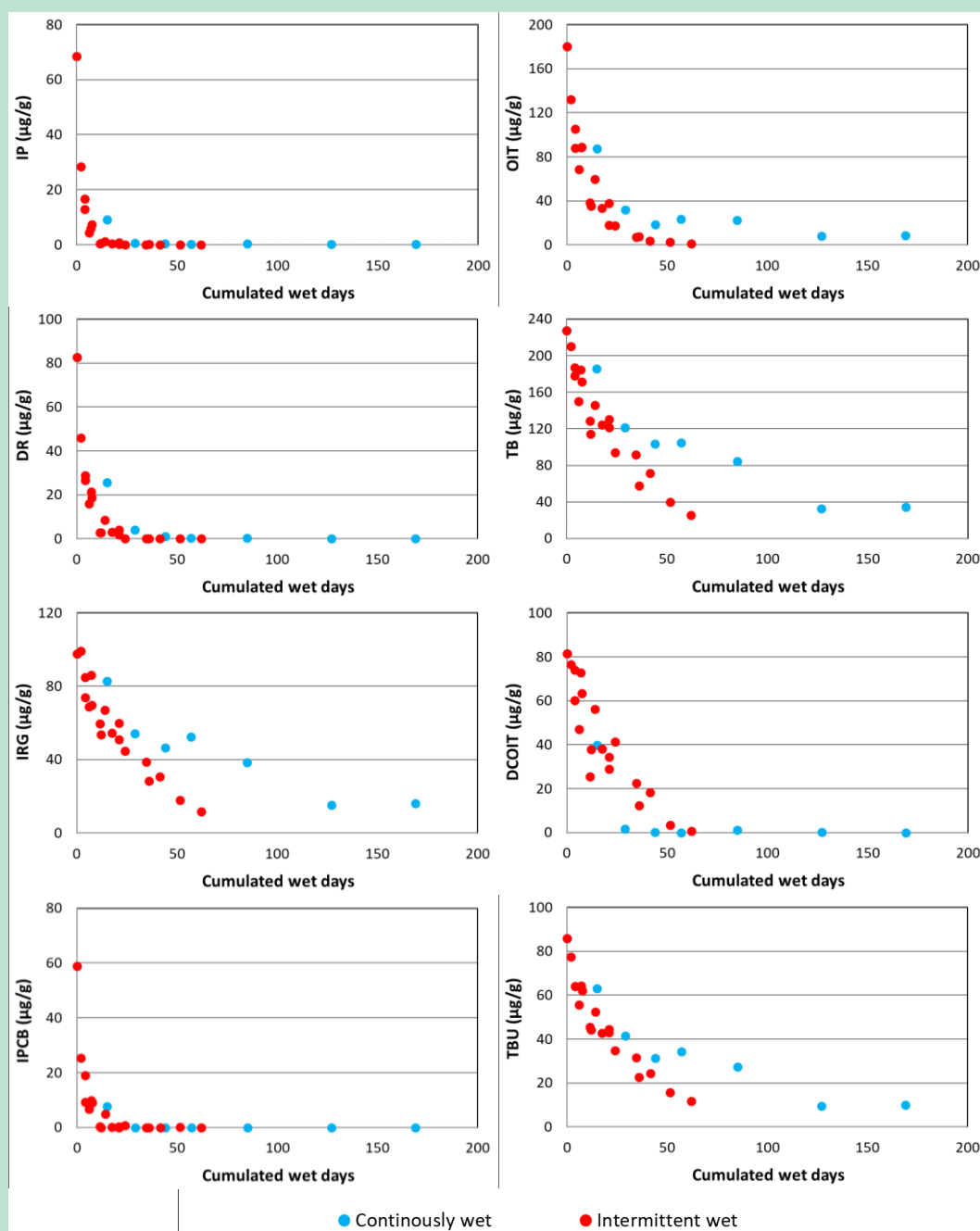


**(c) Intermittent wetting – lowest frequency**



**Figure 3.1-14** Biocide profiles in render tiles subject to intermittent wetting with (a) highest (3 days), (b) medium (3-6 days), and (c) lowest (9 days) wetting frequency.

To test if diffusion is the sole transport mechanism or if advective transport also plays a role, the overall rate of biocide loss from the continuously wet tiles were compared with that of the intermittently wet ones (Figure 3.1-15). The rate of biocide loss from the render per wet day was noticeable larger when the tile was subjected to wet-dry cycles compared to it being continuously wet. Only dichloro-*N*-octylisothiazolinone diverges from this pattern. This indicates that the wetting and drying process in itself creates advective transport of the biocides inside the render pores, which contributes significantly to the overall mass transport inside the render. As a consequence, biocide leaching tests based on submerging render into water can only be indicative in the estimation of leaching rates of real outdoor render surfaces.



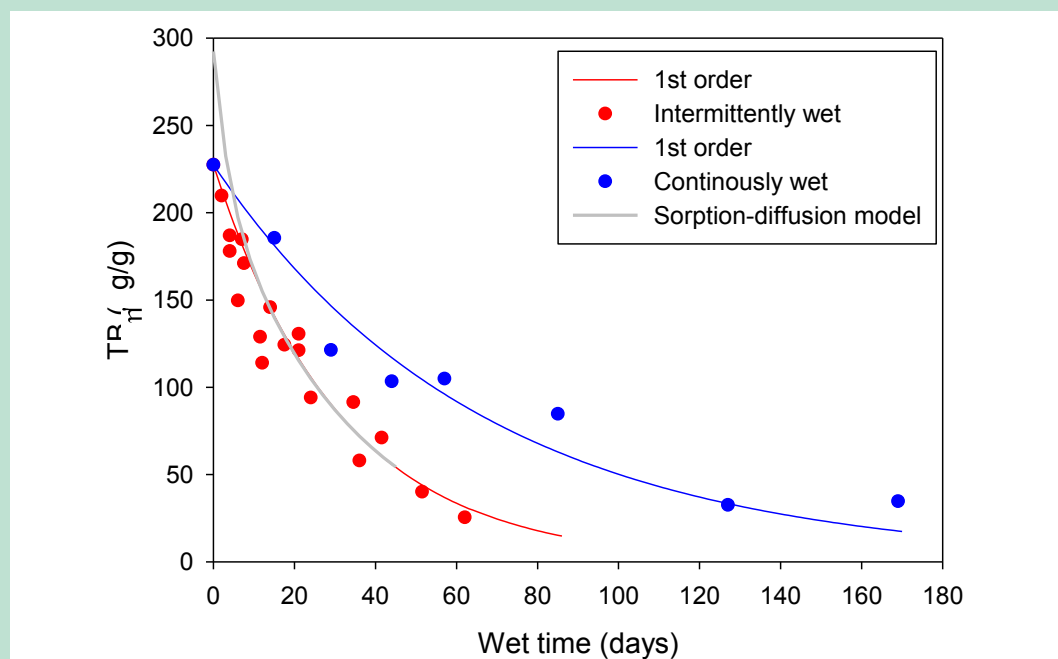
**Figure 3.1-15** Biocide residues in render tiles versus the time they have been wet (submerged).

### Diffusion kinetics

The overall diffusion kinetics – meaning the overall rate by which biocides leached from the render tiles – was generally well-described by a 1<sup>st</sup> order process in the residual biocide mass inside the render. Figure 3.1-16 illustrates this for TB.

A 1D box model was furthermore designed that simulated the diffusion and sorption inside the continuously wet render, taking into account the sorption capacity of the render as well as the pore water pH. Even though this model overestimated the initial mass loss from the render to the water somewhat, it was generally able to reproduce levels of biocides inside the render and did also reproduce the overall residual mass reasonably well. This indicates that both

sorption and diffusion must be taken into account when simulating the transport of biocides inside a polymeric render.



**Figure 3.1-16** Simulation of biocide loss as a simple 1<sup>st</sup> order process in the residual biocide mass in the render as well as simulation by a detailed 1D box model covering diffusion and sorption.

### Depth resolved profiling – Key findings

- Biocides can be inhomogenously distributed in render as its application method can affect how the inorganic constituents are distributed.
- Transport of biocides in renders predominantly occurs through the water-filled pores whereas the transport through the dry render is negligible. Advective transport due to wetting and drying of the render is an important driver for biocide transport to the render surface.
- Biocide transport in a continuously wet render can be described as a combination of sorption and diffusion, while intermittently wet renders need to include advective transport.



## 3.2 Photodegradation of biocides

### 3.2.1 Identification of photodegradation products

#### Terbutryn

Degradation processes are assumed to be the most important loss mechanisms [15] and in particular photodegradation processes in such systems. In order to gain knowledge about possible transformation products, a photodegradation study was performed and samples were analyzed with high resolution mass spectrometry. The following m/z-ratios have been detected in the QToF-spectra for the diverse transformation products (TPs): 140.0933, 184.1194, 168.1253, 212.1518, 196.1568, 226.1674, 239.1988, and 258.1394. In the following the TPs are nominated following the nominal mass and chemical structures of the proposed compounds are listed in Table 3.2-1. An overview over the proposed degradation pathway is shown in Figure 3.2-1. The mass difference between TP-258 and terbutryn corresponds to the insertion of one oxygen atom. This coincides with a compound that has previously been detected in biological wastewater treatment processes (terbutryn sulfoxide) [23]. TP-226 corresponds to an exchange of the sulfur of terbutryn with oxygen which would form terbumeton, another triazine-based herbicide. The remaining products derived from the losses of the side chains of terbutryn (TP-196: -SCH<sub>3</sub>; TP-140: -<sup>1</sup>Bu & -SCH<sub>3</sub>; TP-168: -CH<sub>2</sub>CH<sub>3</sub> & -SCH<sub>3</sub>). This photodegradation pathway has been described by Kiss et al. [24]. In addition, TP-212 and TP-184 refer to the replacement of the thiomethyl-group by hydroxyl (TP-212) followed by a cleavage of the ethyl-group (TP-184). These products have also been described in connection with biological degradation processes in farm ponds [25]. The presence of all suggested transformation products was validated in this study by analytical standards using retention times and MS/MS-data and all transformation products were subsequently quantified. In the present study the cleavage of the ethyl- or the butyl-group before the thiomethyl-group has not been detected. Nonetheless, desethyl-terbutryn (M1) was added to the studied degradation compounds, as it has previously been analyzed in leachates from renders [15].

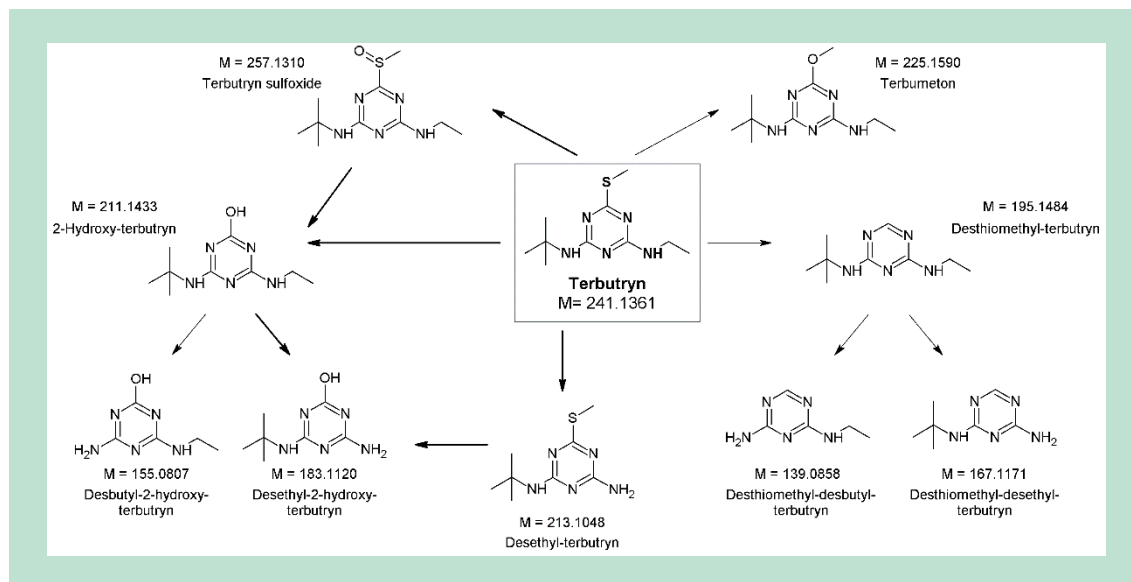
**Table 3.2-1** Terbutryn and the detected photodegradation products: detected m/z in QToF with deviation of measured versus theoretical mass ( $\Delta m/z$ ), compound name, abbreviation and chemical structure.

Transformation product	Detected m/z [Da] $\Delta m/z$ [mDa]	Compound (Abbreviation)	Structure	Properties (calc. with [26])
	242.1445 -0.6	Terbutryn (TB)		WS: 17 mg L <sup>-1</sup> Log K <sub>OW</sub> : 3.77
TP-258	258.1394 -1.1	Terbutryn sulfoxide (TB-SO)		WS: 7 mg L <sup>-1</sup> Log K <sub>OW</sub> : 4.1
TP-196	196.1568 -1.1	Desthiomethyl-terbutryn (TB-DesS)		WS: 264 mg L <sup>-1</sup> Log K <sub>OW</sub> : 2.6
TP-168	168.1253 -0.9	Desthiomethyl-desethyl-terbutryn (TB-DesS-DesE)		WS: 2791 mg L <sup>-1</sup> Log K <sub>OW</sub> : 1.6
TP-140	140.0933 -0.2	Desthiomethyl-desbutyl-terbutryn (TB-DesS-DesB)		WS: 20000 mg L <sup>-1</sup> Log K <sub>OW</sub> : 0.7

**Table 3.2-1** continue.

Transformation product	Detected m/z [Da] $\Delta m/z$ [mDa]	Compound (Abbreviation)	Structure	Properties (calc. with [26])
TP-212	212.1518 -1.2	2-Hydroxy-terbutryn (TB-OH)		WS: 906 mg L <sup>-1</sup> Log K <sub>OW</sub> : 1.5
TP-184	184.1194 -0.1	Desethyl-2-hydroxy-terbutryn (TB-OH-DesE)		WS: 8608 mg L <sup>-1</sup> Log K <sub>OW</sub> : 0.6
TP-226	226.1674 -1.2	Terbumeton (TBM)		WS: 73 mg L <sup>-1</sup> Log K <sub>OW</sub> : 3.6
Added for comparative reasons		Desethyl-terbutryn (M1)		WS: 174 mg L <sup>-1</sup> Log K <sub>OW</sub> : 2.7

The kinetic study on photodegradation of terbutryn in water showed that terbutryn was readily degraded by UV-light following a first-order kinetic with a half-life of 11.9 h (see Bilag 9.2). The most important transformation products were desthiomethyl-terbutryn (TB-DesS), 2-hydroxy-terbutryn (TB-OH), and terbutryn sulfoxide (TB-SO) with concentrations ranging from 1000 to 10000 µg L<sup>-1</sup>. However, terbutryn sulfoxide reached highest concentrations after 20 h, where-upon it was degraded as well. Within the experimental time, the other compounds reached concentrations below 50 µg L<sup>-1</sup>.



**Figure 3.2-1** Proposed terbutryn degradation pathway.

### N-Octylisothiazolinone

The UV-irrigation of OIT led to degradation products with the following signals in electrospray positive ionization (ESI<sup>+</sup>) scans: 214.1252 Da, 158.1527 Da, 198.1486 Da, 184.1701 Da, 172.1696 Da, 130.1954 Da and 216.1595 Da. In the following, the observed peaks are named according to their nominal mass and are listed in Table 3.2-2 together with the suggested

systematic compound name. Differences between theoretical and determined mass ( $\Delta m/z$ ) as well as estimated physico-chemical properties for the suggested compounds are also shown in Table 3.2-2, while the suggested structures are shown in Figure 3.2-2.

TP-214 had the same mass as OIT itself, as well as similar fragmentation pattern, but eluted at a different chromatographic retention time. This suggests photo isomerization as described by Rokach and Hamel [77] for 2-substituted-isothiazol-3(2*H*)-ones: after an initial break of the activated N-S-bond, the isothiazol-3(2*H*)-one isomerized into the corresponding thiazol-2(3*H*)-one (Figure 3.2-3). Additionally, the break of the N-S-bond led to the stepwise degradation of the ring, as the molecular ions of the remaining transformation products correspond to *N*-octylprop-2-enamide (TP-184a), *N*-octylacetamide (TP-172), *N*-octylformamide (TP-158) as well as octylamine (TP-130) as a final product.

A molecular ion of 216.1595 Da, which corresponds to *N*-octyl malonamic acid (TP-216), has been detected in very low intensity, which might be the initial intermediate of the isothiazolinone ring degradation. All previously mentioned transformation products were validated by analytical standards. Octylamine and *N*-octylacetamide were also hypothesised as a degradation product of DCOIT by Sakkas et al. [78]; however, they suggested different intermediate products, which were not detected in the present study. *N*-Octyl malonamic acid has been described as biotransformation product [79], while the remaining four have not been described as transformation products of DCOIT so far. An overview of the proposed photodegradation pathways of OIT is presented in Figure 3.2-2. The environmental assessment report for octylisothiazolinone describes photodegradation resulting in 2-(*n*-octyl)-4-thiazolin-2-one, a mixture of *N*-octyl malonamic acid and oxamic acid metabolites, *N*-octylacetamide and several other not resolved transformation products [80].

**Table 3.2-2** OIT photodegradation products: detected molecular ions in QToF (ESI+) with deviation of measured versus theoretical mass ( $\Delta m/z$ ), product ion spectra, compound name, chemical formula, validation with analytical standard (yes/no), and estimated physico-chemical properties (WS: water solubility; Log  $K_{OW}$ : octanol-water partition coefficient,  $p_{vap}$ : vapour pressure, Log  $K_{OA}$ : octanol-air partition coefficient).

Abbr.	RT [min]	Detected $m/z$ [Da] $\Delta m/z$ [mDa]	Product ion spectrum $m/z$ [Da] CE: 40V	Compound (Abbreviation) Chemical formula	Validation analytical standard	Properties (calc. with EPI suite [81])
OIT	10.12	214.1259 -0.7	102.0023, 57.0749, 43.0615, 83.9922	2-Octylisothiazol-3(2 <i>H</i> )-one $C_{11}H_{19}NOS$	yes	WS: 302 mg L <sup>-1</sup> Log $K_{OW}$ : 2.61 $p_{vap}$ : 0.0266 Pa Log $K_{OA}$ : 8.5
TP-214	14.07	214.1252 -1.4	102.0020, 77.0413, 141.0004, 57.0737, 43.0601	3-Octylthiazol-2(3 <i>H</i> )-one (OT) $C_{11}H_{19}NOS$	yes	WS: 27 mg L <sup>-1</sup> Log $K_{OW}$ : 3.7 $p_{vap}$ : 0.0031 Pa Log $K_{OA}$ : 6.3
TP-158	11.06	158.1527 -1.8	41.0444, 43.0599, 46.0332, 57.0732, 39.0293, 77.0399, 71.0878, 60.0478	<i>N</i> -Octylformamide (OFA) $C_9H_{19}NO$	yes	WS: 776 mg L <sup>-1</sup> Log $K_{OW}$ : 2.29 $p_{vap}$ : 0.0798 Pa Log $K_{OA}$ : 7.3
TP-184a	12.03	184.1701 0	55.0210, 72.0459, 43.0593,	<i>N</i> -Octylprop-2-enamide (OPA) $C_{11}H_{21}NO$	yes	WS: 120 mg L <sup>-1</sup> Log $K_{OW}$ : 3.1 $p_{vap}$ : 0.013 Pa Log $K_{OA}$ : 8.5

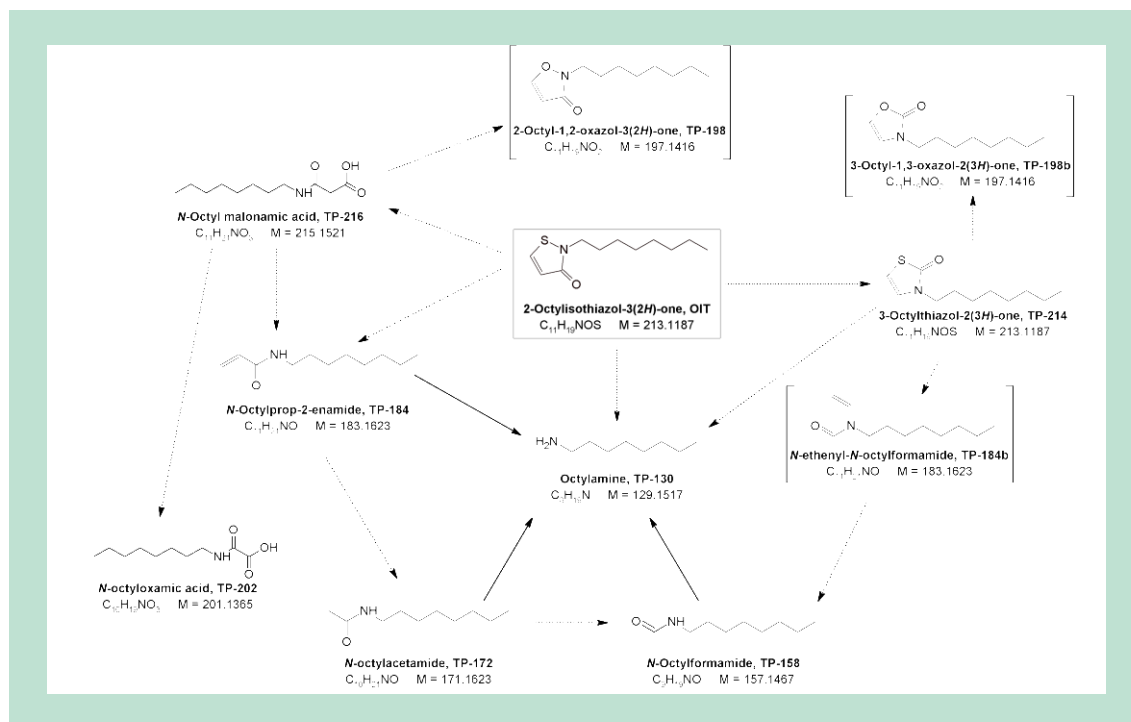
**Table 3.2-2** continue.

Abbr.	RT [min]	Detected m/z [Da] $\Delta m/z$ [mDa]	Product ion spectrum m/z [Da] CE: 40V	Compound Chemical formula	Validation analytical standard	Properties (calc. with EPI suite [81])
TP-172	11.14	172.1696 -0.5	60.0470, 57.0722, 41.0453, 89.9402, 112.9550	<i>N</i> -Octylacetamide (OAA) $C_{10}H_{21}NO$	yes	WS: 276 mg L <sup>-1</sup> Log K <sub>OW</sub> : 2.74 $\rho_{vap}$ : 0.031 Pa Log K <sub>OA</sub> : 7.9
TP-130	6.95	130.1594 -0.4	41.0461, 43.0612, 39.0304, 57.0742, 71.0880	Octylamine (OAM) $C_8H_{19}N$	yes	WS: 3147 mg L <sup>-1</sup> Log K <sub>OW</sub> : 2.8 $\rho_{vap}$ : 131 Pa Log K <sub>OA</sub> : 4.4
TP-216	10.26	216.1595 -0.5	n.a.	$C_{11}H_{21}NO_3$ <i>N</i> -Octyl malonamic acid (OMA)	yes	WS: 720 mg L <sup>-1</sup> Log K <sub>OW</sub> : 2.0 $\rho_{vap}$ : 5.75 10 <sup>-5</sup> Pa Log K <sub>OA</sub> : 12.3
TP-198	12.85	198.1486 -0.8	86.0251, 57.0732, 43.0592, 41.0442	$C_{11}H_{19}NO_2$ 2-Octyl-1,2-oxazol-3(2H)-one? 3-Octyl-1,3-oxazol-2(3H)-one?	no	
TP-184b	11.28	184.17 -0.1	72.0471, 41.0459, 43.0598, 166.1592	$C_{11}H_{21}NO$ <i>N</i> -ethenyl- <i>N</i> -octylformamide?	no	
TP-188	7.36	188.1646	44.0546, 43.0596, 57.0737, 71.0876, 142.1587, 119.9421		no	
TP-182	12.48	182.1533	53.0059, 70.0309, 57.0737, 43.0595		no	
TP-144	9.16	144.139	41.0434, 43.0608, 57.0732, 60.9893, 74.0609, 88.0769		no	

Based on molecular ion and fragmentation pattern, additional transformation products were suggested. Via some intermediate reaction steps, an S-O exchange might have led to the oxazolone derivate (TP-198). TP-184b might be the corresponding degradation product to TP-184a, *N*-ethenyl-*N*-octylformamide, deriving from the degradation of 2-octylthiazol-2(3*H*)-one (TP-214). MS2-scans of those two compounds as well as suggested fragmentation pattern can be found in Bilag 9.1. Other degradation products have been detected at 188.1646 Da (TP-188), 182.1533 Da (TP-182), and 144.139 Da (TP-144). In older studies acetic acid and formic acid were determined as degradation products of CMI and DCOIT [82]. However, as in the present study the lower limit of the MS-scan was set to 100 Da, they would not have been detected. *N*-octyl oxamic acid has been determined as degradation product (bio-/photodegradation, hydrolysis) in previous studies for DCOIT [83] and was added in the following analysis.

The auxiliary kinetics experiments was performed to get a first impression on the stability of OIT and its transformation products. It indicates that the photodegradation of OIT in tap water is following first-order kinetics ( $r^2=0.9538$ ) under the chosen conditions (tap water; 254 nm;  $2.31 \cdot 10^{-10}$  Einstein cm<sup>-2</sup> s<sup>-1</sup>), with a half-life of 28 h and a photodegradation rate constant of 0.026 h<sup>-1</sup> (Bilag 9.2). Dark controls at 4°C showed less than 10% degradation of OIT within one week. For the seven quantified degradation products 3-octylthiazol-2(3*H*)-one, *N*-octylprop-2-enamide, *N*-octylacetamide, *N*-octylformamide as well as octylamine, *N*-octyl malonamic acid, and *N*-octyl oxamic acid maximum concentrations ranging from a few mg mL<sup>-1</sup>

(*N*-octylacetamide) to 2000 mg mL<sup>-1</sup> (octylamine) were detected. Within 48 h of irrigation, the concentrations increased for all compounds besides 3-octylthiazol-2(3*H*)-one. 3-Octylthiazol-2(3*H*)-one peaked after about 10 h at 1000 mg mL<sup>-1</sup>, whereupon it was degraded as well (Bilag 9.2). In the photodegradation experiments of OIT in solution, the concentrations of the seven validated compounds explained more than 97% of the mass balance after 25 h irrigation. However, after 48 h just 80% could be accounted for.



**Figure 3.2-2** Proposed photodegradation pathway of OIT in water [in brackets: suggested compounds based only on HR-MS data, not validated by analytical standard].

With a photodegradation half-life of 28 h in solution while irradiated with  $2.31 \cdot 10^{-10}$  Einstein cm<sup>-2</sup> s<sup>-1</sup>, the degradation rate of OIT is comparable to the chlorinated analogue DCOIT [78]. As known for other isothiazol-3(2*H*)-ones, the photodegradation of OIT is also initiated by a cleavage of the ring structure. However, although being the most important transformation product in previous studies [78, 82], *N*-octyl malonamic acid is not or only tentatively detected in the present study at very low concentrations. This might result from the monochromatic light source (254 nm) or another possibility is that the degradation of *N*-octyl malonamic acid is much faster than its formation.

### 3.2.2 Biocide transformation on facade surfaces

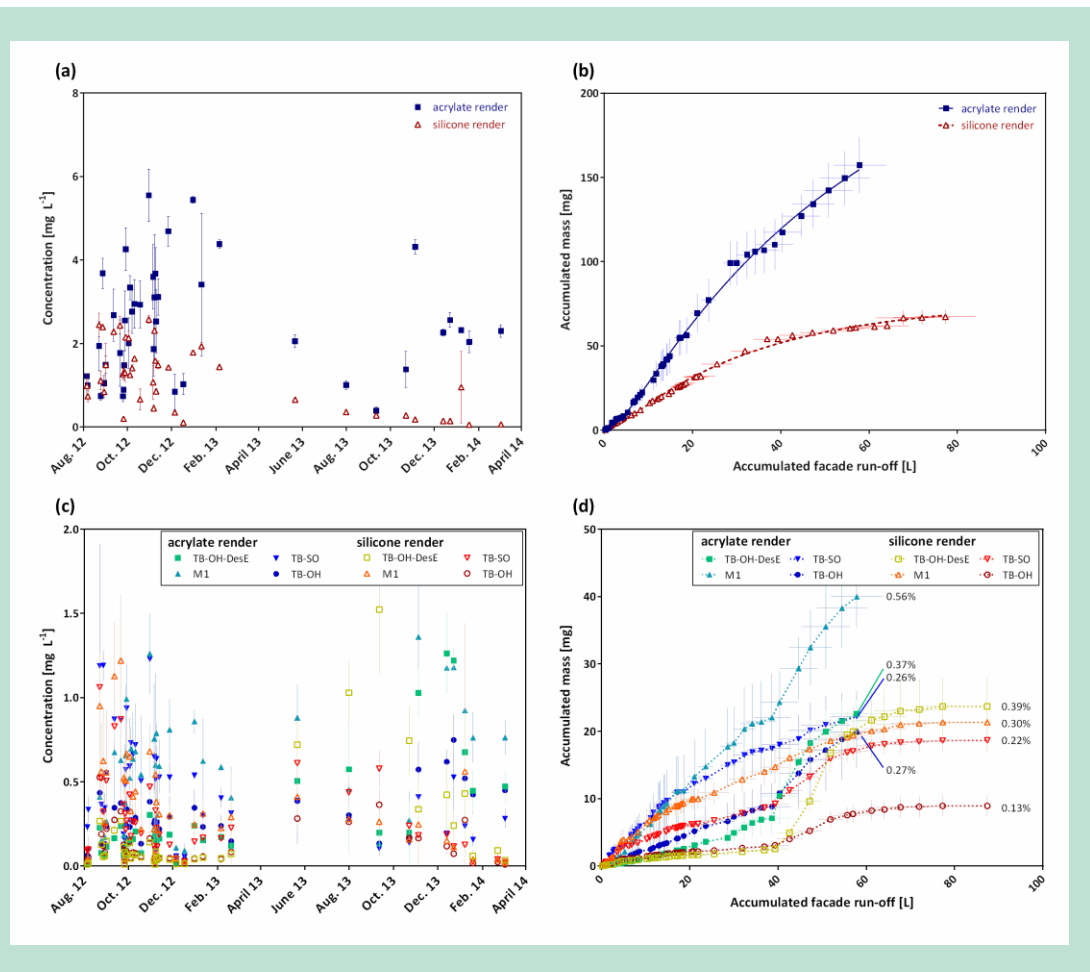
#### Terbutryn

##### *Leaching performance of terbutryn and its metabolites*

As shown in Figure 3.2-3a, the terbutryn concentrations in the runoff were highly varying in the beginning of the panel lifetime and leveled out, as well as became more stable with exposure time. Elevated concentrations of terbutryn from the acrylate render in the end of the exposure time might be due to the heavy storm events in autumn 2013, which might have caused unnoticed micro-cracks in the render or abrasion from the coating surface and, hence, exposed new parts of the render directly to rain. Initial concentrations of about 1-5 mg L<sup>-1</sup> were comparable as those experienced by Burkhardt et al. [15] for the leaching of terbutryn from a model house in Switzerland. Due to different application layer thicknesses, the acrylate rendered panels contained more terbutryn per square meter than the silicone rendered ones. The con-

centration in the leachate  $c_{leachate}$  is expected to be a function of the initially applied concentration  $c_0$  according to Eq. 5.2-1:

$$c_{leachate} = f(c_0) \quad (\text{Eq. 5.2-1})$$



**Figure 3.2-3** Left: concentrations over time of (a) terbutryn and (c) its four most important transformation products in the run-off from artificial walls equipped with acrylate and silicone resin render exposed to natural weather conditions. Right: accumulated mass dependent on the accumulated run-off volume of (b) terbutryn and (d) its four most important transformation products. Error bars: standard error of mean from three panels. M1: Desethyl-terbutryn, TB-SO: Terbutryn sulfoxide, TB-OH: 2-Hydroxy-terbutryn, TB-OH-DesE: Desethyl-2-hydroxy-terbutryn; percentage in (d) represents the fraction of initial terbutryn content transformed into the specific product.

The initial concentration in the acrylate render was 1.5 times higher than the initial concentration in silicone render. Nevertheless, average concentrations in the run-off from acrylate render were five times higher than the ones from silicone render for the single rain events. Hence, in addition to the initial concentrations, different render parameters played an important role and determined the exact amount of leaching. The equilibrium partition constant ( $D_{render/water}$ ) for cybutryn (irgarol), a comparable triazine biocide, is three to five times higher for silicone than for acrylate render [22], which can be the reason for a lower emission from silicone render. Also the total run-off volume differed between the two render types with 57 L (acrylate render) versus 77 L (silicone render), which might be caused by different surface structures of the two render types. In conclusion, the material properties seem to have a strong influence on the leaching amount of terbutryn. The linear correlation of the amount leached and the accu-

mulated facade run-off (Figure 3.2-3b) during the first 30 L (5-6 months of exposure) points towards the fact that driving rain is the main force determining the leaching in the early lifetime of a facade. In the second part of the experiment the emissions decreased. Particularly in the case of the silicone render equipped panels this was remarkable, as the emissions reached a plateau. Comparing the total emissions per panel over the whole experimental time with the initial amount reveals that only about 3% were leached from each panel (different initial masses due to different total render mass per panel). The equality of the values for both render types was most probably only coincidence. Figure 3.2-3b shows clearly that the emissions from silicone render decreased considerably in the end of the exposure time while the emissions from acrylate render were still ongoing. Hence, with longer exposure time the emissions from acrylate render are expected to increase further while the leached-fraction would nearly stay unchanged for silicone render.

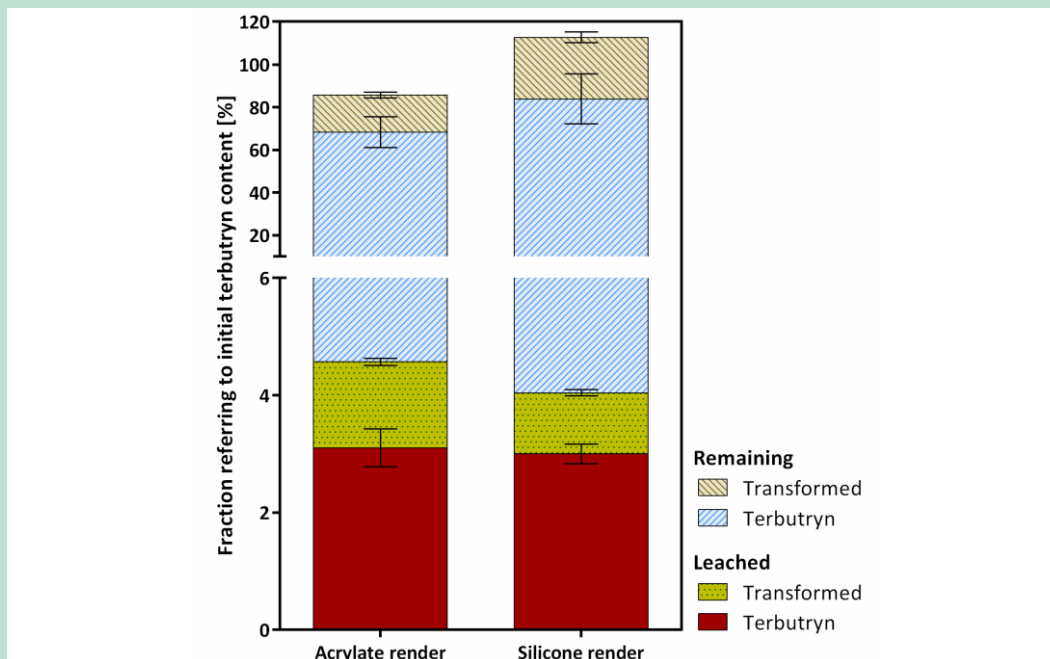
In general, the four main degradation products in the runoff from the panels were terbutryn sulfoxide, 2-hydroxy-terbutryn, desethyl-terbutryn, and desethyl-2-hydroxy-terbutryn. The concentrations varied between 0.05 and 1.5 mg L<sup>-1</sup>. While being the most important degradation compounds under laboratory conditions, desthiomethyl-terbutryn is negligible under natural weather conditions. In contrast, desethyl-terbutryn was detected in as high concentrations as terbutryn sulfoxide or 2-hydroxy-terbutryn, suggesting that either the wider solar spectrum compared to the monochromatic UV-lamp or a specific photosensitizer is promoting its formation. It cannot be excluded that biological degradation is occurring on the coating surface. As shown in Figure 3.2-3c, the general emission of transformation products was rather similar with the terbutryn emissions: slightly higher in the beginning of the exposure and decreasing afterwards as well as a high increase after the storms in autumn 2013. Only for desethyl-2-hydroxy-terbutryn increasing concentrations in the summer months 2013 were detected. An increase in concentrations for degradation products as experienced by Burkhardt et al. [15] was not detected in the present study. In total, 1.5% (acrylate) and 1.0% (silicone) of terbutryn was recovered as transformation products in the run-off. As shown in Figure 3.2-3d, the ratios between the transformation products from the two types of renders were different, which indicates that the different materials have an influence on the individual transformation kinetics.

#### *Closing the mass balance of terbutryn on renders*

The terbutryn fraction remaining in the panel was 64% and 80% for acrylate and silicone render, respectively. As there is still a rather high percentage remaining in the render, the decrease in emissions indicates changes in the controlling factors that determining the leaching. This might include diffusion controlled processes or changes in the surface of the material (including possibly gradients in the system). However, the total mass balances showed gaps of 17 and 33%, respectively, and besides leaching other processes (such as photodegradation) must lead to disappearance of the active ingredient.

The analysis of transformation products remaining in the render revealed that up to 25% terbutryn was transformed and the respective transformation products remained on (or re-entered) the render. About 10% of the initial terbutryn was transformed into M1 and remained in the render. Other products detectable in the render were 2-hydroxy-terbutryn (3 and 4% of terbutryn transformed and remained in the acrylate and silicone render, respectively), desethyl-2-hydroxy-terbutryn (1 and 6%) as well as terbumeton (1 and 3%). Although detectable in run-off water, terbutryn sulfoxide was present in the render only at very low concentrations, while terbumeton, only marginally present in run-off, was detected in the render. As formation and further degradation of the transformation products are ongoing processes, it is difficult to relate the leached amount to its totally formed mass. However, comparing the leached amount of each transformation product with its total amount detected in both, the leachate or the render, the fraction detected in the leachate is ranging between 0.5% (terbumeton) and 77% (terbutryn sulfoxide).





**Figure 3.2-4** Mass balance of terbutryn from artificial walls exposed to natural weather conditions: leached terbutryn - terbutryn detected in run-off water (average from 3 panels), leached transformed - sum of transformation products detected in run-off (average from 3 panels), remaining terbutryn - terbutryn in render after 19 month exposure (average of 10 extracts from one panel), remaining transformed - sum of transformation products in render after 19 month exposure (average of 10 extracts from one panel); error bars: standard error of mean for terbutryn and the sum of transformation products.

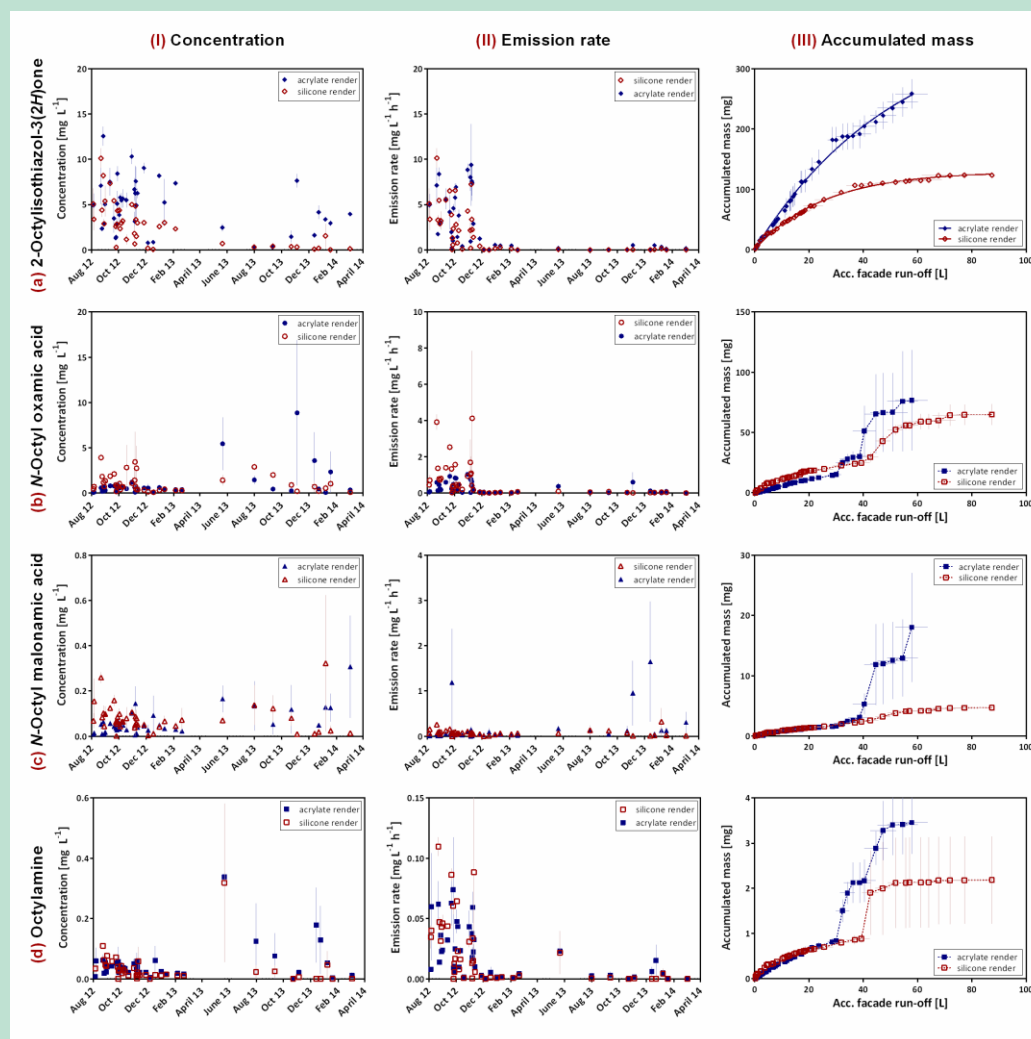
In consideration of the transformation processes and partitioning of the transformation products into the render, the mass balance could be closed (Figure 3.2-4). Contrary to expectations, the major fraction of transformation products is remaining in the material and not washed off immediately. The overall variability was predominantly determined by the variability of the terbutryn fraction remaining in the render, which was high, which might be due to inhomogeneous leaching of terbutryn from the different parts of the wall. Looking at the concentration ratio of the transformation products to terbutryn over time, it is obvious that in the later exposure time the emissions of transformation products were higher than those of terbutryn (see Bilag 10.2). This is particularly visible in the case of silicone render. Hence, the coating is serving as a temporary sink for degradation products, and only slowly, the material is releasing the degradation products with time. For the long-term performance of terbutryn equipped coatings this means that even after terbutryn emissions have ended, emissions of degradation products might still continue.

### **N-Octylisothiazolinone**

#### *Emissions of OIT and its degradation products*

Over the entire exposure time of 19 months, the concentrations of OIT in the wall run-off due to rain events ranged between below detection limit ( $< 0.02 \text{ mg L}^{-1}$ ) and  $12 \text{ mg L}^{-1}$  (silicone render) and  $14 \text{ mg L}^{-1}$  (acrylate render), respectively. The concentrations were varying considerably from event to event. However, a general decreasing trend is visible (Figure 3.2-5.1a). Six of the seven studied degradation products – octylamine, *N*-octyl oxamic acid, *N*-octyl malonic acid, *N*-octylformamide, *N*-octylacetamide, and *N*-octylprop-2-enamide – were detectable in most of the samples in concentrations up to  $8.8 \text{ mg L}^{-1}$  (*N*-octyl oxamic acid). 3-

Octylthiazol-2(3H)-one was detected sporadically in concentrations up to  $10 \mu\text{g L}^{-1}$ . In general, there is no trend detectable for the concentrations of degradation products (Figure 3.2-5.Ib-d).



**Figure 3.2-5** (I) Changes of (a) the OIT concentration and (b-d) its three most important transformation products in the run-off from artificial walls ( $1 \times 1 \text{ m}^2$ ) equipped with acrylate and silicone resin render over time, as well as (II) their emissions rates and (III) the accumulated emitted mass versus the accumulated run-off volume; error bars: standard error of mean from three panels.

Previous studies have shown that the leaching of biocides is correlating with the wind driven rain intensity [23, 26], i.e., the amount of rain hitting the facade (equals run-off volume) per duration of the respective rain event. In order to compare the release of OIT and its transformation products, emission rates (emitted mass of biocide per liter run-off per event duration) were calculated and are presented in Figure 3.2-5.II. The emission rate of OIT was decreasing considerably from about  $5$  to  $10 \text{ mg L}^{-1} \text{h}^{-1}$  to below  $1 \text{ mg L}^{-1} \text{h}^{-1}$  within the first half year of exposure. The emission rates of the degradation products correlated with the emissions of OIT. However, while the OIT emission rate remained low, octylamine was emitted with slightly higher rates in the early summer 2013 (Figure 3.2-5.IId), which might link to higher UV-degradation during this time. For *N*-octyl oxamic acid as well as *N*-octylformamide (not shown) higher emission rates were detected from silicone render within the first half year of exposure

compared to acrylate render, while for the other compounds comparable emission rates were measured.

When considering the accumulated emitted mass in dependency of the accumulated run-off (Figure 3.2-5.IIIa), it appears that OIT emissions declined over time, following an exponential function (Eq. 5.2-2) with  $M_{Acc}$  being the accumulated emitted mass,  $M_{Max}$  the (asymptotic) maximum accumulated emitted mass,  $K$  the emission rate constant and  $V_{run-off}$  the accumulated run-off volume.

$$M_{Acc} = M_{Max} * (1 - e^{(-K * V_{run-off})}) \quad (\text{Eq. 5.2-2})$$

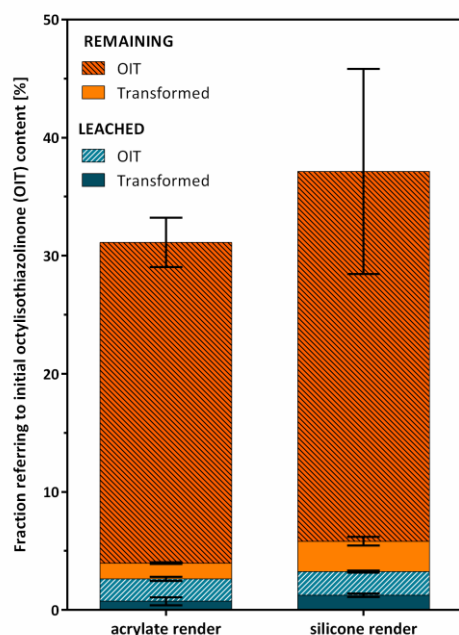
Especially in case of silicone render equipped panels, nearly no OIT was released after about 40 L m<sup>-2</sup> run-off. In contrary, the emissions of the transformation products did not follow a recognizable pattern.

The long-term emissions from biocide-equipped polymer resin render showed that OIT was leaching predominantly within the first half year after application. However, although the emissions decrease, a huge fraction of OIT was still detectable in the material. This raises the question on the limiting processes on the transport of the active substances within the material. For the first months a linear correlation between leached amount and run-off was visible, which suggests that only those biocide molecules that were directly in contact with water (outer and inner surfaces / surface layer) were available for leaching. The refill of this surface layer by diffusion through solid material seems to be too slow. This division of the process into two phases is supporting the suggestion proposed by Wittmer et al. [84]: a fast and a slow diffusion mechanism. Also, the render composition, namely the organic resin binder, seems to have an influence: for most of the events the OIT concentrations in the leachates from the acrylate renders was considerably higher than those from the silicone renders, which was not only an artefact of the higher run-off volume from silicone render. As the exponential functions of the accumulated mass of OIT emitted to the leachate are reaching a plateau, maximum endpoints of 2.1% and 2.8% of the initial OIT amount can be expected for silicone and acrylate render, respectively.

#### *Mass balance of OIT on renders*

The mass balance for OIT on the walls could not be closed based on the presented data, as even including seven transformation products, the mass balance only adds up to 30 - 40% on acrylate and silicone render, respectively. To make matters worse, the material also contained DCOIT, which can photodegrade following a similar degradation pattern (e.g. octylamine and *N*-octyl malonic acid described by Sakkas et al. [78]).

As shown in Figure 3.2-6, the majority of OIT was still remaining in the coating after 19 months of exposure to natural weather (27% acrylate render; 31% silicone render) followed by the OIT fraction leached (2%). The total fraction of transformation products detected in run-off or remaining in the coating was 2% (acrylate) and 4% (silicone), respectively. It is noticeable, that the fraction of transformation products remaining in the material was twice as much as the fraction of transformation products leached. However, the uneven distribution was not detectable for the most important degradation product *N*-octyl oxamic acid, with 1.1% (silicone) and 0.6% (acrylate) leached and 1.4% (silicone) and 0.6% (acrylate) remaining in the material.



**Figure 3.2-6** Mass balance of OIT: leached OIT [OIT detected in run-off water (average from 3 panels)], leached transformed [sum of transformation products detected in run-off (average from 3 panels)], remaining OIT [OIT in render after 19 month exposure (average of 10 extracts from one panel)], remaining transformed [sum of transformation products in render after 19 month exposure (average of 10 extracts from one panel)]; error bars: standard error of mean.

By including seven degradation products (octylamine, *N*-octyl oxamic acid, *N*-octyl malonamic acid, *N*-octylformamide, *N*-octylacetamide, *N*-octylprop-2-enamide and 3-octylthiazol-2(3H)-one) in the analysis of wall run-off as well as the remaining fraction in the render, the mass balance of OIT in facade coatings was still showing gaps of 60-70%. This is also in accordance with the results from the degradation kinetics study in solution: while at earlier time points the studied transformation products can explain the mass balance, the mass balance after 48 h irradiation showed a gap of 23%. However, this gap in the mass balance is in contrast to previous findings for terbutryn on facade render, where the mass balance could be closed by the inclusion of transformation products [85]. These gaps in the OIT mass balance might be due to either vaporisation or reactions to undetected transformation products. While vaporisation of OIT is expected to be low [86], the most important degradation product octylamine is considerably more volatile in comparison (vapour pressure  $p_{\text{vap}}$ : 131 Pa, i.e., about 20000 times higher than OIT). Hence, emissions to the air cannot be excluded. Additionally, complete mineralization via acetic acid and formic acid, as described in earlier studies for MI or DCOIT [78, 82], was not included in our measurements. Products resulting from reactions with OH-radicals were most probably covered based on the laboratory experiments. However, reactions with other reactive atmospheric species as  $\text{N}_x\text{O}_y$ -radicals or ozone might have formed other undetermined products. One could also imagine that activated OIT species have formed molecular bonds with the polymer matrix. 2-Octylcarbamoyl-1-ethene sulfonic acid has been determined as degradation product (bio-/ photodegradation, hydrolysis) in previous studies on DCOIT [83]. As no standard was available at this time, low resolution suspect screening for this compound was performed which revealed, that it might be present in the run-off samples and render extracts from the panel study (see Bilag 10), while it was not present in the UV-degradation study.

Additionally, biodegradation processes cannot be excluded. Nevertheless, as no data is available on the biological activity of biocide-treated facades, no statement can be made at this point and has not been focus of the present report either.

### **Biocide transformation on facade surfaces – Key findings**

- Large fraction of transformation products stays in the coating and is not washed-off immediately: Coating serves as temporarily sink.
- Consideration of transformation products is of high importance for the assessment of biocides in coatings, not only for the emission into the environment, but also for the assessment of the coating film as waste at the end of its lifetime.
- In case of volatile transformation products, also the emissions to air should not be neglected, especially in indoor environments where effects on health are of high concern.

### **3.2.3 Influence of pigments on photodegradation**

#### **Interaction of paint films with solar radiation**

Total solar reflection measurements demonstrate that the black paint absorbs light in the ultra-violet (UV); visible (vis) and infrared (IR) range. The red paint absorbs UV radiation, but only part of Vis and IR radiation. No transmission could be observed for any of these two paint films. The white paint absorbed part of the UV radiation, while large portions of Vis and IR radiation were reflected, and some Vis and IR radiation was transmitted through the paint film. Concerning the transparent paint, parts of the UV, Vis and IR radiation was reflected from the test specimens, and large portions of Vis and IR radiation were transmitted (see Bilag 11.4). This implies that all paints absorbed UV radiation and that energy was potentially available for photolysis of the biocides. Only the white paint almost totally reflected radiation with higher wavelengths than 400 nm that was also applied by the used UVA-340 lamps (see Bilag 11.1 for the spectrum of these lamps).

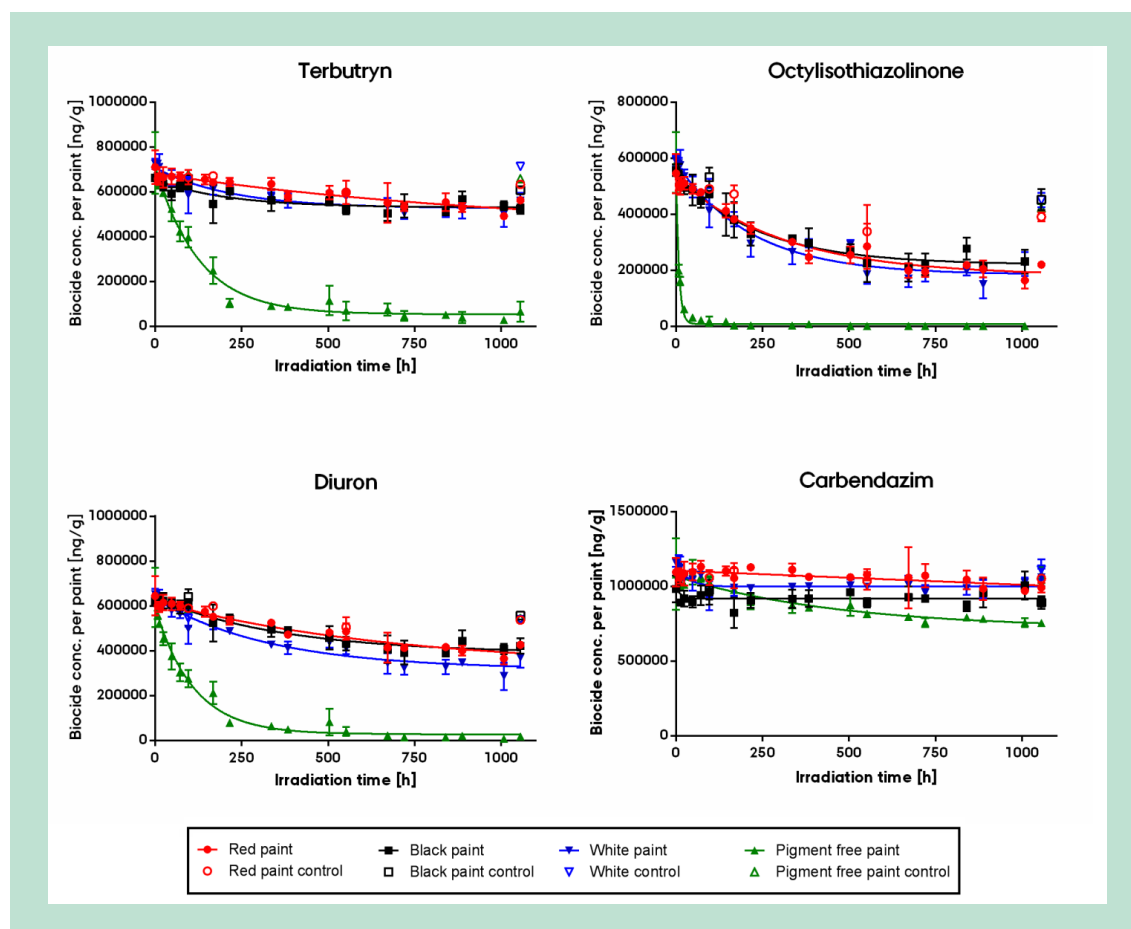
Infrared spectra from paint films mainly represent the polymeric styrene acrylate binder of the paints. Therefore, this technique has been used intensively to describe stability and changes of polymers in coatings [87-90]. It is well known that UV radiation can induce degradation of polymers in coatings. IR spectra from test specimens that were installed in the weathering chamber for the complete duration of the experiment and test specimens that were kept dark for the same time period show different intensities of characteristic signals for chemical bonds in the binder molecules, e.g. C-H in alkanes, C=O and C-O- in esters. This indicates UV induced chemical reactions on the binder molecules, and this way changes of the chemical surrounding of the investigated biocides during the performed UV irradiation experiment. Comparison of IR spectra from the transparent and the different pigmented paints suggests that the pigments protect the styrene acrylic binder from UV induced degradation. Apparently, TiO<sub>2</sub> and the iron oxides have different effects on the reactions that occur at the binder molecules (see Bilag 11.4 for further information). The photocatalytic properties of TiO<sub>2</sub> are well known. However, it has also been observed that certain types of TiO<sub>2</sub>, i.e. rutile TiO<sub>2</sub>, protect coatings from UV degradation. This effect depends on structure, particle size, surface treatment and concentration [87-90].

### Photolysis of biocides within paints

**Figure 3.2-7** shows the concentrations of biocides during the irradiation experiments. All investigated biocides disappeared most rapidly in the pigment free paint with OIT photolyzing the fastest and carbendazim the slowest. The order was the same in the paints with pigments, but at lower photolysis rates. Control experiments with test specimens that were installed in the weathering chamber, but not exposed to UV-A radiation, indicate that transformation was indeed caused by UV-A radiation and not by other experimental parameters (e.g. temperature of 40 °C). First-order-kinetic photolysis rate constants  $k$  as derived from the data in **Figure 3.2-7** for the studied biocides are presented in Table 3.2-3. It is clearly visible, that the highest values were obtained for pigment free formulation for all compounds.

**Table 3.2-3** First-order-kinetic constants  $k$  ( $\text{h}^{-1}$ ) for biocides transformation under UV-A radiation.

	Carbendazim		Diuron		Octylisothiazolinone		Terbutryn	
	$k$	$R^2$	$k$	$R^2$	$k$	$R^2$	$k$	$R^2$
Red paint	-	-	0.0015	0.8722	0.0032	0.9374	0.0009	0.7221
Black paint	-	-	0.0027	0.8624	0.0042	0.9015	0.0048	0.6503
White paint	-	-	0.0030	0.9007	0.0046	0.9319	0.0045	0.7630
Pigment-free paint	0.0021	0.7812	0.0090	0.9608	0.1205	0.9678	0.0079	0.9670



**Figure 3.2-7** Concentration of terbutryn, octylisothiazolinone, diuron and carbendazim in paints with different pigments during UV radiation. Control test specimens were installed in the weathering chamber but not exposed to UV radiation.

### *Terbutryn transformation*

Figure 3.2-8 shows the mass balance of terbutryn including photolysis products identified in paragraph 3.2.1. Primary transformation products found in the analyzed samples were: desethyl-terbutryn, terbutryn sulfoxide and terbumeton. It is hypothesized that terbutryn sulfoxide can further transform to 2-hydroxy-terbutryn. 2-hydroxy-terbutryn produces desethyl-2-hydroxy-terbutryn and desbutyl-2-hydroxy-terbutryn. Another transformation product of terbutryn was desethyl-terbutryn. 2-hydroxy-terbutryn and desethyl-terbutryn can further transform to desethyl-2-hydroxy-terbutryn. A different photolysis pathway of terbutryn leads to the formation of desthiomethyl-terbutryn, which can further transform to desthiomethyl-desethyl-terbutryn and desthiomethyl-desbutyl-terbutryn, although these products were not as abundant as others in our samples. The analysis of transformation products of terbutryn showed that up to 25% percent of the initial terbutryn was transformed within the course of experiment in all formulations with pigments, while higher photolysis rates were observed in the pigment free film, in which a half-life of terbutryn of about 100 h was observed under the experimental conditions. Including the transformation products, the mass balance was closed for all the analyzed paints except the pigment free formulation. For all pigmented paints only increase of the transformation products was observed, while for non pigmented paint usually a maximum was observed for the respective transformation products, indicating generation and secondary photolysis of the transformation products.

The results for the red and the black paint were very similar and indicate slow photolysis of terbutryn. Main transformation products were desethyl-2-hydroxy-terbutryn and desbutyl-2-hydroxy-terbutryn. In both paints the concentrations of terbumeton, desethyl-terbutryn and 2-hydroxy-terbutryn are relatively low. However, the total yield of transformation products was about 40% higher in black than in red paint considering the last time point (Figure 3.2-8).

The results for the white paint were significantly different to the red and black system. In the white paint, terbutryn sulfoxide was the main transformation product of terbutryn, followed by desethyl-2-hydroxy-terbutryn and desbutyl-2-hydroxy-terbutryn (Figure 3.2-8).

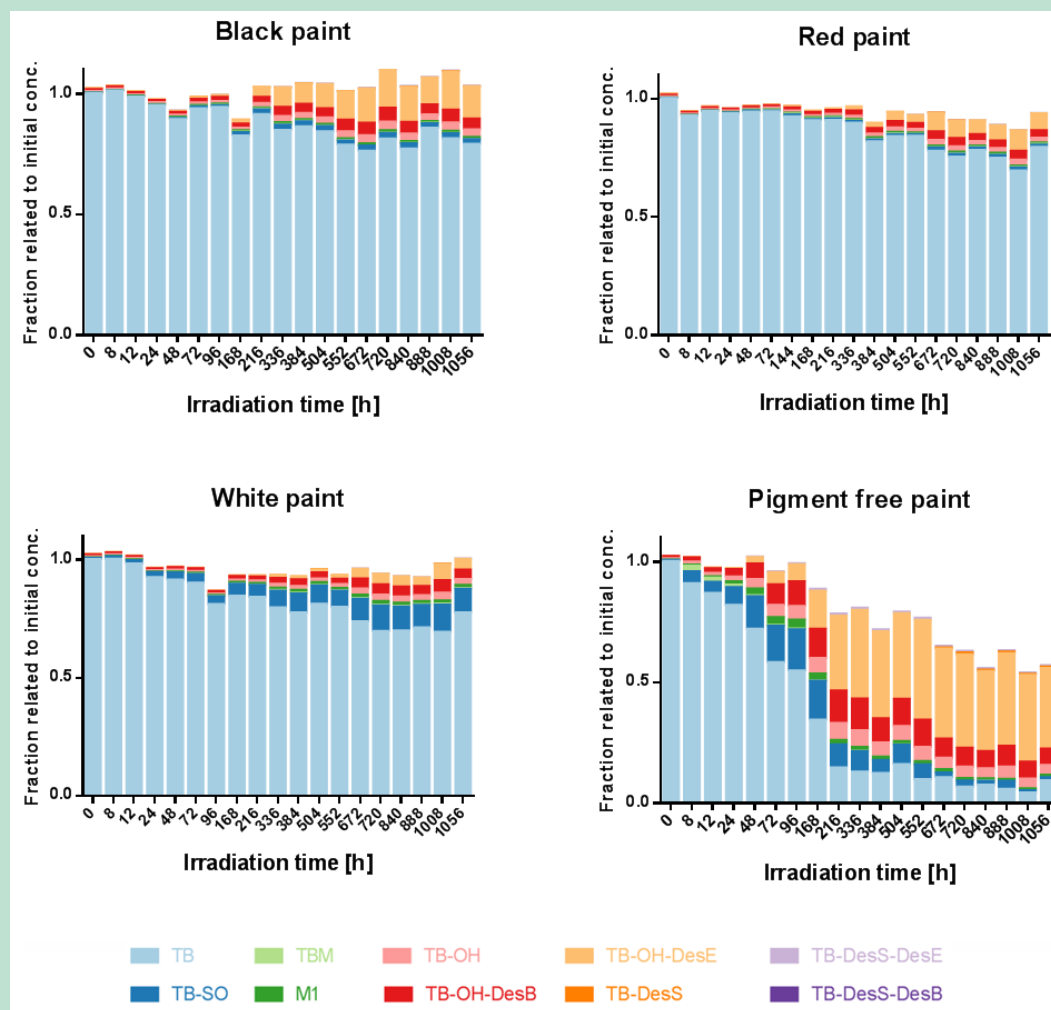
Obviously, terbutryn in the pigment free paint underlies significantly different processes than those in the pigmented paints: Significant amounts of terbumeton are present within few hours from the start of the experiment, succeeded by an increase in terbutryn sulfoxide production, which is then succeeded by desethyl-2-hydroxy-terbutryn, desbutyl-2-hydroxy-terbutryn (Bilag 11.5). The highest concentration of desethyl-2-hydroxy-terbutryn was observed in the pigment free paint. However, also the dynamics of the transformation products of terbutryn in the pigment free paint are interesting: While terbumeton had a nearly immediate concentration maximum and was again photolyzed rapidly, the concentration maximum for terbutryn sulfoxide occurred after about 100 h coinciding with the half-life of the parent compound (Bilag 11.5). The sulfoxide was then further transformed with a half-life of about 300 h (400 h after start of experiment). Approximately the same behavior is observed for desethyl-terbutryn. A considerably slower generation is observed for 2-hydroxy-terbutryn, desbutyl-2-hydroxy-terbutryn, desthiomethyl-desbutyl-terbutryn and desthiomethyl-desethyl-terbutryn. The concentration maximum for all four compounds is observed at about 200 h after start of the experiment (or 100 h post half-life of the parent). All four compounds are then transformed further with a half-life of a bit above 1000 h. Obviously, the photolysis of these transformation products was relatively slow, thus their formation could be observed until no parent was photolyzed any longer (200 h after start of the experiment).

A third type of kinetics was observed for desethyl-2-hydroxy-terbutryn. This compound was formed with its concentrations reaching a maximum at 400 h of the experiment. After that point in time the concentrations did not change. Obviously, this transformation product was either photostable or still formed from other precursors (such as 2-hydroxy-terbutryn or desethyl-terbutryn) during the experiment with similar photolysis rates.

The findings of our research are consistent with previous studies. Lányi and Dinya [91] reported 2-hydroxy-terbutryn as the main phototransformation product of terbutryn in dichloromethane solution exposed to the light of a mercury lamp. Desethyl-2-hydroxy-terbutryn and



desbutyl-2-hydroxy-terbutryn were also detected by these authors, but in oppose to our findings, the concentrations were significantly less.

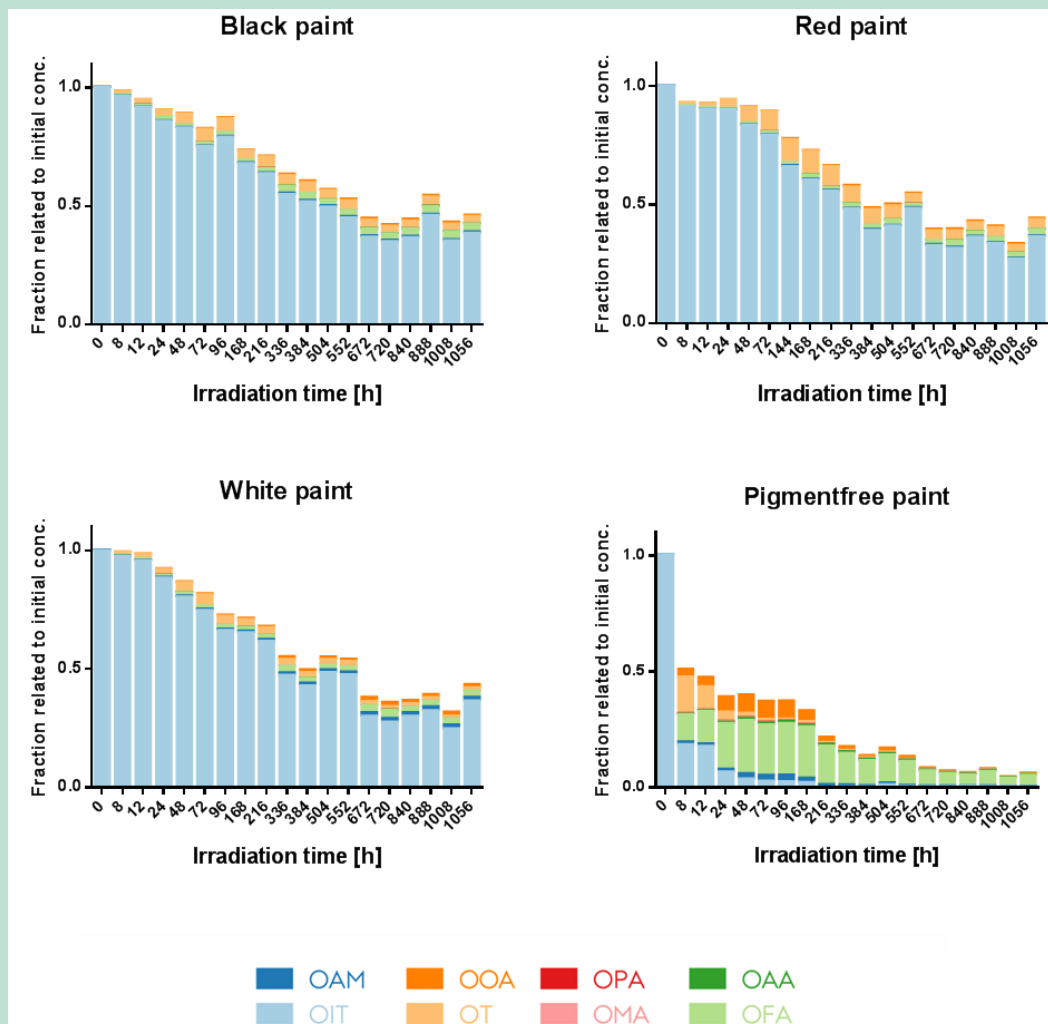


**Figure 3.2-8** Mass balance of terbutryn and its transformation products in paint during the photolysis experiments. TB = Terbutryn, TB-SO = Terbutryn sulfoxide, TB-DesS = Desthiomethyl-terbutryn, TB-DesS-DesE = Desthiomethyl-desethyl-terbutryn, M1 = Desethyl-terbutryn, TB-DesS-DesB = Desthiomethyl-desbutyl-terbutryn, TBM = Terbumeton, TB-OH = 2-hydroxy-terbutryn, TB-OH-DesE = Desethyl-2-hydroxy-terbutryn, TB-OH-DesB = Desbutyl-2-hydroxy-terbutryn. The presented mean values were derived from 3 replicates, relative standard deviations amount to 17 % (not indicated in the graph to keep clarity).

#### Octylisothiazolinone transformation

OIT was the fastest photolyzed compound in our experiment (Table 3.2-3). Figure 3.2-9 presents the mass balances for octylisothiazolinone (OIT). Similar to the degradation studies in aqueous solution (paragraph 3.2.1) and on facade surfaces (paragraph 3.2.2), the mass balances could not be closed, possibly due to vaporization of low molecular mass photolysis products. The pattern of transformation products formed from OIT for all three pigment containing paints is similar and dominated by the photoisomerization product 3-octyl-2(3H)-thiazolone (OT), followed by *N*-octylformamide (OFA), octylamine (OAM) and *N*-octylprop-2-enamide (OPA). OIT was photolyzed with similar reaction constants in the black and red paints. In comparison to the black and red paints, OIT is phototransformed differently in the

white paint, leading to relatively higher concentrations of octylformamide and octylamine and somewhat less OT. Vast differences to all pigmented paints were seen in the pigment free paint. The photolysis rate constants were significantly higher and phototransformation led to a different pattern dominated by octylformamide followed by *N*-Octyl oxamic acid (OAA) indicating different reaction mechanisms.



**Figure 3.2-9** Mass balance of octylisothiazolinone and its transformation products in paint during photolysis experiments. OIT = octylisothiazolinone, OT = 3-octyl-2(3H)-thiazolone, OOA = *N*-Octyl oxamic acid, OPA = *N*-octylprop-2-enamide, OMA = *N*-octyl malonamic acid, OAA = *N*-octylacetamide, OFA = *N*-Octylformamide, OAM = Octylamine. The presented mean values were derived from 3 replicates, relative standard deviations amount to 14 % (not indicated in the graph to keep clarity).

Octylamine, though present in the pigment-free paint in the beginning could only be detected until 168 h. For octyl malonamic acid a clear peak in concentrations can be seen at about 100 h in the pigment-free paint. Successively, this compound was further photolyzed with a half-life of about 400 h. Likewise, this compound has a concentration maximum in the black paint at about 800 h. In the other paints, this compound was formed and then the concentrations did not change within the run of the experiment. For octylprop-2-enamide a clear peak in concentrations could be observed in case of the pigment-free paint a few hours after the start of the experiment with a half-life of about 200 h. In remaining paints the compound was formed and the concentrations stayed somewhat stable after 300 h. For octylamine, a maximum was ob-

served at about 100 h in the pigment-free paint while slow formations have been observed for the red and black paint until 150 h. However, the formation of octylamine in the white paint continues until 600 h after start. For none of the pigmented paints a clear maximum was detectable. Interestingly, for the photoisomerization product (3-octyl-2(3H)-thiazolone) a very sharp maximum was observed for the pigment-free paint after a few hours – this compound was then rapidly further photolyzed. However, also clear maxima were observed for the red paint (200 h) and the black and white paint at about 100 h. In all pigmented paints the concentrations slowly decreased after the maximum.

The literature suggests, that one phototransformation pathway of isothiazolinones is initiated by ring opening through the nitrogen–sulphur bond [92]. After the bond breakage, OIT isomerizes into the corresponding 3-octyl-2(3H)-thiazolone (OT) described first by Rokach and Hamel [77].

The reactions of isothiazolinones using catalyst grade TiO<sub>2</sub> (Degussa P25 – a commercial mixture of anatase and rutile) involving production of holes and excited electrons as well as H<sub>2</sub>O<sub>2</sub> and OH-radicals have been described [92]. In contrary to catalyst grade titanium dioxide, paint grade titanium dioxide did not influence the phototransformation of two isothiazolinones in that study [92].

#### *Diuron transformation*

Diuron was the second fastest photolyzed compound in our study (Table 3.2-3). It was completely degraded from the pigment free formulation within 500 h from the start of the experiment (Figure 3.2-7). Red and black pigment showed 35% photolysis of diuron during the experiment. The photolysis in white paint was higher than in red and black paint and reached 40%. According to Burkhardt et al. [23] DCPMU (1-(3,4-dichlorophenyl)-3-methylurea) is the main transformation product of diuron. Thus, it was also analyzed in the samples of this experiment. However, the mass balance was incomplete even when this transformation product was included (data are not shown). Probably, testing for other transformation products of diuron could shed some more light onto its transformation patterns in paints and complete the mass balance. In a study performed by Mestankova et al. [93] the main products of diuron direct phototransformation were 3-(3-chloro-4-hydroxyphenyl)-1,1-dimethylurea and 3-(4-chloro-3-hydroxyphenyl)-1,1-dimethylurea.

#### *Carbendazim transformation*

Carbendazim was the compound which was photolyzed the least of all tested biocides which is in accordance with previous studies [55]. In none of the pigmented paints, carbendazim was photolyzed significantly. Only in the pigment free formulation, about 30% carbendazim was photolyzed. For carbendazim only one transformation product, 2-aminobenzimidazole, was analyzed in our study. Unfortunately, it was not the main transformation product for pigment free paint, since its concentration accounted to less than 1% of the total mass balance. This means that from all biocides used in this study, carbendazim is least prone to degrade under exposure to light no matter on pigment used. It is worth to mention that carbendazim is a biocide which also does not leach out from renders as fast as diuron or terbutryn [5].

#### **Mechanism of transformation in analyzed paints**

The predominant effect of pigments appears to be shading and thus protection of the biocides from the irradiation. There is a huge difference in the transformation of all observed biocides from paints with pigments compared to paints without pigments. Transformation is always slowed down considerably in paints with pigments. However, there are also clear differences between the white paint on the one hand and the black and red paint on the other hand. No big differences were observed between the black and red paint, although the black and red pigments displayed quite different photochemical properties [black pigment (magnetite) gap of 0.14 eV [94] and red pigment (hematite) gap of 2.0 - 2.3 eV [95]]. Apparently, titanium dioxide acts in a different way than the iron oxides. Considering the iron based pigments: A work by Pulgarin and Kiwi [96] explained the role of  $\alpha$ -Fe<sub>2</sub>O<sub>3</sub> in the phototransformation of phenols.

They argued that the electrons produced cannot react with  $O_2$  bound to the surface. The electron may lead instead to dissolution of  $\alpha\text{-Fe}_2\text{O}_3$ , i.e. electrons react with  $\text{Fe}^{3+}$  to produce  $\text{Fe}^{2+}$ . Hypothetically,  $\text{TiO}_2$  should give a higher yield in terms of transformation products, but this was not observed here. The reason can be that  $\text{TiO}_2$  used in this study is paint grade (rutile), which poses lower photocatalytic properties. The picture concerning the phototransformation of biocides in the paints, especially the formulations containing iron pigments is not 100% clear. However, it needs to be taken into account that chemical interactions of the paint ingredients with the minerals could affect the phototransformation.

### **Influence of pigments on photodegradation – Key findings**

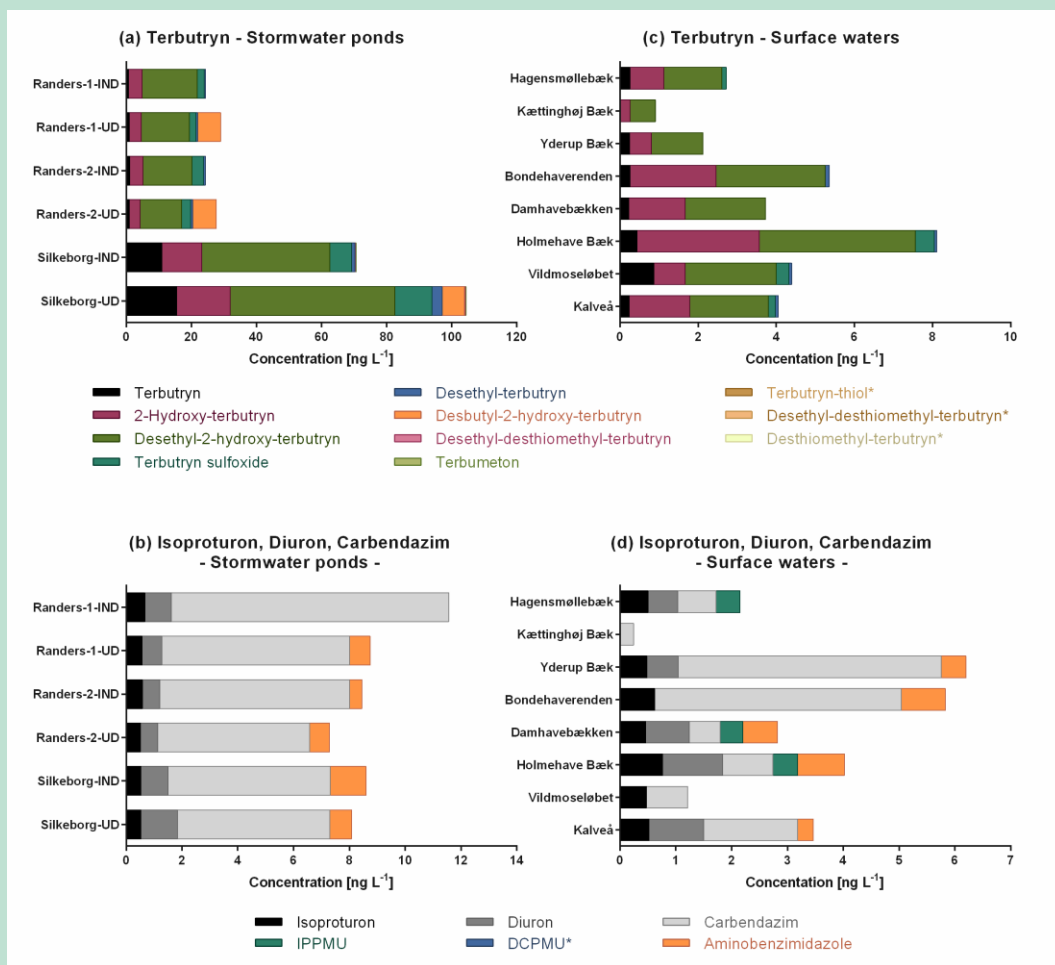
- Pigments shield biocides from photodegradation.
- Pigments interact with biocide photodegradation: transformation pattern are similar in red and black paint, while white and pigment-free paints show different transformation product ratios.
- Mass balance is closed for terbutryn in case of the pigmented paints, but not pigment-free paints.

### **3.2.4 Monitoring of photodegradation products**

Several surface water samples as well as three stormwater ponds were analyzed. Terbutryn and several of its transformation products could be detected in both surface waters and stormwater (Figure 3.2-10, concentrations in Bilag 12) in single compound concentrations up to  $40 \text{ ng L}^{-1}$ . The concentration of transformation products was often as high or even higher than the parent compound. *N*-octylisothiazolinone and its transformation products were only sporadically detected ( $< 1 \text{ ng L}^{-1}$ ). Isoproturon, diuron, and carbendazim were detected together with their most common known transformation products.

The stormwater ponds were sampled both in inlet and outlet. For terbutryn rather similar pattern could be detected for all inlet and for all outlet samples. Especially the detection of desbutyl-2-hydroxy-terbutryn in the outlet has to be mentioned. As this compound was not present in the inflow, it must have formed in the stormwater ponds, either by hydroxylation from desbutyl-terbutryn or by desbutylation from 2-hydroxy-terbutryn. While the first pathway is most probably related to photolysis, the second one is well-known in microbiological processes.

The highest concentrations for terbutryn in the Silkeborg catchment (inlet  $11 \text{ ng L}^{-1}$ , outlet  $15 \text{ ng L}^{-1}$ ) are close to the predicted no effect concentration ( $\text{PNEC}_{\text{aquatic}} 34 \text{ ng L}^{-1}$  [21]). As previous studies showed, during some events even higher concentrations can be expected in this catchment [26]. Similar inlet and outlet concentrations raise the question, if terbutryn might cause a risk to exceed the environmental quality standards of  $64 \text{ ng L}^{-1}$  [20] in catchments with high terbutryn usage. With maximum concentrations of  $1.55 \text{ ng L}^{-1}$  also octylisothiazolinone is close to the predicted no effect concentration ( $\text{PNEC}_{\text{aquatic}}$ ) of  $7.1 \text{ ng L}^{-1}$  [80] likewise in the Silkeborg catchment. However, degradation in the stormwater pond led to a five-time lower concentration in the outlet. Diuron and isoproturon concentrations were considerably lower than  $\text{PNEC}_{\text{aquatic}}$  and AA-EQS-values. It has to be mentioned that these discussions base on a single monitoring campaign and would need verification in future studies.



**Figure 3.2-10** Monitoring of transformation products in (a&b) stormwater ponds and (c&d) surface waters (compounds marked \* were analyzed but not detected in any location).

### Monitoring of transformation products – Key findings

- Persistent transformation products can be detected in stormwater ponds and surface waters.
- Often the concentrations of transformation products are as high as or higher than the respective parent compound.

## 4. General conclusions

This project covered several studies related to (1) the transport of biocides from the deeper layers of a coating film to the surface of the film and into the water and (2) the transformation, i.e. phototransformation, of biocides on facade surfaces that lead to a loss of the active ingredients. In the following the conclusions regarding the five initial hypotheses for this project are summarized.

### 4.1 Transport

**Hypothesis 1:** The evaporating pore water will transport biocides actively to the surface of the material, thus wet/dry cycles will enhance biocide leaching.

The results showed that the transport of biocides in renders predominantly occurs through the water-filled pores, while the transport through the dry render is negligible. As intermittent wetting generated considerably higher leaching rates than continuous wetting, it can be concluded that the equilibration time in between the leaching cycles has a major impact on the leaching as this would be the time to refill the surface layer. However, if the render was kept wet during the equilibration time the leaching was higher than in those cases when the render was left to dry. This indicates that the pore-water diffusion is more important than evaporative (advective) transport for the surface layer refill.

**Hypothesis 2a:** The diffusion of biocides through the render is occurring through the binder and the binder alone controls the diffusion of the biocides through the render.

Comparing the very low dry diffusion rates to diffusion under wet conditions it becomes obvious that the transport rates in a dry render are insignificant compared to those in a wet render. It can hence be concluded that transport via water in the pores of the render is the primary mechanism for biocides being delivered to the render surface.

**Hypothesis 2b:** The polymeric binder and the binder alone controls the partitioning of the biocides between water and render.

The polymeric binder is in fact the most important part in the render-water partitioning. However, some minerals (e.g. talc) show low partitioning as well. The distribution constants to polyacrylate-based render ( $\log D_{\text{render}}$ ) can be predicted linearly from the polyacrylate-water partition constants ( $\log K_{AcW}$ ) as a first assessment.

### 4.2 Transformation

**Hypothesis 3a:** Photochemical transformation products constitute a considerable mass-fraction of the total balance of the biocides in render materials.

As seen in the example of terbutryn, the mass balance can be closed if phototransformation products are included. However, as the mass balance of *N*-octylisothiazolinone cannot be closed, other factors must be considered: still unknown products, mineralization, biodegradation and loss to the atmosphere.

As an important fact, it has to be mentioned that transformation products – though formed on the facade surface – often remain in the material and are not leached immediately. Additionally, transformation products are detected in the stormwater ponds with as high as or higher concentrations than the parent compounds.

**Hypothesis 3b:** The different pigments influence the photo-degradation rates considerably as some might act as photo-catalysts, while others might just shade (protect) the biocides from light.

In general, pigments shade/protect biocides from light irradiation. The influence of pigments on the degradation rates is rather low. However, as different pigments show different degradation pattern, an interaction light-pigment-biocide is evident and cannot be neglected in future assessments.

## 5. Perspectives

This project has generated new important knowledge on both transportation and transformation processes of biocides in render material. This information is of importance for both material design as well as the risk assessment of the biocides.

Considering the results regarding the transport processes, obviously the water filled pores are of uttermost importance for the transport of biocides across render layers. Consequently, the water management within the materials is of highest importance for the leaching of biocides. Thus, it should get focussed attention when designing new materials.

Additionally, minerals like talc can be used to control the partitioning on the surface of the materials and should thus be considered more in the designing of materials.

Photodegradation products of the biocides are quite common in rainwater collection systems. For terbutryn pathways similar to those known for other triazines (atrazine) are relevant. The concentrations of those transformation products that were included in this study exceeded those of the parent compounds significantly.

Future research projects should focus on the identification of transformation pathways and transformation products of (other) biocides, especially of those that do not have an agricultural background. Depending on product group, biodegradation or phototransformation will be of enhanced importance.

Concerning the transformation products and metabolites, it will not only be important to gain data on their formation and presence but also on their toxic effects at least with selected test systems.



## 6. References

1. European Parliament and Council, *Regulation (EU) No 528/2012 concerning the making available on the market and use of biocidal products*. Official Journal of the European Union, 2012. **L167**: p. 1-122.
2. Reichel, A., A. Hochberg, and C. Köpke, *Plaster, Render, Paint and Coatings: Details, Products, Case Studies*. DETAIL Practice. 2004, Basel, Switzerland: Birkhäuser.
3. Paulus, W., *Directory of Microbicides for the Protection of Materials: A Handbook*. 2005, Dordrecht, Netherlands: Springer.
4. European Commission, *List of participants/applicants to the Review Programme of existing active substances used in biocidal products*. [http://ec.europa.eu/environment/biocides/pdf/list\\_participants\\_applicants\\_subs.pdf](http://ec.europa.eu/environment/biocides/pdf/list_participants_applicants_subs.pdf) (assessed 22/09/2011). Brussels, Belgium. 2011.
5. Burkhardt, M., et al., *Leaching of additives from construction materials to urban storm water runoff*. Water Science and Technology, 2011. **63**(9): p. 1974-1982.
6. Schultz, T.P., D.D. Nicholas, and A.F. Preston, *Perspective - A brief review of the past, present and future of wood preservation*. Pest Management Science, 2007. **63**(8): p. 784-788.
7. Amorisco, A., et al., *Photocatalytic degradation of the herbicide isoproturon: characterisation of by-products by liquid chromatography with electrospray ionisation tandem mass spectrometry*. Rapid Communications in Mass Spectrometry, 2005. **19**(11): p. 1507-1516.
8. Blanchoud, H., F. Farrugia, and J.M. Mouchel, *Pesticide uses and transfers in urbanised catchments*. Chemosphere, 2004. **55**(6): p. 905-913.
9. Bucheli, T.D., et al., *Occurrence and behavior of pesticides in rainwater, roof runoff, and artificial stormwater infiltration*. Environmental Science & Technology, 1998. **32**(22): p. 3457-3464.
10. Bucheli, T.D., et al., *Bituminous roof sealing membranes as major sources of the herbicide (R,S)-mecoprop in roof runoff waters: Potential contamination of groundwater and surface waters*. Environmental Science & Technology, 1998. **32**(22): p. 3465-3471.
11. Gerecke, A.C., et al., *Sources of pesticides in surface waters in Switzerland: pesticide load through waste water treatment plants-current situation and reduction potential*. Chemosphere, 2002. **48**(3): p. 307-315.
12. Kahle, M., et al., *Azole fungicides: Occurrence and fate in wastewater and surface waters*. Environmental Science & Technology, 2008. **42**(19): p. 7193-7200.
13. Quednow, K. and W. Puettmann, *Temporal concentration changes of DEET, TCEP, terbutryn, and nonylphenols in freshwater streams of Hesse, Germany: possible influence of mandatory regulations and voluntary environmental agreements*. Environmental Science and Pollution Research, 2009. **16**(6): p. 630-640.
14. Albanis, T.A., et al., *Antifouling paint booster biocide contamination in Greek marine sediments*. Chemosphere, 2002. **48**(5): p. 475-485.
15. Cassi, R., I. Tolosa, and S. de Mora, *A survey of antifoulants in sediments from Ports and Marinas along the French Mediterranean coast*. Marine Pollution Bulletin, 2008. **56**(11): p. 1943-1948.
16. Harino, H., et al., *Degradation of antifouling booster biocides in water*. Journal of the Marine Biological Association of the United Kingdom, 2005. **85**(1): p. 33-38.
17. Konstantinou, I.K. and T.A. Albanis, *Worldwide occurrence and effects of antifouling paint booster biocides in the aquatic environment: a review*. Environment International, 2004. **30**(2): p. 235-248.
18. Lambropoulou, D.A., V.A. Sakkas, and T.A. Albanis, *Analysis of antifouling biocides Irgarol 1051 and Sea Nine 211 in environmental water samples using solid-phase microextraction and gas chromatography*. Journal of Chromatography A, 2002. **952**(1-2): p. 215-227.

19. Thomas, K.V., M. McHugh, and M. Waldock, *Antifouling paint booster biocides in UK coastal waters: inputs, occurrence and environmental fate*. Science of the Total Environment, 2002. **293**(1-3): p. 117-127.
20. European Parliament and Council, *DIRECTIVE 2013/39/EU amending Directives 2000/60/EC and 2008/105/EC as regards priority substances in the field of water policy*. Official Journal of the European Communities, 2013. **L 226**: p. 1-17.
21. Burkhardt, M., et al., *Biozide in Gebäudefassaden – ökotoxikologische Effekte, Auswaschung und Belastungsabschätzung für Gewässer (Biocides in building facades – ecotoxicological effects, leaching and environmental risk assessment for surface waters)*. Umweltwissenschaften und Schadstoff-Forschung, 2009. **21**(1): p. 36-47.
22. ECHA. *Biocidal Active Substances*: <https://echa.europa.eu/information-on-chemicals/biocidal-active-substances> (last assessed 19/06/2018). 2018.
23. Burkhardt, M., et al., *Leaching of Biocides from Facades under Natural Weather Conditions*. Environmental Science & Technology, 2012. **46**(10): p. 5497-5503.
24. Bester, K., J. Vollertsen, and U.E. Bollmann, *Water-driven leaching of biocides from paints and renders: Methods for the improvement of emission scenarios concerning biocides in buildings*. 2014, The Danish Environmental Protection Agency: Copenhagen, Denmark. p. 108.
25. Gasperi, J., et al., *Micropollutants in urban stormwater: occurrence, concentrations, and atmospheric contributions for a wide range of contaminants in three French catchments*. Environmental Science and Pollution Research, 2014. **21**(8): p. 5267-5281.
26. Bollmann, U.E., et al., *Dynamics of biocide emissions from buildings in a suburban stormwater catchment - Concentrations, mass loads and emission processes*. Water Research, 2014. **56**: p. 66-76.
27. Masiá, A., et al., *Combined use of liquid chromatography triple quadrupole mass spectrometry and liquid chromatography quadrupole time-of-flight mass spectrometry in systematic screening of pesticides and other contaminants in water samples*. Analytica Chimica Acta, 2013. **761**: p. 117-127.
28. Singer, H., et al., *Determination of biocides and pesticides by on-line solid phase extraction coupled with mass spectrometry and their behaviour in wastewater and surface water*. Environmental Pollution, 2010. **158**(10): p. 3054-3064.
29. Chen, Z.F., et al., *Determination of biocides in different environmental matrices by use of ultra-high-performance liquid chromatography-tandem mass spectrometry*. Analytical and Bioanalytical Chemistry, 2012. **404**(10): p. 3175-3188.
30. Bollmann, U.E., et al., *Biocides in urban wastewater treatment plant influent at dry and wet weather: Concentrations, mass flows and possible sources*. Water Research, 2014. **60**: p. 64-74.
31. Wick, A., G. Fink, and T.A. Ternes, *Comparison of electrospray ionization and atmospheric pressure chemical ionization for multi-residue analysis of biocides, UV-filters and benzothiazoles in aqueous matrices and activated sludge by liquid chromatography-tandem mass spectrometry*. Journal of Chromatography A, 2010. **1217**(14): p. 2088-2103.
32. Wittmer, I.K., et al., *Significance of urban and agricultural land use for biocide and pesticide dynamics in surface waters*. Water Research, 2010. **44**(9): p. 2850-2862.
33. Bollmann, U.E., et al., *Biocide Runoff from Building Facades: Degradation Kinetics in Soil*. Environ Sci Technol, 2017. **51**(7): p. 3694-3702.
34. Coutu, S., et al., *Modeling of facade leaching in urban catchments*. Water Resources Research, 2012. **48**: p. W12503.
35. Schoknecht, U., et al., *Leaching of Biocides Used in Facade Coatings under laboratory Test Conditions*. Environmental Science & Technology, 2009. **43**(24): p. 9321-9328.
36. Wangler, T.P., et al., *Laboratory scale studies of biocide leaching from facade coatings*. Building and Environment, 2012. **54**(0): p. 168-173.
37. Breuer, K., et al., *Wirksamkeit und Dauerhaftigkeit von Bioziden in Bautenbeschichtungen (Effectiveness and durability of biocidal ingredients in façade coatings)*. Bauphysik, 2012. **34**(4): p. 170-182.

38. Styszko, K., et al., *Desorption of biocides from renders modified with acrylate and silicone*. Chemosphere, 2014. **95**: p. 188-192.
39. Zuleeg, S. *Auswaschung von Bioziden aus praxisnahen wärmegeprägten Fassaden*. in *Biozide und Nanopartikel in Fassaden, Meeting at the EAWAG/EMPA*. 2008. Zurich.
40. Simmler, H. *Fassadenabfluss unter natürlichem Witterungseinfluss*. in *Biozide und Nanopartikel in Fassaden, Meeting at the EAWAG/EMPA*. 2008. Zurich.
41. Burkhardt, M. *Auswaschung von Bioziden aus Fassaden unter natürlichem Witterungseinfluss und deren Vorkommen im Regenwasserabfluss*. in *Biozide und Nanopartikel in Fassaden, Meeting at the EAWAG/EMPA*. 2008. Zurich.
42. Glotfelty, D.E., et al., *Volatilisation and wind erosion of soil surface applied atrazine, simazine alachlor, and toxaphene*. J. Agric. Food Chem, 1989. **37**: p. 546-551.
43. European Parliament and Council, *REGULATION (EC) No. 1223/2009 on cosmetic products*. Official Journal of the European Union, 2009. **L342**: p. 59-209.
44. Danish Environmental Protection Agency, *Bekæmpelsesmiddelstatistik 2016 (Pesticides and biocides statistic 2016)*. Copenhagen, Denmark. 2017.
45. Danish Environmental Protection Agency, *Salg af sprøjtemidler til brug i private haver 2015 og 2016 (Sales of pesticides for private gardening - 2015/2016)*. Copenhagen, Denmark. 2017.
46. Danish Veterinary and Food Administration, *Pesticidrester i fødevarer 2016 (Pesticide residues in food 2016)*. Glostrup, Denmark. 2017.
47. Synthomer Deutschland, *Technical Data Sheet PLEXTOL D 498*. 2014: Marl, Germany.
48. Brunauer, S., P.H. Emmett, and E. Teller, *Adsorption of gases in multimolecular layers*. Journal of the American Chemical Society, 1938. **60**: p. 309-319.
49. Schwarzenbach, R.P., P.M. Gschwend, and D.M. Imboden, *Environmental Organic Chemistry*. 2nd ed. 2003, Hoboken, New Jersey: Wiley-Interscience.
50. Mayer, P., W.H.J. Vaes, and J.L.M. Hermens, *Absorption of hydrophobic compounds into the poly(dimethylsiloxane) coating of solid-phase microextraction fibers: High partition coefficients and fluorescence microscopy images*. Analytical Chemistry, 2000. **72**(3): p. 459-464.
51. Crank, J., *The mathematics of diffusion*, 2nd ed. 1975, Oxford: Clarendon Press.
52. Saltzman, W.M., *Drug Delivery: Engineering Principles for Drug Therapy*. 2001, New York: Oxford University Press.
53. Vergnaud, J.-M. and *Controlled drug release of oral dosage forms*. 1993, New York: Ellis Horwood.
54. Baker, R.W., *Controlled Release of Biologically Active Agents*. 1987, New York: John Wiley and Sons.
55. Minelgaite, G., et al., *Photodegradation of three stormwater biocides*. Urban Water Journal, 2015: p. 1-8.
56. Schlüsener, M.P., U. Kunkel, and T.A. Ternes, *Quaternary Triphenylphosphonium Compounds: A New Class of Environmental Pollutants*. Environmental Science & Technology, 2015. **49**(24): p. 14282-1429.
57. Mayer, P., et al., *Equilibrium sampling devices*. Environmental Science & Technology, 2003. **37**(9): p. 184A-191A.
58. Vaes, W.H.J., et al., *Partitioning of Organic Chemicals to Polyacrylate-Coated Solid Phase Microextraction Fibers: Kinetic Behavior and Quantitative Structure-Property Relationships*. Analytical Chemistry, 1996. **68**(24): p. 4458-4462.
59. Benhabib, K. and G. Mimanne, *Optimized parameters of SPME analysis for atrazine and its application to measure speciation*. Applied Clay Science, 2014. **87**(0): p. 260-264.
60. Endo, S., S.T.J. Droge, and K.U. Goss, *Polyparameter Linear Free Energy Models for Polyacrylate Fiber-Water Partition Coefficients to Evaluate the Efficiency of Solid-Phase Microextractions*. Analytical Chemistry, 2011. **83**(4): p. 1394-1400.
61. Haftka, J.J.H., et al., *Using Polyacrylate-Coated SPME Fibers To Quantify Sorption of Polar and Ionic Organic Contaminants to Dissolved Organic Carbon*. Environmental Science & Technology, 2013. **47**(9): p. 4455-4462.

62. Verbruggen, E.M.J., et al., *Polyacrylate-Coated SPME Fibers as a Tool To Simulate Body Residues and Target Concentrations of Complex Organic Mixtures for Estimation of Baseline Toxicity*. Environmental Science & Technology, 1999. **34**(2): p. 324-331.
63. Zambonin, C.G. and F. Palmisano, *Determination of triazines in soil leachates by solid-phase microextraction coupled to gas chromatography–mass spectrometry*. Journal of Chromatography A, 2000. **874**(2): p. 247-255.
64. SRC. *PhysProp Database* <http://esc.syrres.com/fatepointer/search.asp> (assessed 25/02/2014). 2014.
65. Schoknecht, U., et al., *Interlaboratory comparison for a laboratory leaching test procedure with façade coatings*. Progress in Organic Coatings, 2013. **76**(2–3): p. 351-359.
66. Juergensen, L., et al., *Fate, behavior, and aquatic toxicity of the fungicide IPBC in the Canadian environment*. Environmental Toxicology, 2000. **15**(3): p. 201-213.
67. Bob, M. and H.W. Walker, *Enhanced adsorption of natural organic matter on calcium carbonate particles through surface charge modification*. Colloids and Surfaces a-Physicochemical and Engineering Aspects, 2001. **191**(1-2): p. 17-25.
68. Ciullo, P.A., *Industrial Minerals and Their Uses*. 1996, Saddle River, New Jersey: Noyes Publications.
69. Giese, R.F., P.M. Costanzo, and C.J. Vanoss, *The Surface Free-Energies of Talc and Pyrophyllite*. Physics and Chemistry of Minerals, 1991. **17**(7): p. 611-616.
70. Vijay, M. and C.J. Patel, *Understanding Coatings Raw Materials*. 2015, Hanover.: Vincentz Network.
71. Berglof, T., et al., *Carbendazim sorption-desorption in Vietnamese soils*. Chemosphere, 2002. **48**(3): p. 267-273.
72. Haderlein, S.B. and R.P. Schwarzenbach, *Adsorption of Substituted Nitrobenzenes and Nitrophenols to Mineral Surfaces*. Environmental Science & Technology, 1993. **27**(2): p. 316-326.
73. Ulusoy, U., C. Hiciilmaz, and M. Yekeler, *Role of shape properties of calcite and barite particles on apparent hydrophobicity*. Chemical Engineering and Processing, 2004. **43**(8): p. 1047-1053.
74. Jaffe, H.W., *Introduction to Crystal Chemistry: Student Edition*. 1988, Cambridge.: Cambridge University Press.
75. Styszko, K. and K. Kupiec, *Determination of diffusion coefficients of biocides on their passage through organic resin-based renders*. Chemosphere, 2016. **160**: p. 273-279.
76. Bergek, J., et al., *Controlled release of microencapsulated 2-n-octyl-4-isothiazolin-3-one from coatings: Effect of microscopic and macroscopic pores*. Colloids and Surfaces A: Physicochemical and Engineering Aspects, 2014. **458**(0): p. 155-167.
77. Rokach, J. and P. Hamel, *Photoisomerization of 2-substituted-isothiazol-3(2H)-ones to 3-substituted-thiazol-2(3H)-ones*. Journal of the Chemical Society, Chemical Communications, 1979(18): p. 786-787.
78. Sakkas, V.A., I.K. Konstantinou, and T.A. Albanis, *Aquatic phototransformation study of the antifouling agent Sea-Nine 211: identification of byproducts and the reaction pathway by gas chromatography-mass spectroscopy*. Journal of Chromatography A, 2002. **959**(1-2): p. 215-227.
79. Williams, T.M. and A.H. Jacobson. *Paper No. 303: Environmental fate of isothiazolone biocides*. in *Corrosion*. 1999. NACE International, Houston, TX, USA.
80. European Parliament and Council, *Assessment Report OIT (PT8 wood preservative)*. 2017.
81. US EPA. *EPI Suite™ v4.10* <http://www.epa.gov/oppt/exposure/pubs/episuitedi.htm>. 2011.
82. Krzeminski, S.F., et al., *Fate of microbicidal 3-isothiazolone compounds in the environment: Products of degradation*. Journal of Agricultural and Food Chemistry, 1975. **23**(6): p. 1068-1075.
83. European Parliament and Council, *Assessment Report DCOIT (PT8 wood preservative)*. 2011.
84. Wittmer, I.K., et al., *Modelling biocide leaching from facades*. Water Research, 2011. **45**(11): p. 3453-3460.

85. Bollmann, U.E., et al., *Leaching of Terbutryn and Its Photodegradation Products from Artificial Walls under Natural Weather Conditions*. Environmental Science & Technology, 2016. **50**(8): p. 4289-95.
86. Horn, W., O. Jann, and O. Wilke, *Suitability of small environmental chambers to test the emission of biocides from treated materials into the air*. Atmospheric Environment, 2003. **37**(39–40): p. 5477-5483.
87. Allen, N.S., et al., *Behaviour of nanoparticle (ultrafine) titanium dioxide pigments and stabilisers on the photooxidative stability of water based acrylic and isocyanate based acrylic coatings*. Polymer Degradation and Stability, 2002. **78**(3): p. 467-478.
88. Miklecic, J., et al., *Influence of TiO<sub>2</sub> and ZnO nanoparticles on properties of waterborne polyacrylate coating exposed to outdoor conditions*. Progress in Organic Coatings, 2015. **89**: p. 67-74.
89. Nguyen, T.V., et al., *Effect of R-TiO<sub>2</sub> and ZnO nanoparticles on the UV-shielding efficiency of water-borne acrylic coating*. Progress in Organic Coatings, 2017. **110**: p. 114-121.
90. Nguyen, T.V., et al., *Accelerated degradation of water borne acrylic nanocomposites used in outdoor protective coatings*. Polymer Degradation and Stability, 2016. **128**: p. 65-76.
91. Lányi, K. and Z. Dinya, *Photodegradation study of some triazine-type herbicides*. Microchemical Journal, 2003. **75**(1): p. 1-13.
92. Kandavelu, V., H. Kastien, and K.R. Thampi, *Photocatalytic degradation of isothiazolin-3-ones in water and emulsion paints containing nanocrystalline TiO<sub>2</sub> and ZnO catalysts*. Applied Catalysis B: Environmental, 2004. **48**(2): p. 101-111.
93. Mestankova, H., et al., *Evolution of algal toxicity during (photo)oxidative degradation of diuron*. Aquatic Toxicology, 2011. **101**(2): p. 466-473.
94. Reza, K.M., A. Kurny, and F. Gulshan, *Photocatalytic Degradation of Methylene Blue by Magnetite+H<sub>2</sub>O<sub>2</sub>+UV Process*. Int J Environ Sci Develop, 2016. **7**(5): p. 325-329.
95. Li, F.B., et al., *Effect of alumina on photocatalytic activity of iron oxides for bisphenol A degradation*. Journal of Hazardous Materials, 2007. **149**(1): p. 199-207.
96. Pulgarin, C. and J. Kiwi, *Iron Oxide-Mediated Degradation, Photodegradation, and Biodegradation of Aminophenols*. Langmuir, 1995. **11**(2): p. 519-526.

# Bilag 1.

## Material properties

### Bilag 1.1 Paint composition

Provided by Dr.-Robert-Murjahn-Institut, Ober-Ramstadt, Germany

Ingredient	Pigment-free paint	Red paint	Black paint	White paint
	Wt.-%	Wt.-%	Wt.-%	Wt.-%
Water	17.32	17.32	17.32	17.32
Cellulose ether	0.19	0.19	0.19	0.19
Sodium hydroxide solution 20%	0.19	0.19	0.19	0.19
Na-Polyacrylate 35%	0.28	0.28	0.28	0.28
Polymer defoaming agent	0.28	0.28	0.28	0.28
Methylisothiazolinone/ Benzisothiazolinone	0.19	0.19	0.19	0.19
TiO <sub>2</sub> chloride type Color index: P.W. 6	0.00	0.00	0.00	<b>9.21</b>
Iron oxide red / Fe <sub>2</sub> O <sub>3</sub> / color index P.R. 101	0.00	<b>9.21</b>	0.00	0.00
Iron oxide black / Fe <sub>3</sub> O <sub>4</sub> / color index: P.Bk. 11	0.00	0.00	<b>9.21</b>	0.00
CaCO <sub>3</sub> D: 50 15 µ	<b>31.98</b>	22.77	22.77	22.77
Mica D: 50 38 µ	4.46	4.46	4.46	4.46
CaCO <sub>3</sub> D: 50 5 µ	13.86	13.86	13.86	13.86
Styrolacrylate 50% MFT ca. 20 Grad	27.72	27.72	27.72	27.72
Silicon-resin emulsion mod. polysiloxane 55 %	0.99	0.99	0.99	0.99
Acrylate thickener 25 %	0.28	0.28	0.28	0.28
Dipropyleneglycole n-Butyl- ether	1.29	1.29	1.29	1.29
25% Terbutryn <sup>1</sup>	0.20	0.20	0.20	0.20
50% Diuron <sup>1</sup>	0.10	0.10	0.10	0.10
8% OIT <sup>1</sup>	0.63	0.62	0.62	0.63
50% Carbendazim <sup>1</sup>	0.11	0.10	0.10	0.11

(1) only in paint formulation with biocides

# Bilag 2.

## Extraction and analytical method

### Bilag 2.1 Extraction recoveries transformation products

ID	Name	Recovery [%] (St. Dev.)	
		Water	Render
OT	3-Octylthiazol-2(3H)-one	100 (11)	55 (0.8)
OFA	N-Octylformamide	87 (10)	54 (0.9)
OPA	N-Octylprop-2-enamide	99 (10)	62 (1)
OAA	N-Octylacetamide	99 (12)	59 (0.9)
OAM	Octylamine	113 (4)	46 (1)
OMA	N-Octyl malonamic acid	113 (2)	36 (4)
OOA	N-Octyl oxamic acid	112 (12)	35 (4)
TB-OH	2-Hydroxy-4-N-ethyl-6-N-tertbutyl-1,3,5-triazine-4,6-diamine	105 (3)	76 (3)
MEBT	2-N-Tertbutyl-4-N-ethyl-6-methoxy-1,3,5-triazine-2,4-diamine		120 (10)
TB-SO	2-N-Tertbutyl-4-N-ethyl-6-methane-sulfinyl-1,3,5-triazine-2,4-diamine	86 (6)	9 (0.8)
M1	2-N-Tertbutyl-6-methylsulfonyl-1,3,5-triazine-2,4-diamine	109 (9)	86 (9)
TB-OH-DesE	2-Hydroxy-4-N-tertbutyl-1,3,5-triazine-4,6-diamine	101 (10)	69 (2)
TB-OH-DesB	2-Hydroxy-4-N-ethyl-1,3,5-triazine-4,6-diamine		147 (3)
TB-DesS	2-N-Tertbutyl-4-N-ethyl-1,3,5-triazine-2,4-diamine		78 (8)
TB-DesS-DesB	2-N-Ethyl-1,3,5-triazine-2,4-diamine	94 (14)	64 (7)
TB-DesS-DesE	2-N-Tertbutyl-1,3,5-triazine-2,4-diamine	84 (10)	77 (5)
DCPMU	1-(3,4-Dichlorophenyl)-3-methyl urea	92 (2)	
Am-BIZ	2-Aminobenzimidazole	98 (3)	
IPPMU	1-(4-Isopropylphenyl)-3-methyl urea	110 (16)	

## Bilag 2.2 Mass spectrometric data of biocides

DP: Declustering potential, EP: Entrance potential, CE: Collision cell energy, CXP: Collision cell exit potential

ID	Name	Supplier	Precursor	Product	DP	EP	CE	CXP
MI	Methylisothiazolinone	Sigma-Aldrich	116	101	77	10	32	20
				98	75	10	25	18
BIT	Benzisothiazolinone	Sigma-Aldrich	152	134	80	10	32	26
				109	90	10	28	21
OIT	<i>N</i> -Octylisothiazolinone	Sigma-Aldrich	214	102	55	10	22	19
				57	84	10	30	10
DCOIT	Dichloro- <i>N</i> -octylisothiazolinone	Thor	282	170	67	10	21	32
				71	68	10	27	27
IPBC	Iodocarb	Sigma-Aldrich	282	165	62	10	26	32
				57	62	10	22	10
CD	Carbendazim	Sigma-Aldrich	192	160	82	10	29	31
				132	73	10	42	24
IP	Isoproturon	Sigma-Aldrich	207	72	84	10	36	29
				165	81	10	23	31
DR	Diuron	Sigma-Aldrich	233	72	70	10	38	13
			235	72	72	10	38	13
TB	Terbutryn	Sigma-Aldrich	242	186	65	10	35	19
				158	58	10	34	31
IRG	Cybutryn (Irgarol 1051)	Dr. Ehrenstorfer	254	198	83	10	30	22
				156	77	10	36	30
TBU	Tebuconazole	Dr. Ehrenstorfer	308	70	85	10	47	13
				125	81	10	51	12
PPZ	Propiconazole	Sigma-Aldrich	342	159	91	13	40	15
				69	34	7	37	13
MCP	Mecoprop*	Dr. Ehrenstorfer	213	141	-65	-10	-22	-10
				71	-64	-10	-15	-10

\*Analyzed with electron spray ionization in negative mode (ESI(-)).



### Bilag 2.3 Mass spectrometric data of surrogate standards

DP: Declustering potential, EP: Entrance potential, CE: Collision cell energy, CXP: Collision cell exit potential

ID	Name	Supplier	Precursor	Product	DP	EP	CE	CXP
MI-D3	Methylisothiazolinone-D3	TRC	119	101	55	10	29	19
				74	45	10	31	13
OIT-D17	N-Octylisothiazolinone-D17	TRC	231	103	47	10	22	5
				66	54	10	34	12
IPBC-D6	Iodocarb-D6	TRC	291	165	55	10	24	9
				66	55	10	24	11
CD-D4	Carbendazim-D4	Dr. Ehrenstorfer	196	164	78	10	28	11
				136	81	10	45	13
IP-D6	Isoproturon-D6	Sigma-Aldrich	213	78	77	10	31	15
				171	79	10	22	17
DR-D6	Diuron-D6	Sigma-Aldrich	239	78	48	10	38	8
			240	78	51	10	35	8
TB-D5	Terbutryn-D5	Dr. Ehrenstorfer	247	191	89	10	32	9
				91	91	10	39	8
IRG-D9	Cybutryn-D9 (Irgarol-D9)	CDN Isotopes	263	199	87	10	29	14
				126	90	10	36	12
TBU-D5	Tebuconazole-D6	Dr. Ehrenstorfer	314	72	91	10	44	13
				125	57	10	54	23
PPZ-D5	Propiconazole-D5	Dr. Ehrenstorfer	347	159	74	10	42	9
				74	63	10	35	13
MCPP-D3	Mecoprop-D3*	Dr. Ehrenstorfer	216	71	-65	-10	-15	-10
				144	-64	-10	-22	-10

\*Analyzed with electron spray ionization in negative mode (ESI(-)).

## Bilag 2.4 Mass spectrometric data of transformation products

DP: Declustering potential, EP: Entrance potential, CE: Collision cell energy, CXP: Collision cell exit potential

ID	Name	Supplier	Precursor	Product	DP	EP	CE	CXP
OT	3-Octylthiazol-2(3 <i>H</i> )-one	Uorsy	214	57	84	10	30	10
				57	60	10	35	9
OFA	<i>N</i> -Octylformamide	TCI-Chemicals	158	57	68	10	25	10
				71	64	10	19	12
OPA	<i>N</i> -Octylprop-2-enamide	Uorsy	184	55	61	10	42	9
				43	45	10	41	7
OAA	<i>N</i> -Octylacetamide	Uorsy	172	60	61	10	26	12
				43	69	10	44	7
OA	Octylamine	Sigma-Aldrich	130	57	60	10	25	12
				71	48	10	22	12
OMA	<i>N</i> -Octyl malonamic acid	Chemspace	216	71	48	10	27	13
				156	50	10	17	9
OOA	<i>N</i> -Octyl oxamic acid	Chemspace	202	71	48	10	17	13
				156	45	10	13	9
TB-OH	2-Hydroxy-4- <i>N</i> -ethyl-6- <i>N</i> -tertbutyl-1,3,5-triazine-4,6-diamine	Sigma-Aldrich	212	86	35	10	35	4
				156	33	10	22	9
TBM	2- <i>N</i> -Tertbutyl-4- <i>N</i> -ethyl-6-methoxy-1,3,5-triazine-2,4-diamine	Sigma-Aldrich	226	114	46	10	35	7
				170	46	10	32	24
TB-SO	2- <i>N</i> -Tertbutyl-4- <i>N</i> -ethyl-6-methane-sulfinyl-1,3,5-triazine-2,4-diamine	MicroCombiChem	258	184	48	10	26	12
				240	50	10	20	15
M1	2- <i>N</i> -Tertbutyl-6-methylsulfonyl-1,3,5-triazine-2,4-diamine	MicroCombiChem	214	158	50	10	36	16
				85	50	10	37	16
TB-OH-DesE	2-Hydroxy-4- <i>N</i> -tertbutyl-1,3,5-triazine-4,6-diamine	Synchem	184	128	60	10	22	7
				86	45	10	35	17
TB-OH-DesB	2-Hydroxy-4- <i>N</i> -ethyl-1,3,5-triazine-4,6-diamine	Synchem	156	114	70	10	23	6
				128	68	10	24	7
TB-DesS	2- <i>N</i> -Tertbutyl-4- <i>N</i> -ethyl-1,3,5-triazine-2,4-diamine	FCH Group	196	140	77	10	32	8
				70	49	10	45	12
TB-DesS-DesB	2- <i>N</i> -Ethyl-1,3,5-triazine-2,4-diamine	FCH Group	140	70	45	10	31	12
				98	43	10	24	10
TB-DesS-DesE	2- <i>N</i> -Tertbutyl-1,3,5-triazine-2,4-diamine	FCH Group	168	112	46	10	25	10
				70	42	10	36	12
DCPMU	1-(3,4-Dichlorophenyl)-3-methyl urea	Sigma-Aldrich	219	127	66	10	37	7
			221	127	66	10	37	7
Am-BIZ	2-Aminobenzimidazole	Sigma-Aldrich	134	65	75	10	47	12
				92	56	10	31	17
IPPMU	1-(4-Isopropylphenyl)-3-methyl urea	Sigma-Aldrich	193	94	73	10	30	5
				136	54	10	22	8

# Bilag 3.

## Additional data: influence of wet & dry cycles

**Bilag 3.1 Water uptake during the wet/dry-experiments.**

time sec	Silicone render		Acrylate render	
	water uptake in each exp. step [g]	in respect to the render [% of render]	water uptake in each exp. step [g]	in respect to the render [% of render]
<b>Wet/Dry</b>				
3	0.07	4.0	0.14	8.2
5	0.04	2.3	0.18	10.3
10	0.07	4.0	0.21	11.8
15	0.08	4.6	0.27	15.4
30	0.09	4.9	0.27	15.6
60	0.13	7.4	0.34	19.4
600	0.18	10.0	0.28	15.8
1800	0.27	15.1	0.29	16.6
3600	0.32	18.0	0.23	13.0
<b>Wet/Wet 24h</b>				
3	0.09	5.0	0.15	8.4
5	0.12	6.9	0.10	5.9
10	0.09	5.0	0.08	4.6
15	0.09	5.3	0.03	1.9
30	0.05	2.9	0.01	0.6
60	0.05	3.0	0.03	1.5
600	0.09	5.0	0.01	0.4
1800	0.11	6.5	0.01	0.8
3600	0.17	9.5	0.00	0.0
<b>Wet/Wet</b>				
3	0.07	4.0	0.10	5.7
5	0.01	0.9	0.03	1.7
10	0.04	2.6	0.05	2.6
15	0.00	0.3	0.01	0.6
30	0.02	1.1	0.02	1.1
60	0.04	2.0	0.01	0.6
600	0.04	2.6	0.00	0.0
1800	0.09	5.1	0.01	0.6
3600	0.11	6.0	0.04	2.3

# Bilag 4.

## Additional data: mobility controlled by the polymeric binder

### Bilag 4.1 Mass balance for confirmation of complete extraction.

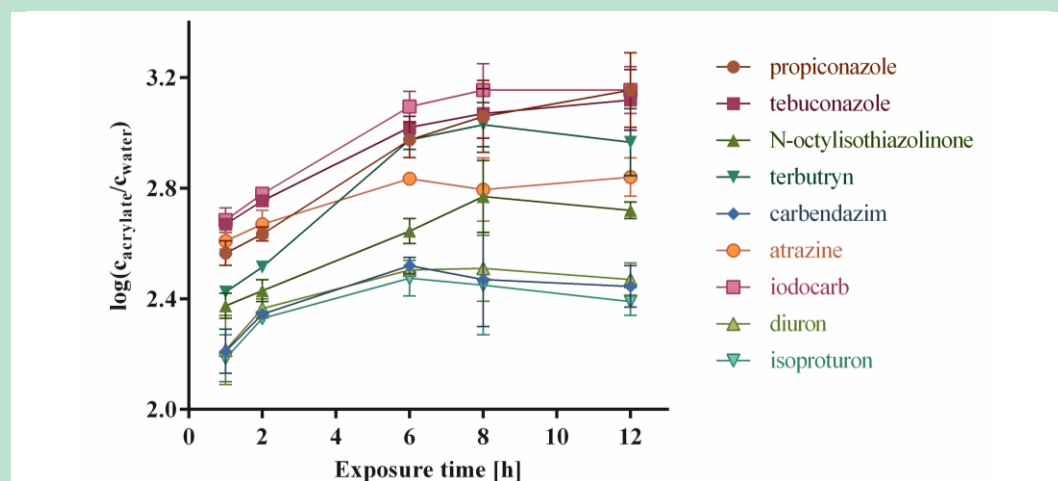
Mass balance for confirmation of complete extraction according to Eq. B4-1 with  $n_W(T_{eq})$  measured amount in the aqueous and  $n_{Ac}(T_{eq})$  measured amount in the polyacrylate phase after equilibration,  $n_0$  initial amount added to the system.

$$M = \frac{n_W(T_{eq}) + n_{Ac}(T_{eq})}{n_0} \cdot 100 \quad (B4-1)$$

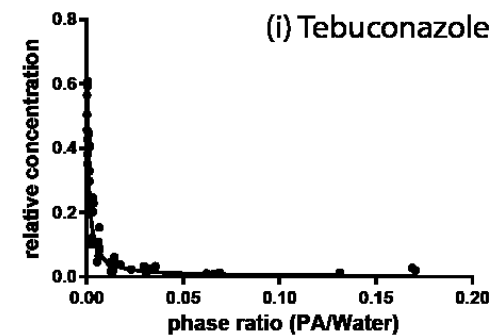
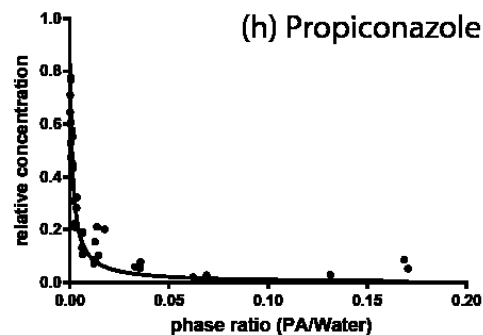
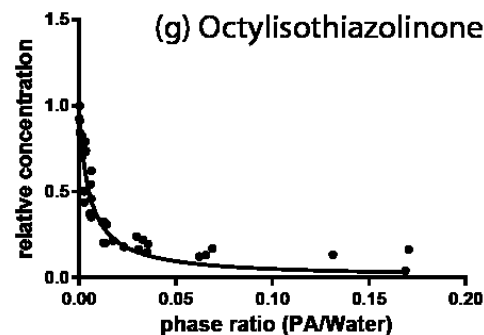
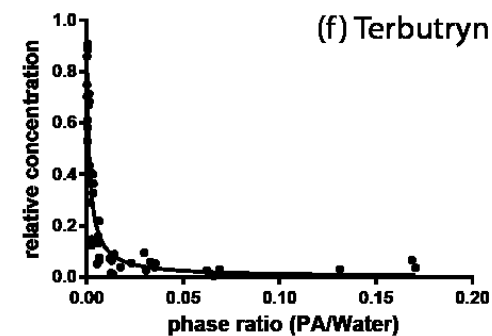
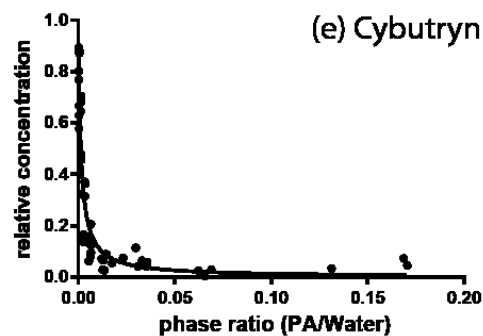
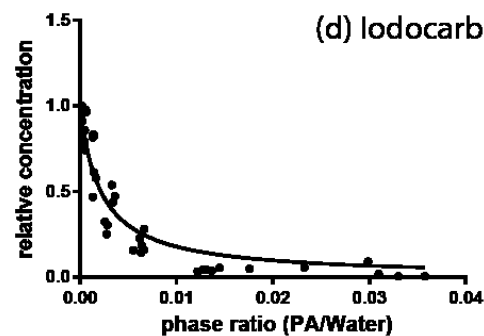
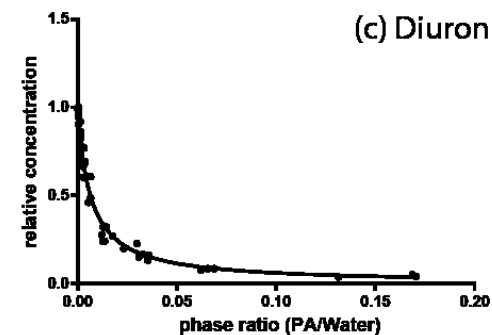
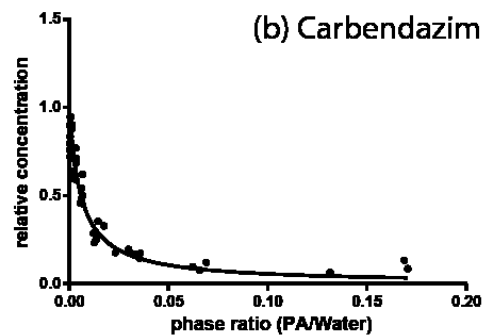
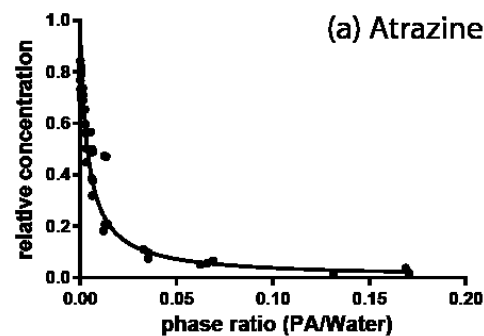
	Mass balance [%]
Carbendazim	79
Isoproturon	91
Diuron	105
Iodocarb	109
Atrazine	101
Terbutryn	87
Cybutryn	82
N-Octylisothiazolinone	81
Tebuconazole	58
Dichloro-N-otylisothiazolinone	74
Propiconazole	72

### Bilag 4.2 Kinetic profiles of the glass fiber filter extraction.

Changes in the concentration ratio over time (average from duplicate analysis, error bars denote standard error of mean).



Bilag 4.3 Non-linear regressions for all studied compounds.

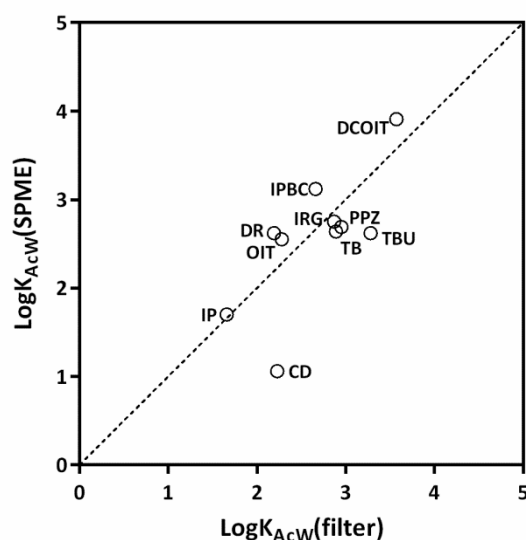


#### Bilag 4.4 Solid phase micro extraction (SPME).

For comparative reasons the polyacrylate-water partition constants were determined using solid phase micro extraction (SPME) fibers as well. SPME fiber assemblies with polyacrylate coating (length 10 mm, 85 µm coating) were purchased from Supelco (Bellefonte, Pennsylvania, USA). Prior usage the fibers were cleaned with methanol. 100 mL aqueous biocide solution, both 10 ng mL<sup>-1</sup> and 100 ng mL<sup>-1</sup>, were exposed to SPME fibers for 18 h, while stirring with glass coated magnetic stirrers at room temperature. Afterwards the fibers were extracted by 100 µL methanol for 6 h. Both, 100 µL of the extracted aqueous biocide solution as well as the methanol extract were spiked with 10 µL surrogate standard and analyzed by HPLC-MS/MS. The experiments were performed in triplicates. The polyacrylate-water partition constant of the solid phase micro extraction  $\log K_{AcW}(SPME)$  was determined according to Eq. B4-2.

$$\log K_{AcW}(SPME) = \frac{n_{Ac}(T_{eq})}{n_W(T_{eq})} \quad (B4-2)$$

In particular, the polyacrylate-water partition constant determined by solid phase micro extraction of carbendazim differs significantly from the one determined by coated glass fiber filters, while all other biocides scatter around the 1:1-line (Figure B4-1).



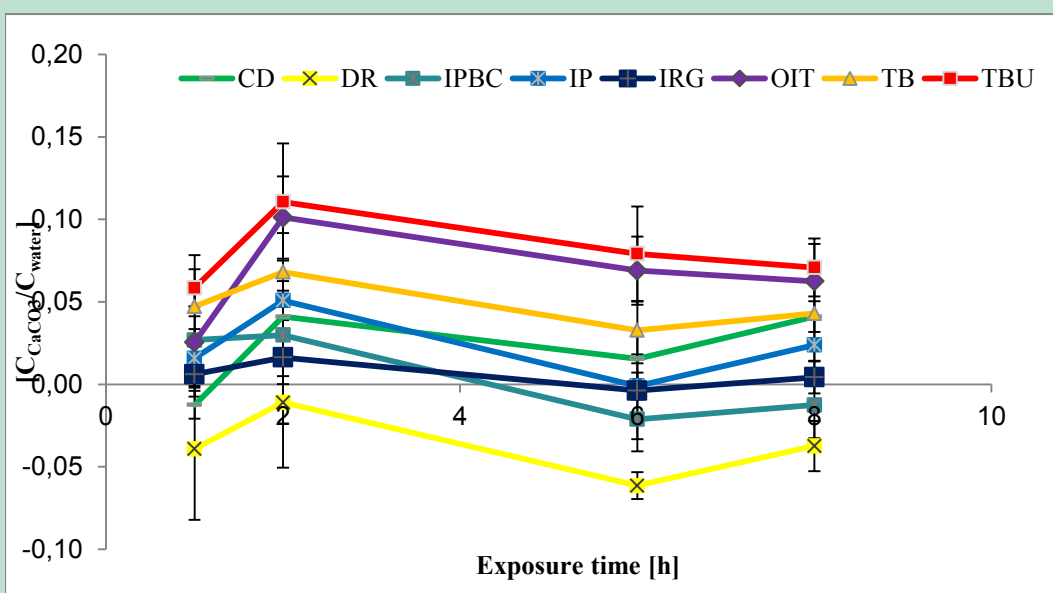
**Figure B4-1** Comparison acylate-water partition constants determined by SPME ( $\log K_{AcW}(SPME)$ ) and coated glass fiber filter ( $\log K_{AcW}(\text{filter})$ ); DCOIT: dichloro-*N*-octylisothiazolione, IPBC: iodocarb, IRG: cybutryn, PPZ: propiconazole, TB: terbutryn, TBU: tebuconazole, DR: diuron, OIT: *N*-octylisothiazolinone, IP: isoproturon, CD: carbendazim.

# Bilag 5.

## Additional data: mobility controlled by the minerals

### Bilag 5.1 Kinetic profiles for calcium carbonate.

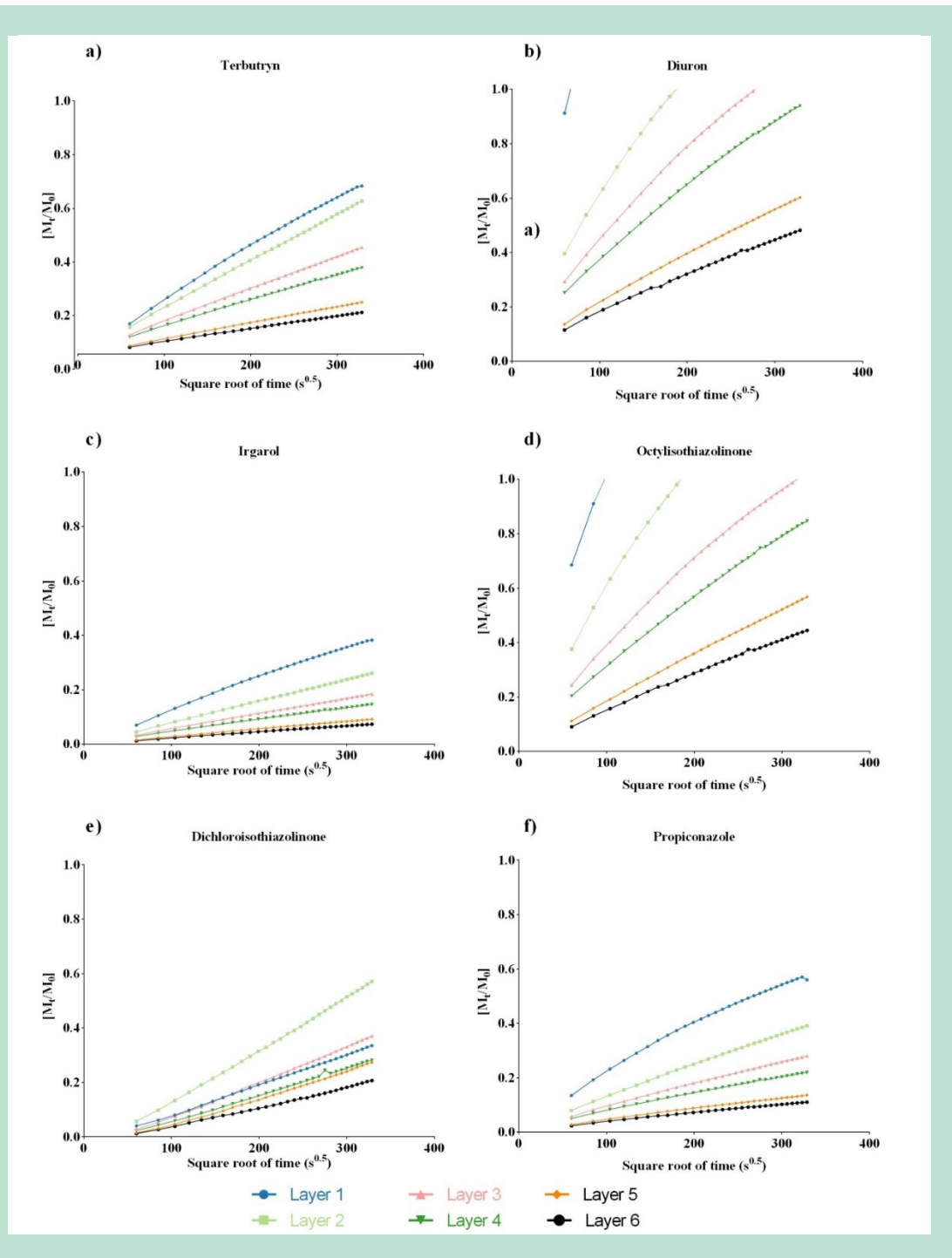
Kinetic profiles for calcium carbonate: changes in the concentration ratio over time (average from duplicate analysis).



# Bilag 7.

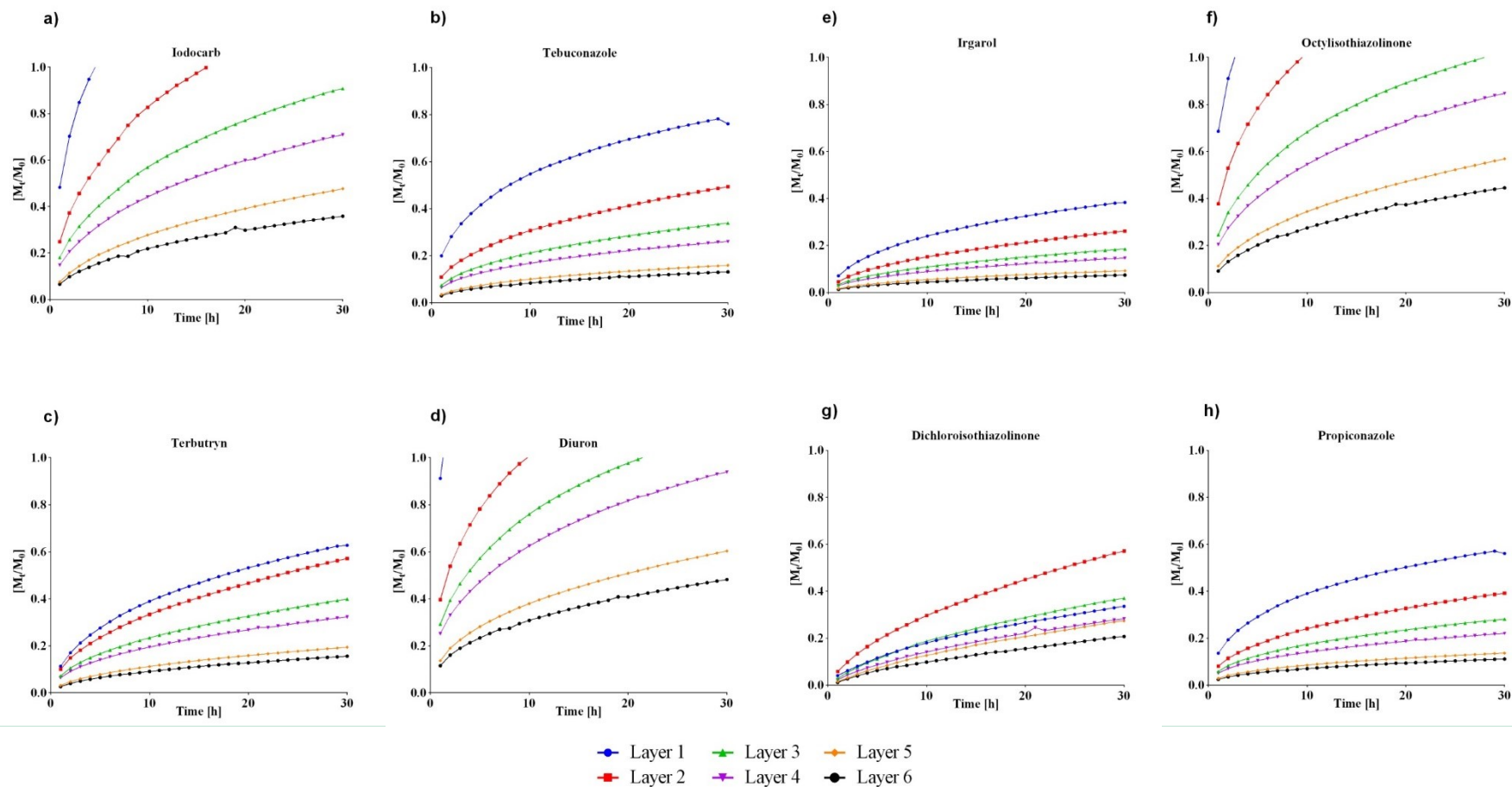
## Additional data: diffusion controlled mobility

Bilag 7.1 Mass transfer of biocides through layered paint films into water.





## Bilag 7.2 Depletion of biocides amount in paint film

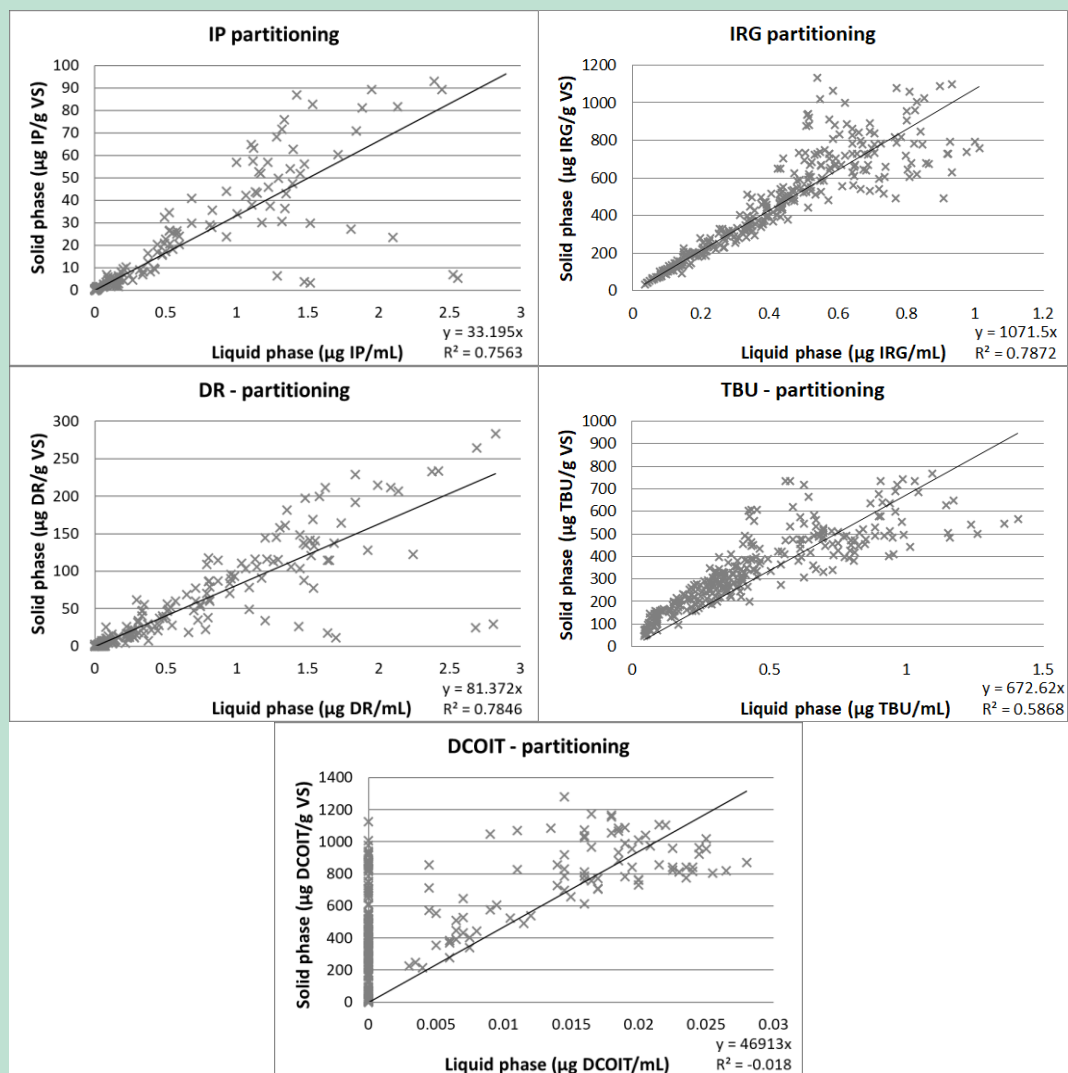


# Bilag 8.

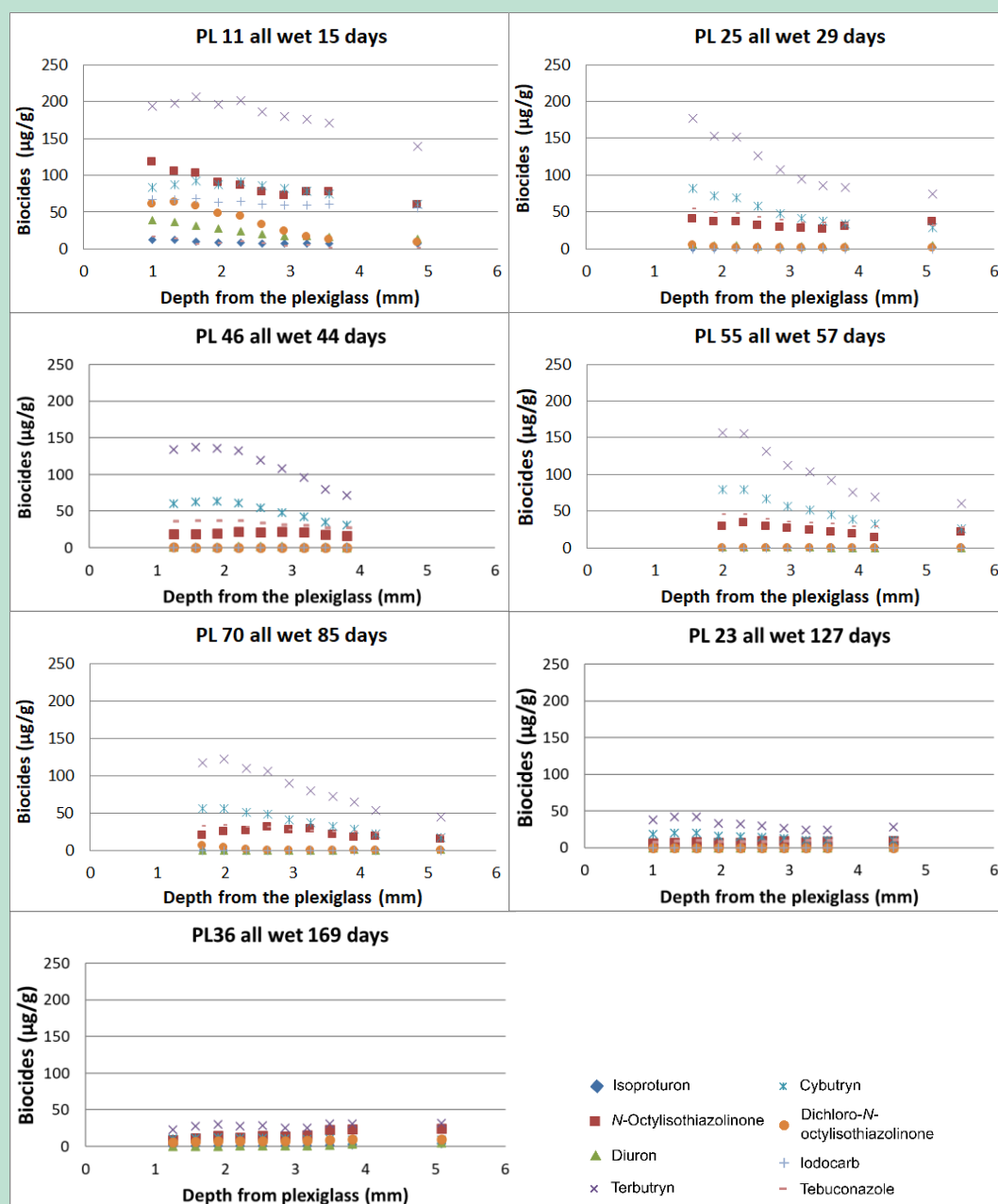
## Additional data: depth resolved profiling

### Bilag 8.1 Render-water distribution of biocides.

The regression line was forced through zero.

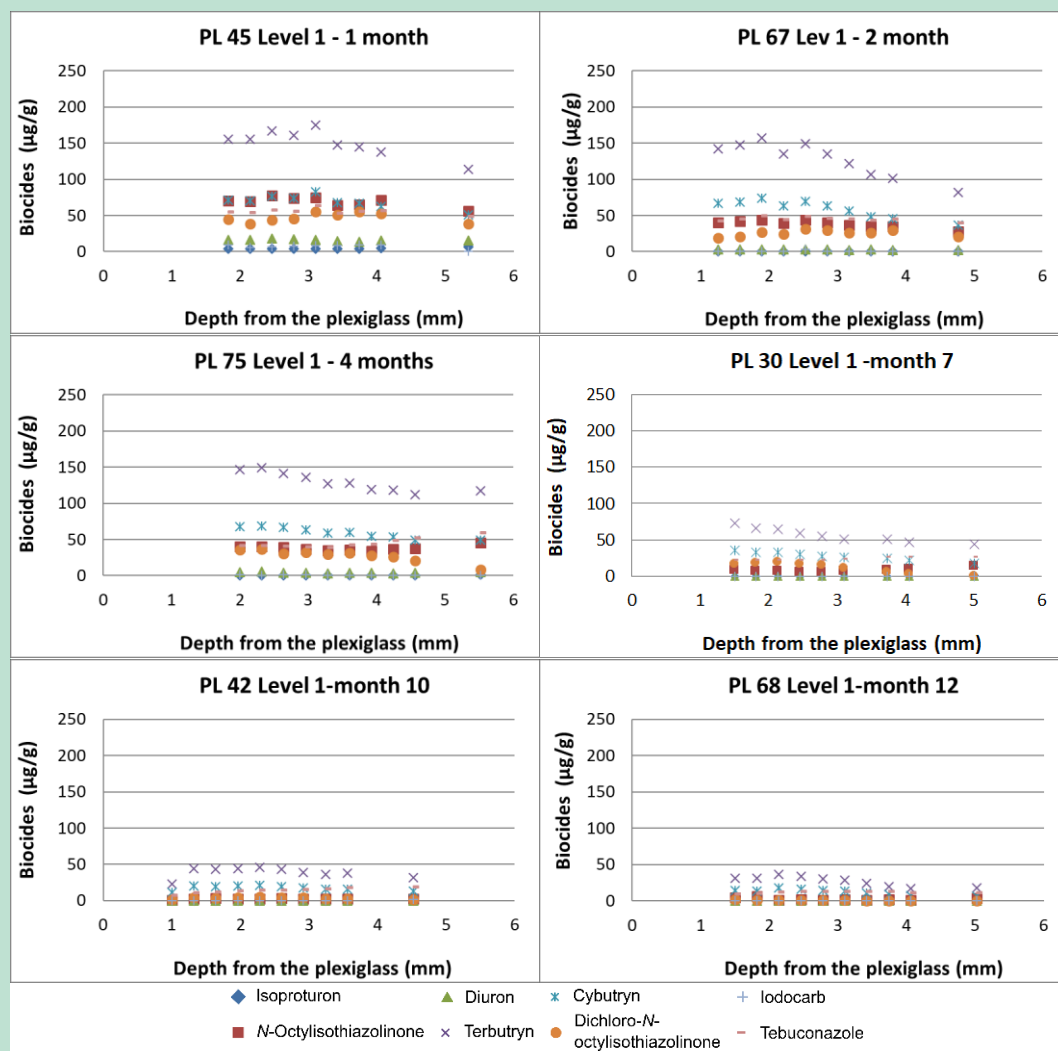


## Bilag 8.2 Biocides in render tiles subject to continuous wetting.



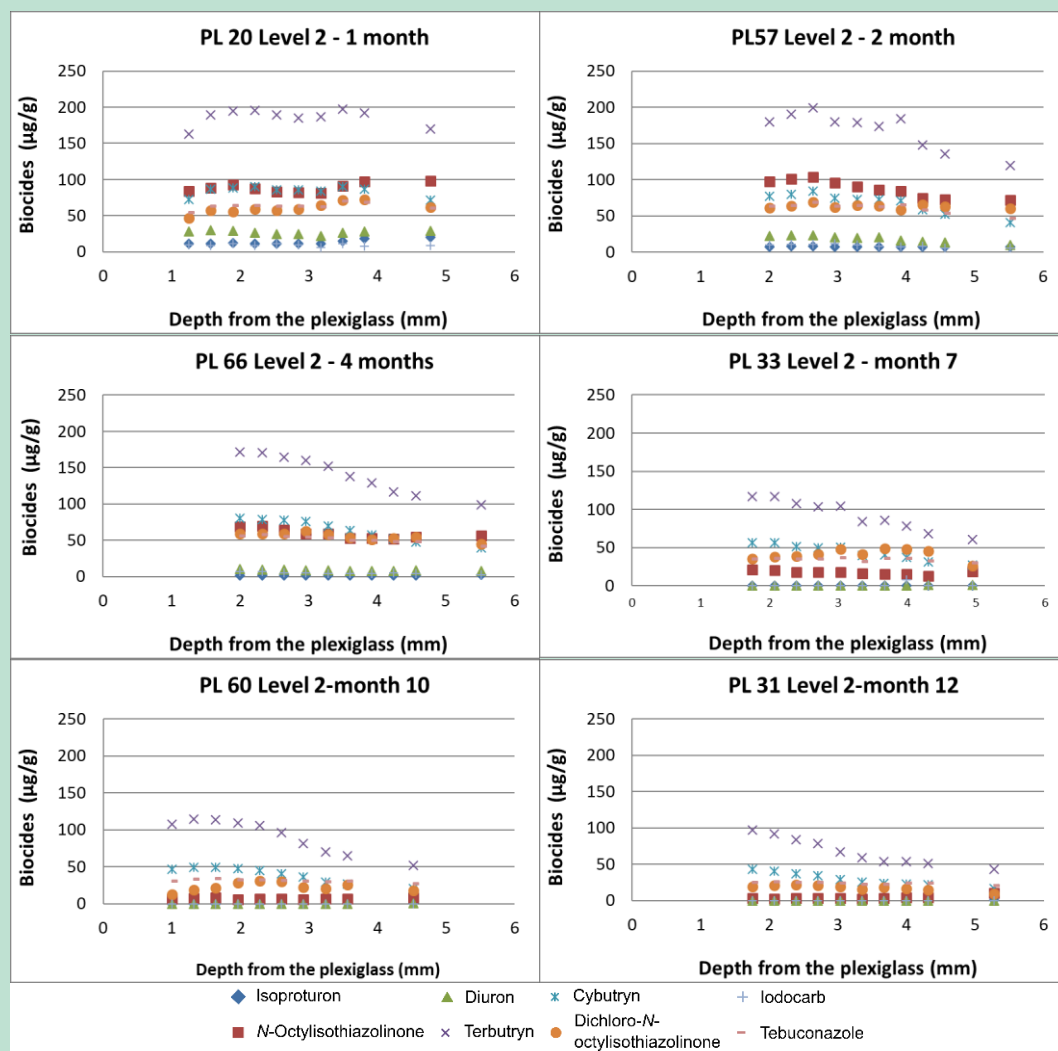
### Bilag 8.3

### Biocides in render tiles subject to intermittent wetting – highest wetting frequency (3 days).



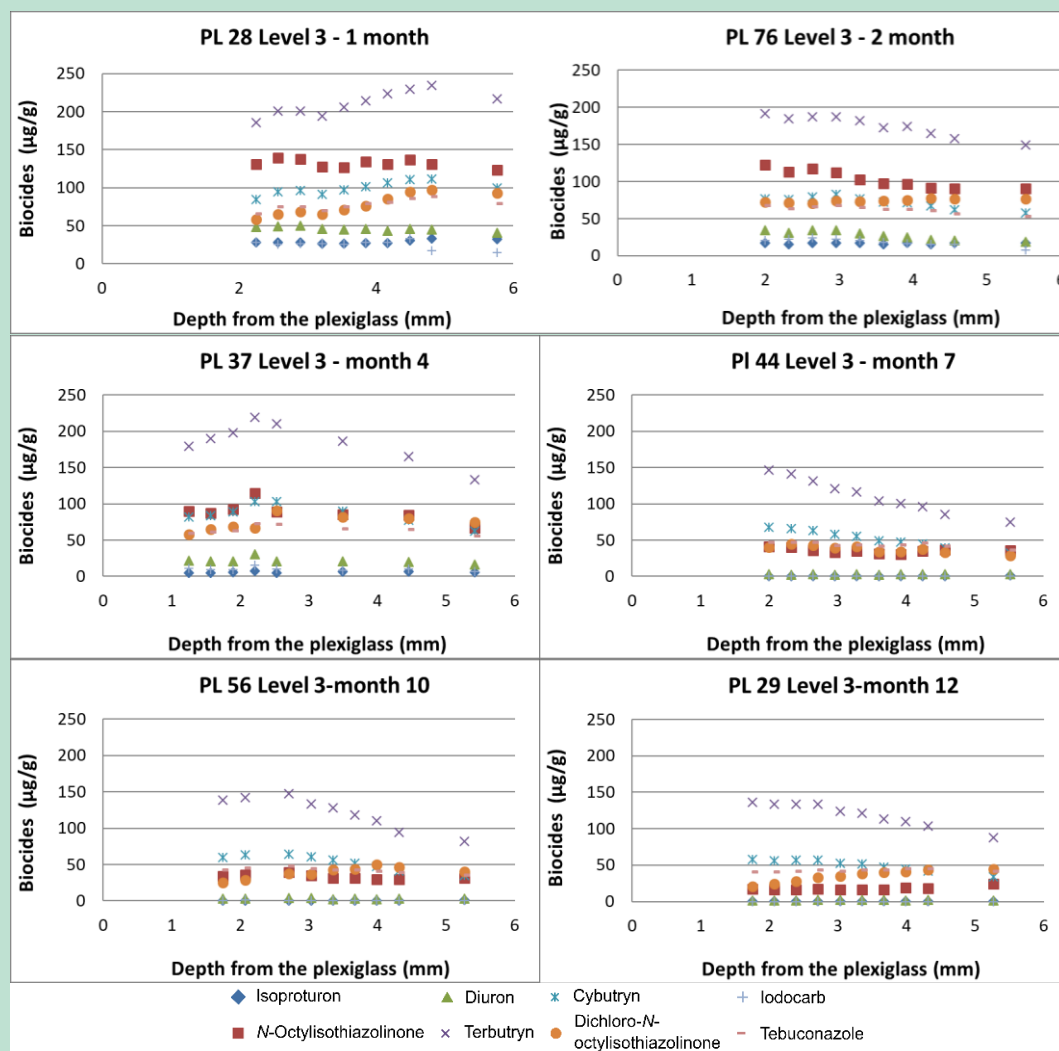
# Bilag 8.4

## Biocides in render tiles subject to intermittent wetting – medium wetting frequency (6 days).



## Bilag 8.5

### Biocides in render tiles subject to intermittent wetting – lowest wetting frequency (9 days).

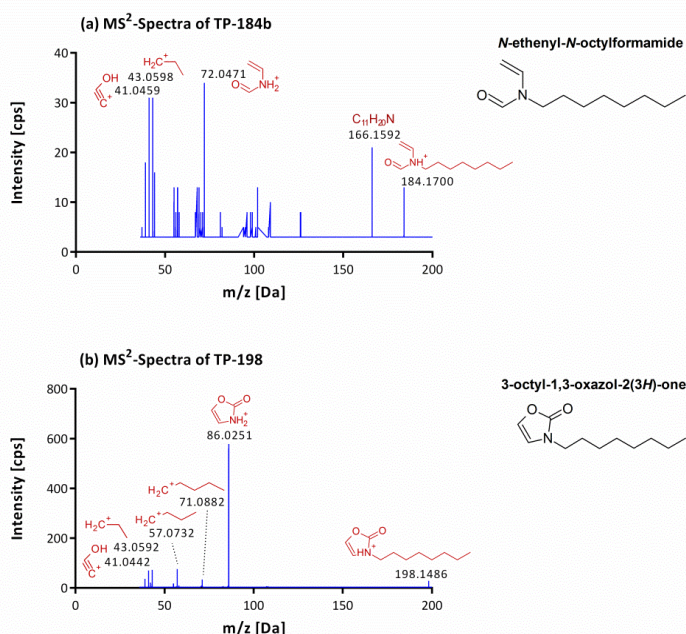


# Bilag 9.

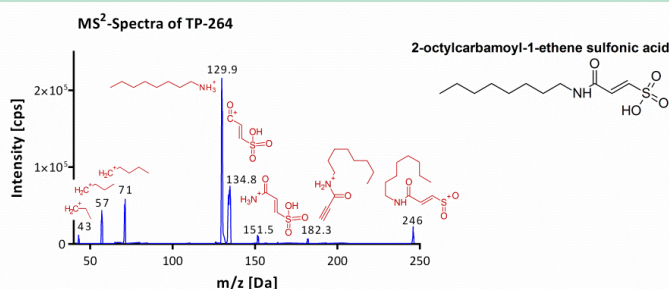
## Additional data: photodegradation products

### Bilag 9.1 MS<sup>2</sup> spectra and possible fragmentation pattern of suggested chemical structures.

MS<sup>2</sup> spectra (ESI+, CE = 40 V, TripleToF 5600), chemical structures and suggested fragmentation pattern of (a) TP-184b (suggestion: *N*-ethenyl-*N*-octylformamide) and (b) TP-198 (suggestion: 3-octyl-1,3-oxazol-2(3*H*)-one) from the HR-MS analysis of the laboratory degradation study.



MS<sup>2</sup> spectra (ESI+, CE = 40 V, API4000), chemical structures and suggested fragmentation pattern of TP-264 (suggestion: 2-octylcarbamoyl-1-ethene sulfonic acid) detected in a suspect screening in runoff samples and extracts of the render of the studied panels.

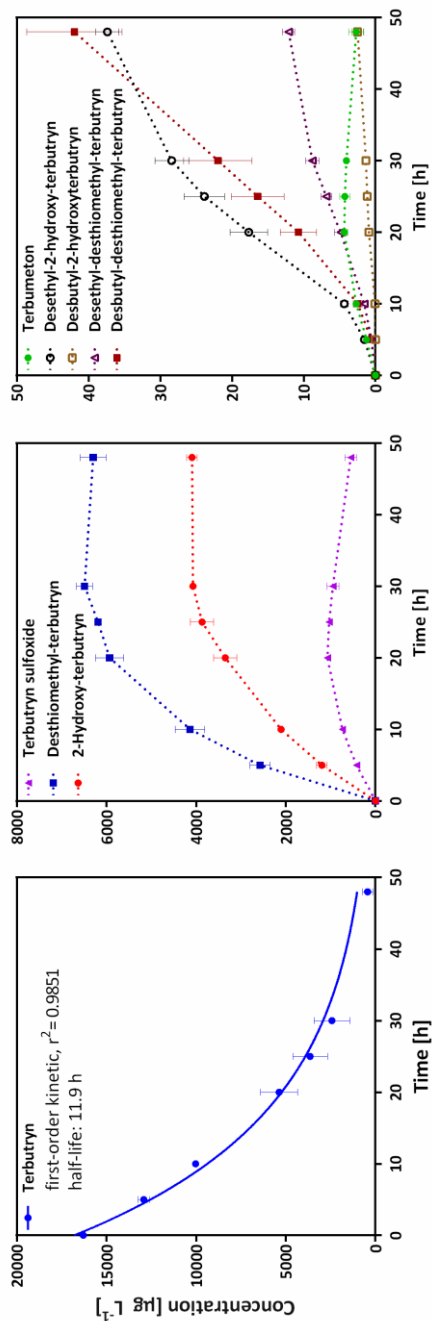


## Bilag 9.2

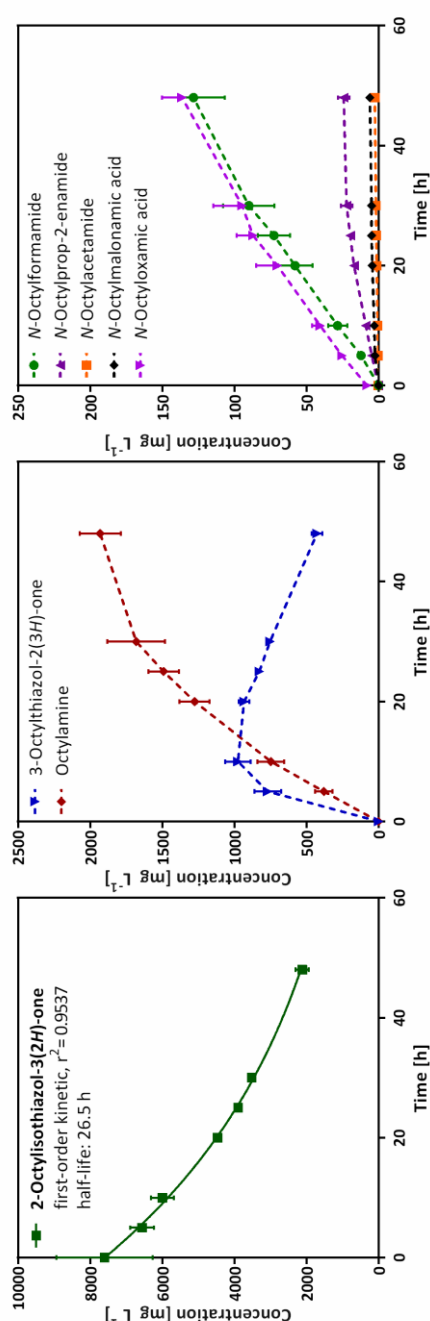
### Kinetic profiles for *N*-octylisothiazolinone and terbutryn in laboratory experiments.

Photodegradation of (a) terbutryn and (b) *N*-octylisothiazolinone dissolved in tap water under UV-light (254 nm;  $2.31 \cdot 10^{-10}$  Einstein  $\text{cm}^{-2} \text{s}^{-1}$ ) and formation of degradation products over time (error bars: standard error of the mean of two replicates).

(a) Terbutryn and its transformation products



(b) *N*-Octylisothiazolinone and its transformation products

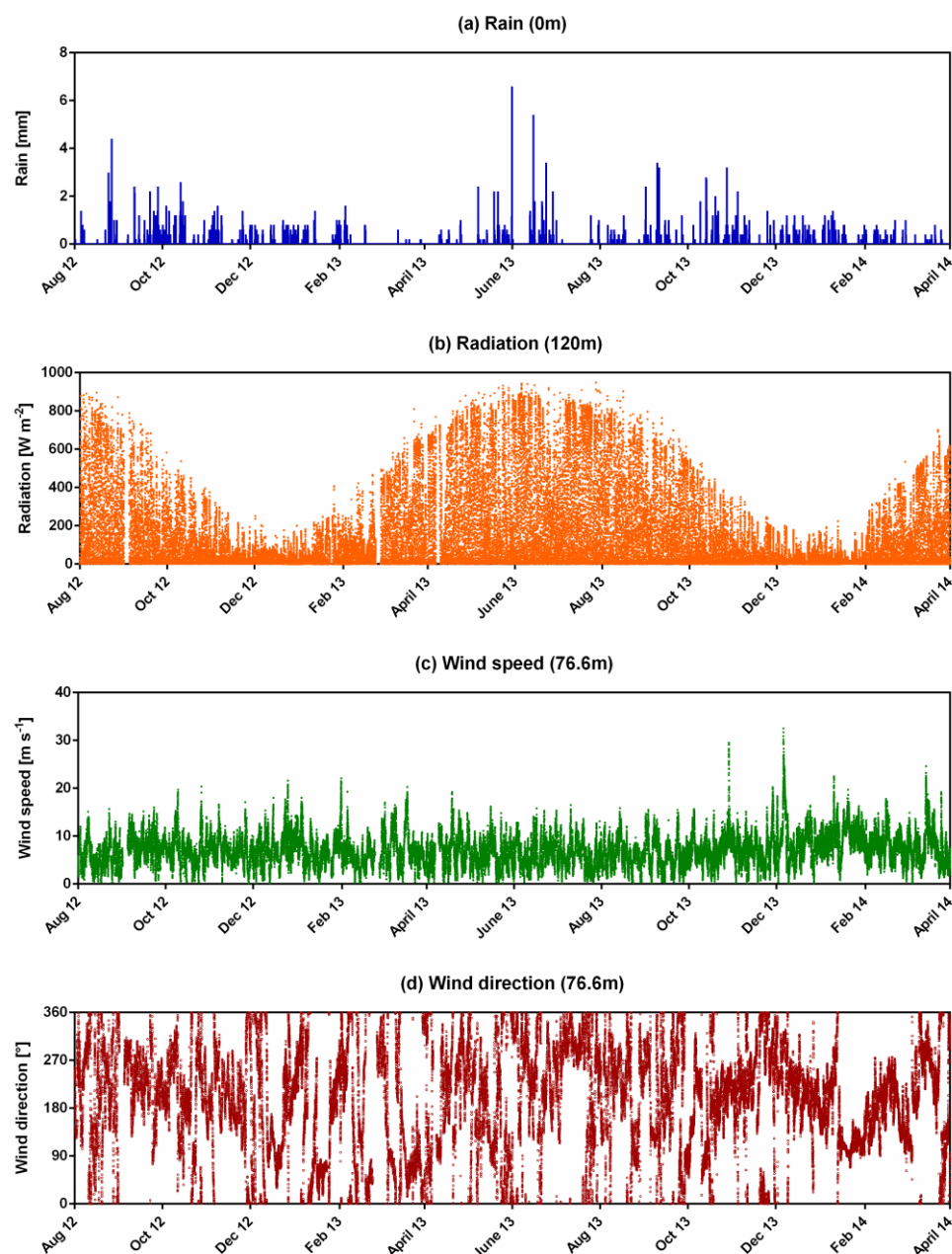




# Bilag 10.

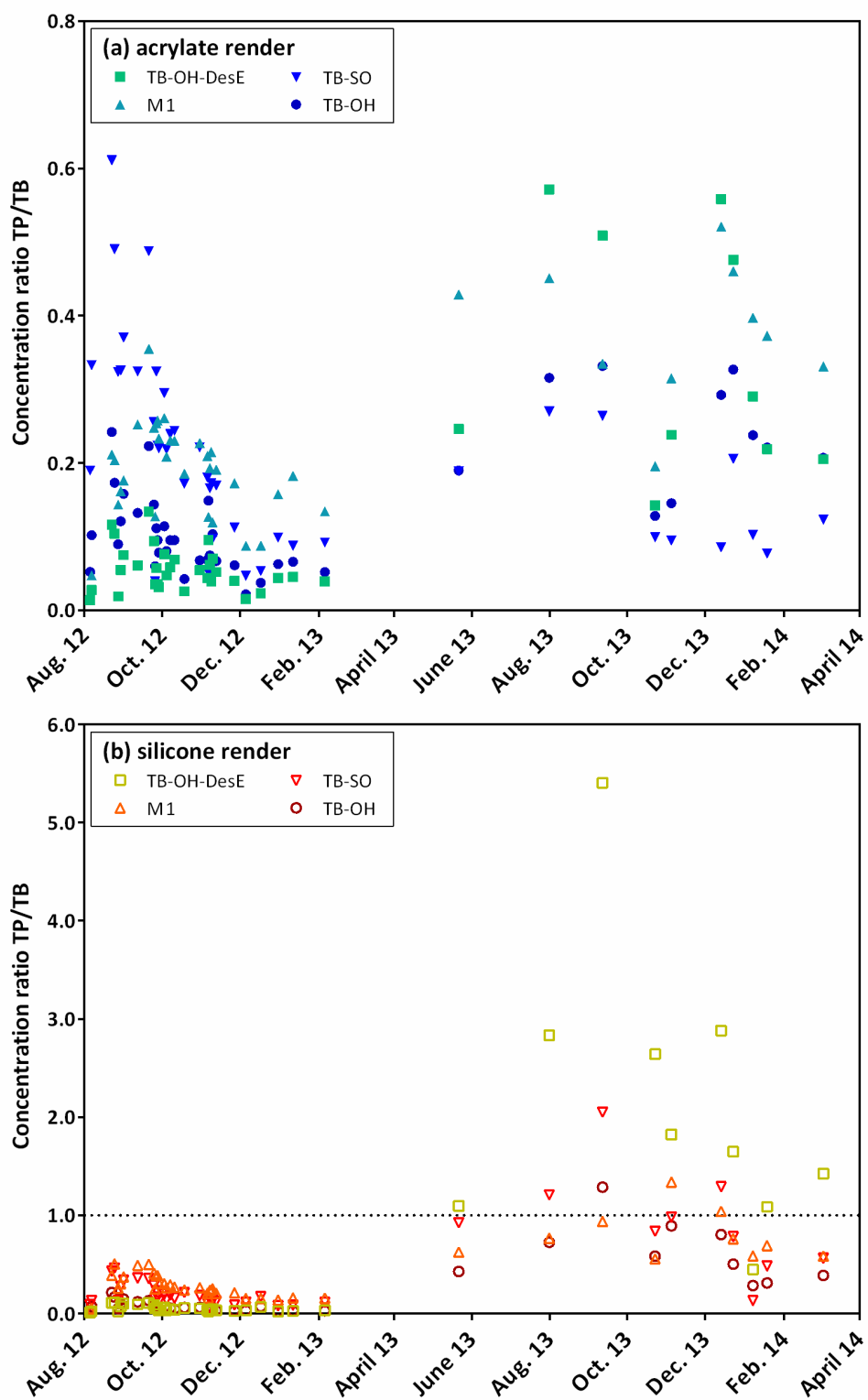
## Additional data: photodegradation on facade surfaces

**Bilag 10.1** Weather data for field experiments (data points: 10 min average).



## Bilag 10.2

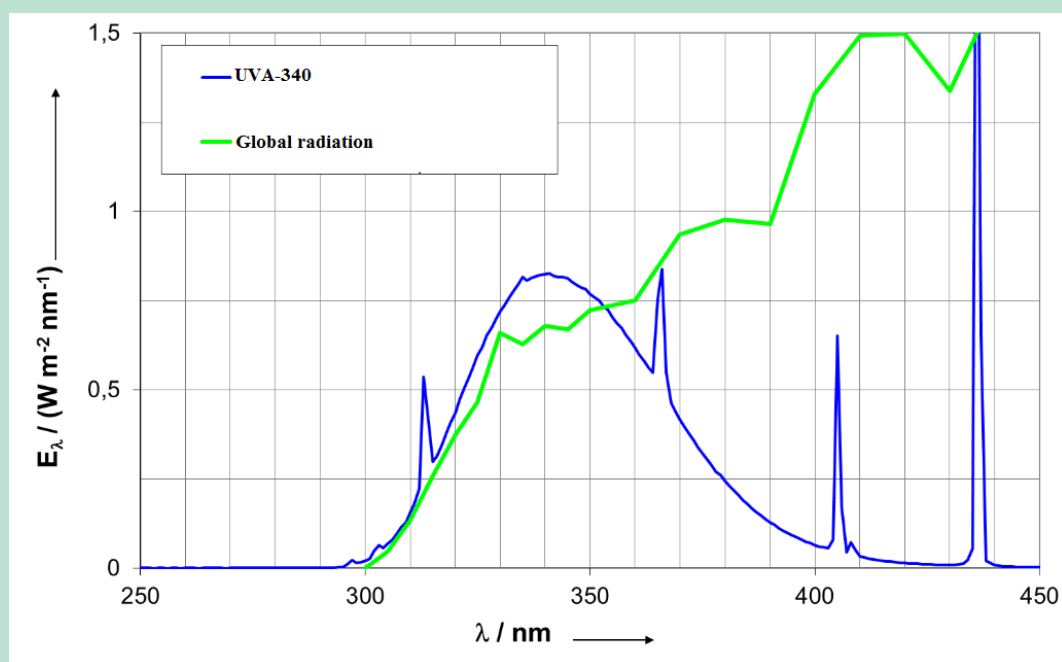
Concentrations of the transformation products in relation to the terbutryn concentration over time (average values for three panels each).



# Bilag 11.

## Additional data: influence of pigments on photodegradation

**Bilag 11.1** Typical spectrum of the used UVA-340 lamps compared to global radiation



**Bilag 11.2** Recovery rates for biocides extracted from paint spiked with biocides.

Name	Recovery (STD Dev.) [%]
Carbendazim	137 (4)
Diuron	108 (3)
N-Octylisothiazolinone	131 (5)
Terbutryn	112 (4)

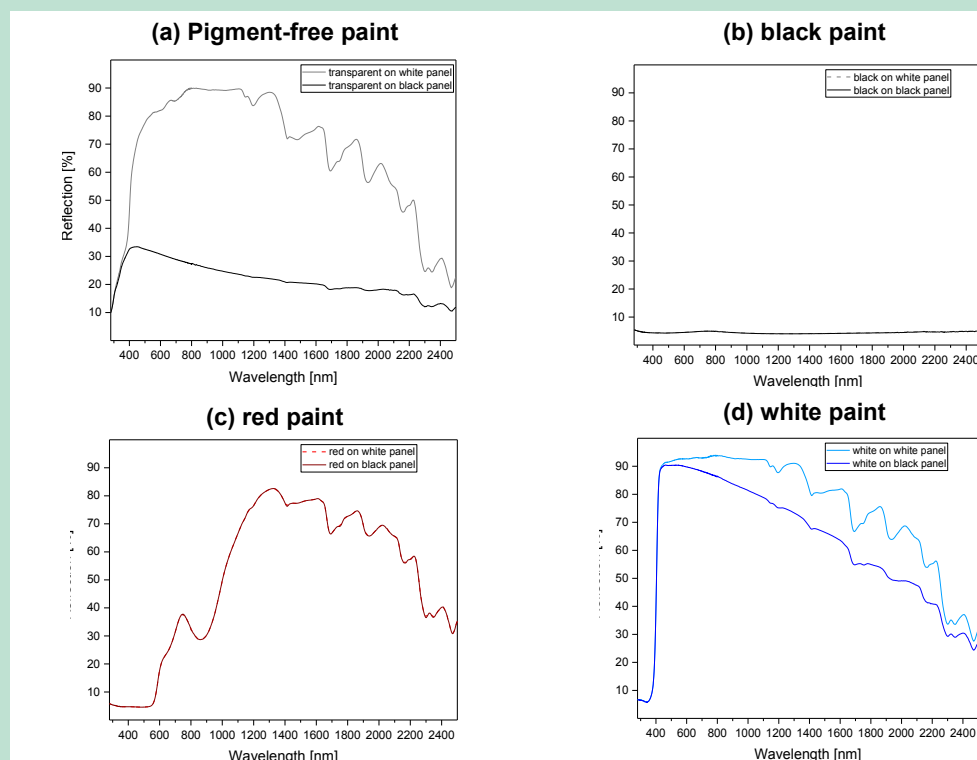
### Bilag 11.3 Total solar reflection (TSR).

The optical properties and switching characteristics of paints were measured by UV-VIS-NIR spectrophotometer (Type Cary 5000, Agilent Technologies, Waldbronn, Germany) equipped with a 150 mm Ulbricht sphere for measurements of diffuse reflection. The TSR determination was performed following the ASTM G173-03 standard for calculations. The discrete wavelength change was set to 1 nm between 280 nm and 800 nm, and 5 nm between 800 nm and 2500 nm. The paint samples were applied with a spreading knife to reach a film thickness of 400 µm to Leneta-2DX test slides. The test specimens thus prepared were dried for at least 24 hours in standard conditions according to DIN EN 23270 at  $23 \pm 2$  °C and a relative humidity of  $50 \pm 5\%$ .

The paints were applied to white and black surfaces in order to get information on transmission through the paint film. The measured signal represents solely reflected radiation in case of black background (radiation is totally absorbed) and reflected and transmitted radiation in case of white background (radiation that is transmitted through the paint film is reflected). The difference between the two signals represents transmission. Note that the radiation transmitted has passed the coating film twice.

**Table B11-1** Results from TSR measurements assigned to different types of radiation.

Colour	TSR, paint on white panel				TSR, paint on black panel				Transmission			
	Total	UV	Vis	IR	Total	UV	Vis	IR	Total	UV	Vis	IR
<b>Pigment-free</b>	78.2	30.9	78.2	82.8	27.1	27.4	30.9	23.5	51.1	3.5	47.3	59.3
<b>red</b>	31.6	4.1	12.9	51.9	29.4	4.1	12.8	47.6	2.2	0	0.1	4.3
<b>black</b>	4.0	4.0	4.0	4.0	4.0	4.0	4.0	4.0	0	0	0	0
<b>white</b>	85.1	11.4	90.4	87.1	78.5	11.4	88.1	75.9	6.6	0	2.3	11.2



**Figure B11-1** TSR spectra.

#### Bilag 11.4 FT-IR-spectrometry

FT-IR spectra (obtained by a Nicolet NEXUS 670 FTIR (Thermo Fisher Scientific, Waltham, MA, USA) of paints were measured by ATR infrared spectroscopy (attenuated total reflection) in order to expose the differences between irradiated and non-irradiated samples. Two samples for each paint were analyzed, one not exposed to light and one irradiated for 1056 h. Paint films were removed from the glass plates and fixed on top of the ATR crystal (diamond coated zinc selenide). Infrared light passed the ATR crystal from the bottom and was reflected by the paint film surface. Extinction of the reflected infrared signal was recorded. Different spots of about 2 mm<sup>2</sup> on the film surfaces were analyzed at least three times both from the UV-radiated top side and the lower side (that was in contact with glass). Position and intensity of characteristic signals (signal height) of the FTIR spectra were analyzed using the software programme called OMNIX.

Characteristic IR signals were selected. It is supposed that the IR spectra mainly represent the styrene acrylate binder of the investigated paints. Substituents that are indicated by the characteristic signals (see Table SI 7-1) can be assigned to chemical bonds that occur in either styrene or acrylates.

Intensities of signals at the selected wave numbers were recorded. The intensities varied for the IR spectra from different spots of the film surfaces, especially from the top sides. This is probably caused by irregular surface structure. Differences in signal intensities were less pronounced for the lower sides that were rather even due to the former contact to the glass plates. Mean values of these intensities were calculated for up to five IR spectra from each sample (each for the top and lower side for all four paints) to equalize differences within the samples and obtain representative 'semi-quantitative' results. Ratios between these mean values from the UV irradiated and non-irradiated samples were calculated. The ratios for the lower sides differed only slightly, i.e. UV irradiation did not cause changes on the lower sides of the paints for the duration of the experiments. A number of characteristic signals were less intensive after UV irradiation on the irradiated top sides of the paints. Differences were observed for the paints depending on the added pigments (see Table SI 7-1). As expected, the binder was affected by UV irradiation. The investigated pigments caused different protection of the binder from UV irradiation, i.e. the red pigment protects the binder more effectively than the black and white pigments (see IR-spectra in the figures below). Chemical reactions of the binder were not further investigated. However, it can be concluded that the chemical surroundings for the biocides changes differently during the experiment in the presence of different pigments.

**Table B11-2** Changed intensities in the IR-spectra of the test specimen (mostly the styrene-acrylate binder) due to the UV irradiation.

IR signal Wave number [cm <sup>-1</sup> ]	Possible assignment to chemical bond	Ratio between signal intensities for UV irradiated and non-irradiated test specimens [%]			
		Black	Red	White	Pigment-free
697	C=C-H	65	55	27	42
711	C=C-H	75	82	106	42
757	C=C-H	71	63	82	45
871	C=C-H	76	54	107	47
1027	C-O	66	57	85	47
1063	C-O	63	57	82	43
1154	C-O-C	60	63	97	47
1259	C-O	66	53	107	43
1395	OCOCH <sub>3</sub>	73	62	61	37
1727	C=O	62	57	45	44
2929	CH <sub>2</sub> , CH <sub>3</sub>	67	60	80	42

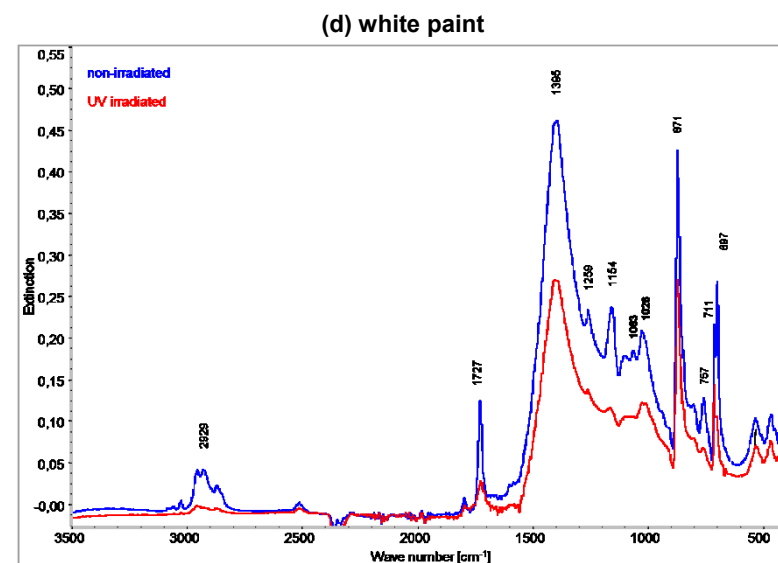
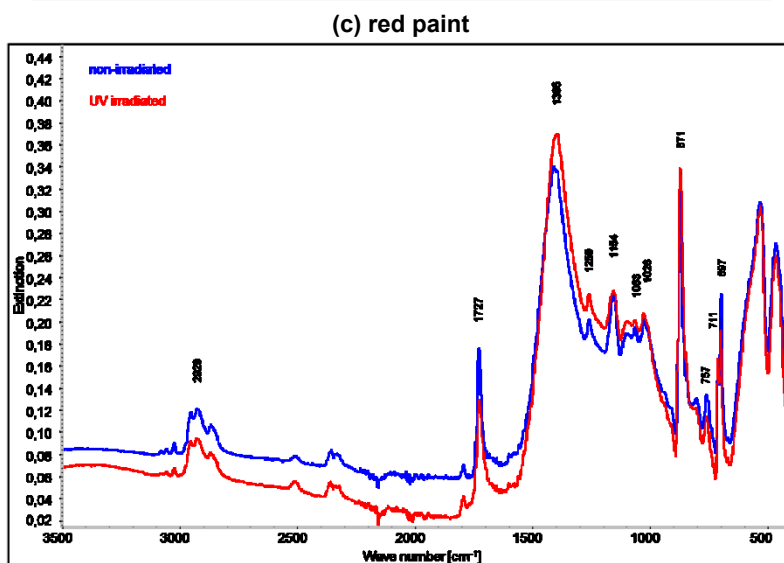
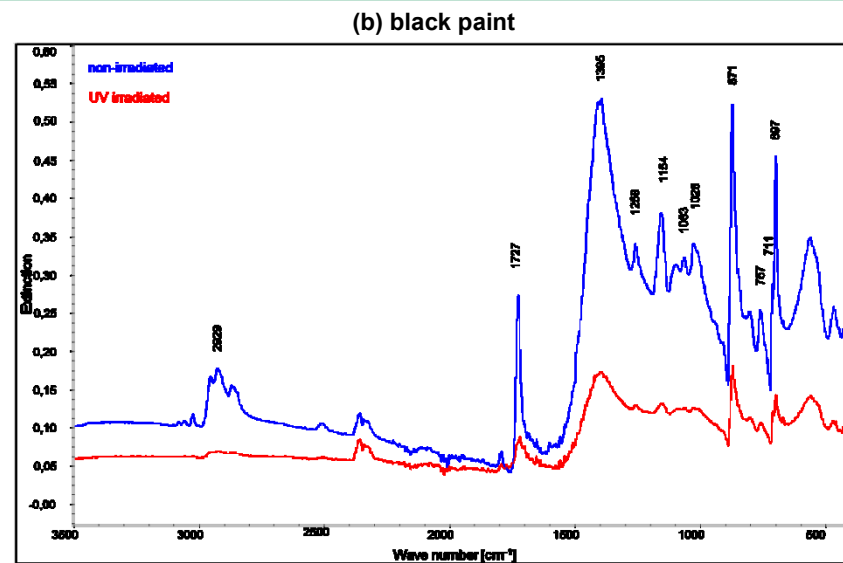
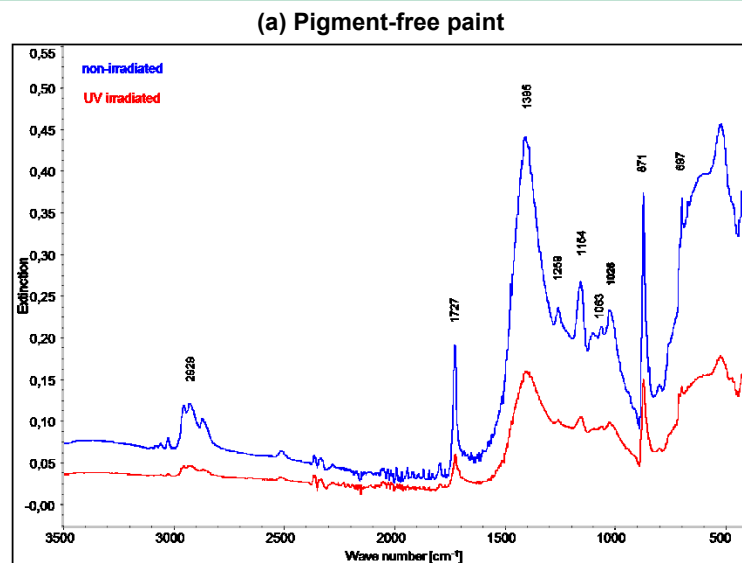
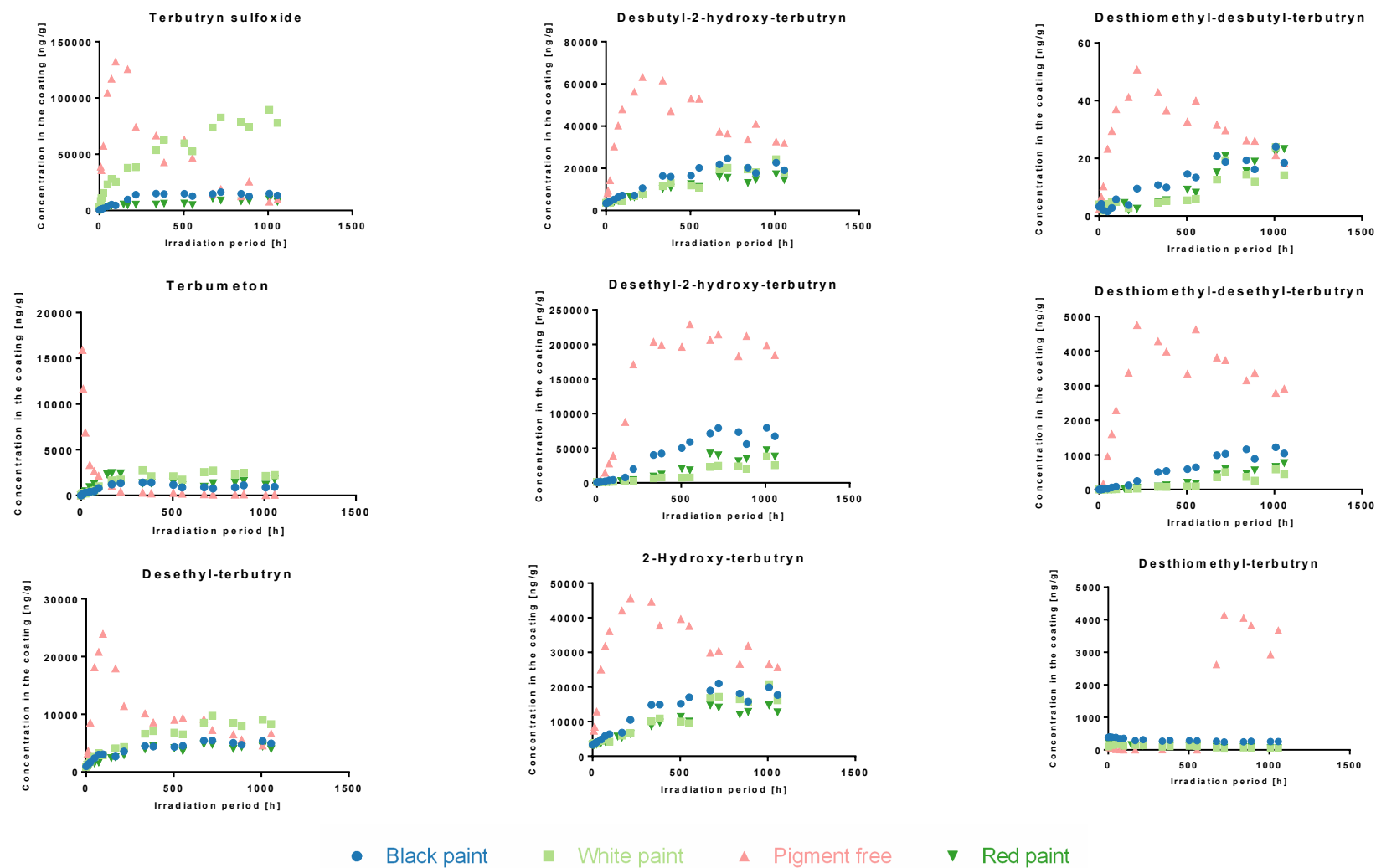
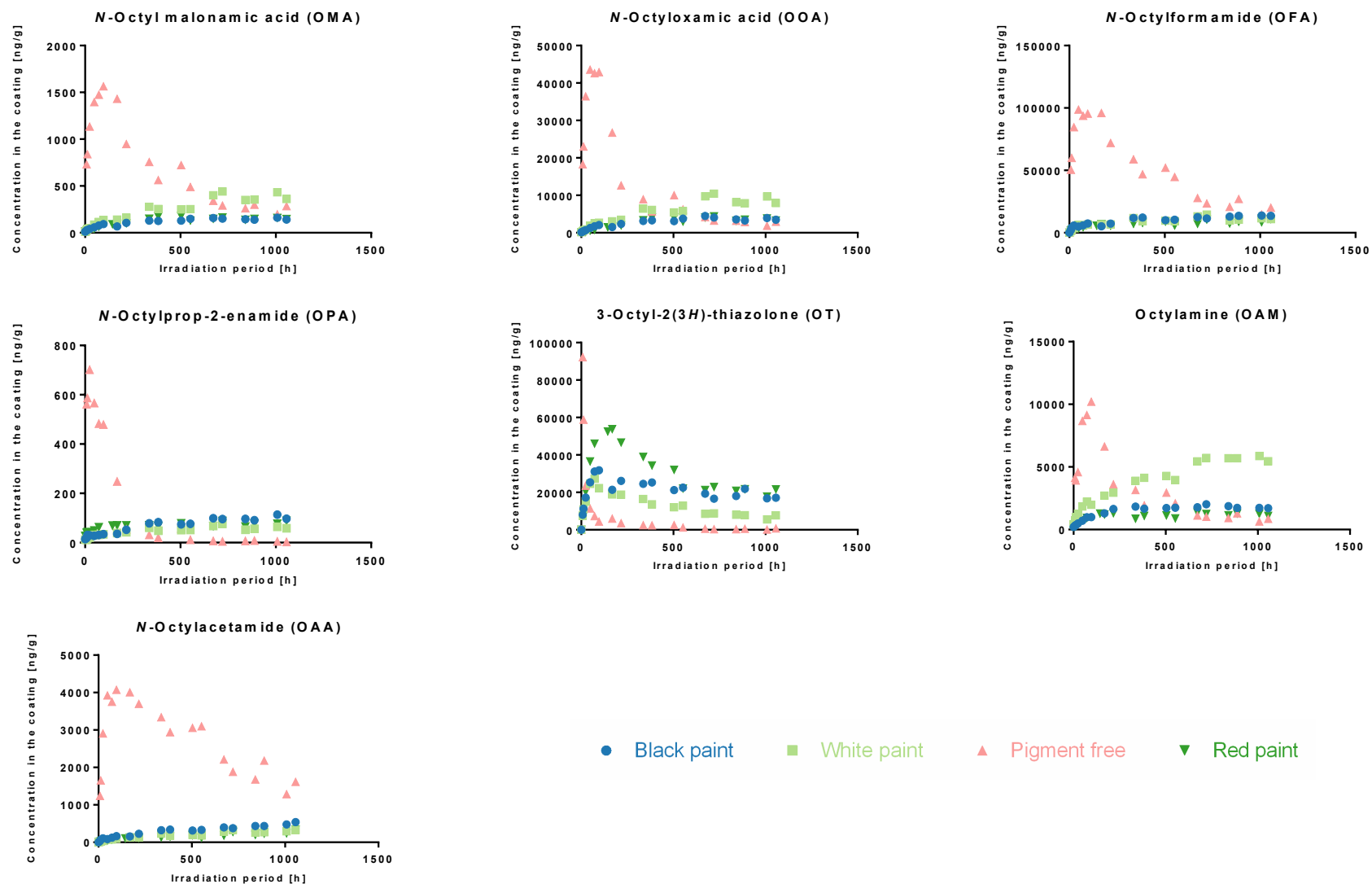


Figure B11-2 Selected examples of IR spectra from UV irradiated samples compared to non-irradiated top sides of paint films.

## Bilag 11.5 Concentrations of Terbutryn transformation products during the experiments.



## Bilag 11.6 Concentrations of *N*-Octylisothiazolinone transformation products during the experiments.





# Bilag 12.

## Additional data: transformation products in the environment

**Bilag 12.1** Monitoring of transformation products in stormwater ponds and surface waters: Terbutryn [ng L<sup>-1</sup>].

	Stormwater						Surface water							
	Silkeborg UD	Silkeborg IND	Randers-2 UD	Randers-2 IND	Randers-1 UD	Randers-1 IND	Kalveå	Vildmose- løbet	Holmehave Bæk	Damhave- bækken	Bondehave- renden	Yderup Bæk	Kættinghøj Bæk	Hagensmøl- lebæk
Terbutryn	15.5	10.97	0.9	1.02	0.96	0.72	0.23	0.86	0.43	0.22	0.25	0.24	<LOD	0.25
Terbutryn sulfoxide	11.38	6.61	2.7	3.55	2.07	2.1	0.17	0.32	0.48	<LOD	<LOD	<LOD	<LOD	0.12
Desethyl- terbutryn	3.11	1.01	0.66	0.58	0.48	0.38	0.08	0.07	0.07	<LOD	0.1	<LOD	<LOD	<LOD
Terbumeton	0.27	0.36	<LOD	<LOD	<LOD	<LOD	<LOD	<LOD	<LOD	<LOD	<LOD	<LOD	<LOD	<LOD
2-Hydroxy- terbutryn	16.43	12.28	3.41	4.18	3.66	4.2	1.55	0.8	3.13	1.44	2.2	0.56	0.25	0.87
Desbutyl-2- hydroxy- terbutryn	6.91	<LOD	7.21	<LOD	7.06	<LOD	<LOD	<LOD	<LOD	<LOD	<LOD	<LOD	<LOD	<LOD
Desethyl-2- hydroxy- terbutryn	50.66	39.37	12.77	15	14.74	16.96	2.02	2.34	4	2.06	2.8	1.32	0.65	1.48
Desthiomethyl- terbutryn	<LOD	<LOD	<LOD	<LOD	<LOD	<LOD	<LOD	<LOD	<LOD	<LOD	<LOD	<LOD	<LOD	<LOD
Desbutyl-des- thiomethyl- terbutryn	<LOD	<LOD	<LOD	<LOD	<LOD	<LOD	<LOD	<LOD	<LOD	<LOD	<LOD	<LOD	<LOD	<LOD
Desethyl-des- thiomethyl- terbutryn	0.14	0.1	0.04	0.03	<LOD	0.05	<LOD	<LOD	<LOD	<LOD	<LOD	<LOD	<LOD	<LOD
Terbutryn-thiol	<LOD	<LOD	<LOD	<LOD	<LOD	<LOD	<LOD	<LOD	<LOD	<LOD	<LOD	<LOD	<LOD	<LOD

**Bilag 12.2 Monitoring of transformation products in stormwater ponds and surface waters: Octylisothiazolinone [ng L<sup>-1</sup>].**

	Stormwater						Surface water							
	Silkeborg UD	Silkeborg IND	Randers-2 UD	Randers-2 IND	Randers-1 UD	Randers-1 IND	Kalveå	Vildmose- løbet	Holmehave Bæk	Damhave- bækken	Bondehave- renden	Yderup Bæk	Kættinghøj Bæk	Hagensmøl- lebæk
<i>N</i> -Octyliso- thiazolinone	0.29	1.55	0.31	0.42	0.42	0.56	0.32	0.7	0.65	0.4	0.33	0.46	0.32	0.31
<i>N</i> -Octyl- formamide	<LOD	<LOD	<LOD	<LOD	<LOD	<LOD	<LOD	<LOD	<LOD	<LOD	<LOD	<LOD	<LOD	<LOD
<i>N</i> -Octylacet- amide	<LOD	<LOD	<LOD	<LOD	<LOD	<LOD	<LOD	<LOD	<LOD	<LOD	<LOD	<LOD	<LOD	<LOD
<i>N</i> -Octylprop-2- enamide	<LOD	<LOD	<LOD	<LOD	<LOD	<LOD	<LOD	<LOD	<LOD	<LOD	<LOD	<LOD	<LOD	<LOD
<i>N</i> -Octylamine	<LOD	<LOD	<LOD	<LOD	<LOD	<LOD	<LOD	<LOD	<LOD	<LOD	<LOD	<LOD	<LOD	<LOD
3-Octylthiazol- 2(3 <i>H</i> )-one	<LOD	<LOD	<LOD	<LOD	<LOD	<LOD	<LOD	<LOD	<LOD	<LOD	<LOD	<LOD	<LOD	<LOD
<i>N</i> -Octyl oxamic acid	<LOD	<LOD	<LOD	<LOD	<LOD	<LOD	<LOD	<LOD	<LOD	<LOD	<LOD	<LOD	<LOD	<LOD
<i>N</i> -Octyl malonamic acid	<LOD	<LOD	<LOD	<LOD	<LOD	0.96	<LOD	<LOD	<LOD	<LOD	<LOD	<LOD	<LOD	<LOD

**Bilag 12.3 Monitoring of transformation products in stormwater ponds and surface waters: Others [ng L<sup>-1</sup>].**

	Stormwater						Surface water							
	Silkeborg UD	Silkeborg IND	Randers-2 UD	Randers-2 IND	Randers-1 UD	Randers-1 IND	Kalveå	Vildmose- løbet	Holmehave Bæk	Damhave- bækken	Bondehave- renden	Yderup Bæk	Kættinghøj Bæk	Hagensmøl- lebæk
Carbendazim	5.46	5.81	5.45	6.79	6.73	9.94	1.68	0.74	0.9	0.55	4.42	4.72	0.24	0.69
Aminobenz- imidazole	0.78	1.29	0.71	0.45	0.74	<LOD	0.28	<LOD	0.84	0.62	0.79	0.44	<LOD	<LOD
Diuron	1.31	0.97	0.62	0.63	0.7	0.95	0.98	<LOD	1.08	0.78	<LOD	0.56	<LOD	0.53
DCPMU	<LOD	<LOD	<LOD	<LOD	<LOD	<LOD	<LOD	<LOD	<LOD	<LOD	<LOD	<LOD	<LOD	<LOD
Isoproturon	0.53	0.53	0.51	0.58	0.57	0.67	0.52	0.47	0.76	0.46	0.62	0.48	<LOD	0.5
IPPMU	<LOD	<LOD	<LOD	<LOD	<LOD	<LOD	<LOD	<LOD	0.44	0.41	<LOD	<LOD	<LOD	0.43

# Bilag 13.

## Conference contributions

### Bilag 13.1 Platform presentations

U.E. Bollmann, G. Minelgaite, M. Schlüsener, J. Vollertsen, T. Ternes, K. Bester: Biocide leaching from building material: Semi-field emissions influenced by driving-rain and photodegradation. 16th EuCheMS International Conference on Chemistry and the Environment, June 2017, Oslo, Norway.

U.E. Bollmann, K. Styszko, Y. Ou, P. Mayer, S. Trapp, J. Vollertsen, K. Bester: Biocides from façade coatings in urban surface waters: Estimating the leaching of biocides from render by polyacrylate-water partitioning constants. SETAC Europe 25th Annual Meeting, May 2015, Barcelona, Spain.

### Bilag 13.2 Poster

M.M. Urbanczyk, K. Bester, N. Borho, U. Schoknecht, U.E. Bollmann: Biocides in facade coatings: Influence of pigments on the phototransformation of biocides. SETAC Europe 28th Annual Meeting, May 2018, Rome, Italy.

M. Urbanczyk, U.E. Bollmann, N. Borho, U. Schoknecht, K. Bester: Influence of pigments on phototransformation rates of biocides in paints. 16<sup>th</sup> EuCheMS International Conference on Chemistry and the Environment, June 2017, Oslo, Norway.

E.A. Rudelle, U.E. Bollmann, A.H. Nielsen, K. Bester, J. Vollertsen: Transport mechanisms of biocides in renders. SETAC Europe 27<sup>th</sup> Annual Meeting, May 2017, Bruxelles, Belgium.

U.E. Bollmann, G. Minelgaite, M. Schlüsener, J. Vollertsen, T. Ternes, K. Bester: Emissions and photo-transformation of biocides on building facades using the example of terbutryn. SETAC Europe 26<sup>th</sup> Annual Meeting, May 2016, Nantes, France.

K. Bester, U.E. Bollmann, M. Escola Casas, K. Koefoed Brandt, T. Lv, P.N. Carvalho, H. Brix: Biodegradation of biocides in soils, soil filters and other biofilm reactors. SETAC Europe 26<sup>th</sup> Annual Meeting, May 2016, Nantes, France.

U.E. Bollmann, K. Styszko, K. Bester: Leaching of biocides from polymer renders: Determine transport processes through the material during wet and dry cycles. 15<sup>th</sup> EuCheMS International Conference on Chemistry and the Environment, September 2015, Leipzig, Germany.

M. Urbanczyk, U.E. Bollmann, K. Bester: Partitioning of biocides between water and inorganic phases of render. SETAC Europe 25<sup>th</sup> Annual Meeting, May 2015, Barcelona, Spain.



## **Transport and transformation of biocides in construction materials - Factors controlling release and emissions**

It is state-of-the-art in material production, to equip polymeric resin-based paints and renders with biocides (i.e. algaecides, fungicides, bactericides) to prevent the materials and the final coating films from biological deterioration. Nevertheless, it is well-known that these biocides leach from the materials when they get in contact with rainwater and, thus, end up in the environment. However, although the water contact is crucial for the leaching, other factors need to be taken into consideration: the transport of the biocides to the coating surface as well as the transformation reactions.



The Danish Environmental  
Protection Agency  
Haraldsgade 53  
DK-2100 København Ø

[www.mst.dk](http://www.mst.dk)